

Curriculum Vitae

Nivedita Uday Hegdekar
Nivedita.Hegdekar@gmail.com

EDUCATION

- Aug 2014 – Ph.D. in Biochemistry and Molecular Biology
May 2022 (transferred from the M.S. program in Fall 2016)
University of Maryland, Baltimore
- Aug 2019 – M.S. in Law (majoring in Patent Law)
May 2021 University of Maryland, Baltimore
- Sept 2010 – Bachelor of Pharmacy
May 2014 Institute of Chemical Technology, Mumbai, India.

PUBLICATIONS

Hegdekar, N., Sarkar, C., Ritzel R.M., Hanscom, Bustos, S., Loane D.J., Faden A.I., Lipinski, M.M. Autophagy Dysregulation in Microglia and Infiltrating Macrophages Exacerbates Neuroinflammation and Functional Defects following Traumatic Brain Injury. (in preparation)

Morel, Y., **Hegdekar, N.**, Sarkar, C., Lipinski, M.M., Kane, M., Jones, J. (2021) Structure-Specific, Accurate Quantitation of Plasmalogen Glycerophosphoethanolamine: Application to Traumatic Brain Injury. *Analytica Chimica Acta*, Volume 1186.

Hegdekar, N., Lipinski, M. M., & Sarkar, C. (2021). N-Acetyl-L-leucine improves functional recovery and attenuates cortical cell death and neuroinflammation after traumatic brain injury in mice. *Scientific Reports*, 11(1), 9249. <https://doi.org/10.1038/s41598-021-88693-8>

Hanscom M., Loane D.J., Aubretch T., Leser J., Molesworth K., **Hegdekar N.**, Ritzel R.M., Abulwerdi G., Shea-Donohue T., Faden A.I. (2021) Acute colitis during chronic experimental traumatic brain injury in mice induces dysautonomia and persistent extraintestinal, systemic, and CNS inflammation with exacerbated neurological deficits. *J Neuroinflammation*, 18(1):24. <https://doi.org/10.1186/s12974-020-02067-x>.

Thayer, J. A., Awad, O., **Hegdekar, N.**, Sarkar, C., Tesfay, H., Burt, C., Zeng, X., Feldman, R. A., & Lipinski, M. M. (2020). The *PARK10* gene *USP24* is a negative regulator of autophagy and ULK1 protein stability. *Autophagy*, 16(1), 140–153. <https://doi.org/10.1080/15548627.2019.1598754>

Sarkar, C., Jones, J. W., **Hegdekar, N.**, Thayer, J. A., Kumar, A., Faden, A. I., Kane, M. A., & Lipinski, M. M. (2020). PLA2G4A/cPLA2-mediated lysosomal membrane

damage leads to inhibition of autophagy and neurodegeneration after brain trauma. *Autophagy*, 16(3), 466–485. <https://doi.org/10.1080/15548627.2019.1628538>.

POSTER PRESENTATIONS

- Nov 2021 Autophagy Dysregulation in Microglia and Macrophages Exacerbates Neuroinflammation Following Traumatic Brain Injury.
Society for Neuroscience 2021 Meeting (Virtual)
- Mar 2019 The Molecular Crosstalk between Autophagy Dysregulation and Neuroinflammation Following Traumatic Brain Injury.
UMB Graduate Research Conference
- Mar 2019 The Molecular Crosstalk between Autophagy Dysregulation and Neuroinflammation Following Traumatic Brain Injury.
2019 National Capital Area Traumatic Brain Injury Research Symposium, Bethesda, MD.
- Jan 2019 The Molecular Crosstalk between Autophagy Dysregulation and Neuroinflammation Following Traumatic Brain Injury.
UMB Program in Biochemistry and Molecular Biology Retreat, Baltimore, MD.
- Nov 2018 The Molecular Crosstalk between Autophagy Dysregulation and Neuroinflammation Following Traumatic Brain Injury.
Society for Neuroscience 2018 Meeting: San Diego, CA.
- Oct 2018 The Molecular Crosstalk between Autophagy Dysregulation and Neuroinflammation Following Traumatic Brain Injury.
Greater Baltimore Society for Neuroscience, Baltimore, MD.
- Jun 2018 The Molecular Crosstalk between Autophagy Dysregulation and Neuroinflammation Following Traumatic Brain Injury.
Program in Neuroscience Annual Retreat, Baltimore, MD.
- Jan 2018 The Molecular Crosstalk between Autophagy Dysregulation and Neuroinflammation Following Traumatic Brain Injury.
2018 National Capital Area Traumatic Brain Injury Research Symposium, Bethesda, MD.
- Jan 2018 The Molecular Crosstalk between Autophagy Dysregulation and Neuroinflammation Following Traumatic Brain Injury
UMB Program in Biochemistry and Molecular Biology Retreat, Baltimore, MD.
- Nov 2017 The Molecular Crosstalk between Autophagy Dysregulation and Neuroinflammation Following Traumatic Brain Injury

Greater Baltimore Society for Neuroscience, Baltimore, MD.

- Nov 2017 The Molecular Crosstalk between Autophagy Dysregulation and Neuroinflammation Following Traumatic Brain Injury
Society for Neuroscience 2017 Meeting: Washington D.C.
- Jun 2017 The Molecular Crosstalk between Autophagy Dysregulation and Neuroinflammation Following Traumatic Brain Injury.
Program in Neuroscience Annual Retreat, Baltimore, MD.
- Jan 2017 The Molecular Crosstalk between Autophagy Dysregulation and Neuroinflammation Following Traumatic Brain Injury.
2017 National Capital Area Traumatic Brain Injury Research Symposium, Bethesda, MD.

ORAL PRESENTATION

- May 2021 Autophagy Dysregulation in Microglia and Macrophages Exacerbates Neuroinflammation Following Traumatic Brain Injury.
Society for Neuroscience 2021 Meeting (Virtual)
- Mar 2019 Autophagy Dysregulation in Microglia and Macrophages Exacerbates Neuroinflammation Following Traumatic Brain Injury.
2021 Baltimore Brain Series.
- Mar 2019 Autophagy Dysregulation in Microglia and Macrophages Exacerbates Neuroinflammation Following Traumatic Brain Injury.
2020 National Capital Area Traumatic Brain Injury Research Symposium

HONORS.

- Oct 2021 Elaine Miye Otani Memorial Award for service to GPILS community
- Mar 2021 2021 Presidential Core Values Leadership Award
- Nov 2017 UMB President Entrepreneurial Fellowship
- Mar 2016 Spring 2016 Employee of the Semester (part-time job at URecFit, University of Maryland, Baltimore)
- Mar 2014 1st place- Best Pharmacy Student Award (selected from over 1,000 state-wide pharmacy students)

ABSTRACT

Title of Dissertation: Inhibition of Autophagy in Microglia and Infiltrating Monocytes/Macrophages Exacerbates Neuroinflammation and Functional Defects Following Traumatic Brain Injury

Dissertation directed by: Dr. Marta M. Lipinski., Associate Professor, Department of Anesthesiology, University of Maryland, Baltimore.

Committee Members: Dr. Marta M. Lipinski (Committee Chair), Dr. Alan Faden, Dr. Brian Polster, Dr. David Loane, Dr. Mervyn Monteiro.

The autophagy-lysosomal pathway serves an important role in cellular homeostasis and protection against neurodegeneration. Recently autophagy has been also implicated in regulation of immune and inflammatory responses. Specifically, high levels of autophagy flux are generally associated with anti-inflammatory, and inhibition of flux with pro-inflammatory phenotypes.

To determine if autophagy may be involved in modulation of brain inflammation after traumatic brain injury (TBI), we assessed the levels of autophagy in resident microglia and infiltrating macrophages following moderate controlled cortical impact (CCI) in C57Bl/6 mice. Consistent with a potential function in neuroinflammation, our data demonstrated accumulation of autophagosomes and inhibition of autophagy flux specifically in the activated microglia and infiltrating macrophages starting by day 1 and continuing through day 28 post-CCI. Our immunofluorescence studies in transgenic *Cx3Cr1-GFP* microglial and *Ccr2-RFP* monocyte reporter mice confirmed inhibition of autophagy flux and demonstrated that while both activated resident microglia and infiltrating macrophages are affected, inhibition of autophagy is much more prominent in

macrophages. We used flow cytometry analysis to demonstrate that immune cells with inhibited autophagy flux after CCI expressed increased levels of pro-inflammatory markers, including IL-1 β and TNF- α , as compared to corresponding immune cells with normal levels of autophagy. Furthermore, inhibition of autophagy flux correlated with impaired phagocytic function, indicating microglial/macrophage dysfunction. These trends persisted through day 28- post CCI, suggesting that autophagy flux impairment following TBI has long-term consequences. Consistent with ability of autophagy to affect inflammation, our *in vitro* experiments in microglial and macrophage cell lines demonstrated that inhibition of autophagy can potentiate pro-inflammatory activation induced by lipopolysaccharide (LPS) treatment. *In vivo*, mice with microglia/macrophage-specific knockout of the autophagy gene *Becn1* (*Beclin1*^{*fllox/fllox*}, *LysM*^{*Cre/Cre*}) subjected to CCI showed increased expression of pro-inflammatory genes and proteins as compared to controls. This included a marked exacerbation of the innate immune responses, including activation of the NLRP3 inflammasome and the type-I IFN pathways, indicating the importance of autophagy in suppression of innate-immunity mediated inflammation. Finally, *Beclin1*^{*fllox/fllox*}, *LysM*^{*Cre/Cre*} mice performed worse than *LysM*^{*Cre/Cre*} controls on behavioral tasks after CCI. Overall, these findings indicate that inhibition of autophagy in microglia/macrophages exacerbates neuroinflammation after TBI and contributes to functional deficits.

Inhibition of Autophagy in Microglia and Infiltrating Monocytes/Macrophages
Exacerbates Neuroinflammation and Functional Defects
Following Traumatic Brain Injury

by
Nivedita Uday Hegdekar

Dissertation submitted to the Faculty of the Graduate School of the
University of Maryland, Baltimore in partial fulfillment
of the requirements for the degree of
Doctor of Philosophy
2022

DEDICATION

This thesis is dedicated to

My parents *Mrs. Nandita Hegdekar* and *Dr. Uday Hegdekar* for their selfless sacrifices, love, and guidance. You both have always pushed me to be the best version of myself, and believed in me, especially at times when I had lost faith in myself;

My younger sister *Namita Hegdekar*, for being my best friend, confidant, and fiercest cheerleader. You will always be the greatest gift life has given me;

My late paternal grandparents *Mrs. Sharada Hegdekar* and *Mr. Venkatesh Hegdekar*, whose legacy and life inspired me to live a value-driven life. Through your life, I learned that life isn't about how much stuff you manage to accumulate, it's about how well you loved and were loved by the people who mattered most;

My maternal grandfather *Dr. Ullal Balkrishnan Rao*, who epitomized selflessness, service above self and dedication to one's craft. You made the world a better place through your infinite kindness, wisdom, and humor. If I amount to even half the person you were, I will consider this a life well-lived;

and finally, to my late maternal grandmother *Mrs. Radha B. Rao*, for her endless love through the years. There is nothing I wouldn't give to spend just one more day with you. While I cherish the many memories we created together, please know that I will miss you dearly till my last breath.

ACKNOWLEDGEMENTS

My 7.5 years of graduate school life have been a time of immense learning, joy, growth, and self-reflection. I would gratefully like to extend my thanks to the many, many individuals who helped me get here.

First, I would like to thank my mentor, Dr. Marta Lipinski, for welcoming me into her laboratory and providing excellent guidance since January 5th, 2015. Her mentorship and constant encouragement to think independently have helped me grow into a confident scientist. I was very fortunate to have had a wonderful thesis advisory committee. Dr. David Loane, Dr. Brian Polster, Dr. Mervyn Monteiro, and Dr. Alan Faden. Thank you for being willing to discuss my research and find ways to improve my project. Your suggestions were invaluable in the course of my thesis research, committee meeting, and dissertation preparations.

My time here has helped my critical thinking skills in and out of the lab. I am incredibly grateful to members (both current and former) of the Lipinski Lab- Dr. Chinmoy Sarkar- thanks for training me during the early days after joining the lab and laying the foundations for this research work. Dr. Julia Thayer, (to-be Dr.) Sabrina Bustos, Denisha Odie, Amir Mehrabani Tabari, and Ruchel McNair- thanks for making the lab a fun workplace and helping me get through the everyday ups and downs of research life! I want to think I've become a better researcher due to your help and unconditional support over the years.

I would like to thank the members of Shock, Trauma, and Anesthesiology Research (STAR) group for their support and bring amazing co-workers: Dr. Marie Hanscom, Courtnet Colson, Dr. Gelareh Vinueza, Dr. Boris Sabirzhaniv, Dr. Rebecca Henry, Dr. James Barrett, Dr. Aidan Smith, Dr. Niaz Khan, Dr. Yun Li, Dr. Taryn Aubretch, Victoria Meadows, and Kara Molesworth. Kelly Sikorski deserves all the hugs and praise in the world for being my #1 go-to person on all matters, big or small, on good days and bad days. A big thank you to the UMB Flow Cytometry Core (in particular Bryan Hahn and Dr. Xiaoxuan Fan) and Dr. Rodney Ritzel for their expertise on several flow cytometry experiments in this study. To collaborators on numerous projects over the years- Dr. Ola Awad, Dr. Jace Jones and Yulemni Morel- working with you has been a phenomenal experience. I have grown so much through your wisdom and knowledge.

I am also indebted to the Program in Biochemistry and Molecular Biology and notably Dr. Gerald Wilson for allowing me to pursue my dream of becoming a research scientist. The program has provided a supportive learning environment. I owe a debt of thanks to the staff at UMB, have helped me navigate through numerous hurdles, paperwork, form, and general grad school stress. These include Kiriaki (Koula) Cozmo, Ali Squires, Elice Baca- Garcia, Jennifer Aumiller- you have always been willing to put aside what you were doing to talk to me, whether it was for a good reason or not. Dr. Renee Cockerham and Dr. Georgia Rogers, thank you for welcoming me as an unofficial member of the Program in Neuroscience (PIN), and inviting me to PIN-related events and seminars! I would also like to thank Dr. Erin Golembewski and Jamila Savage for always being so helpful and assisting me on so many grad school issues over the years.

I truly lucked out when it came to making friends in grad school, and there's a reason I consider 2014-2022 to be the happiest period of my life. To my family in Baltimore and beyond- Nathan Hardenbrook, Christian Kinney, Quinton Banks, Jennifer McFarland, Amber Plante, Amanda Labuza, Alli Mancini, Will Gustafson, Mashhood Wani, Ramon Martinez, Laura Bozzi, Heather Mutchie, Daniel Garman, Katie Boyle, Kelson Shilling-Scrive, Emily Boydston, Ryan Mayers, Kaila Noland, Megan Lynch, Utsav Gyawali, Sydney Ashton, Ashley Marquardt, Jack Hussey, Sin Chan, Kelsey Gustaveson, Maria Larossa Garcia, Shane Breighner, Bryan Mackowiak, Gina Salvatore, Pranjali Kanvinde, Aakash Gandhi, Chintal Shah, Devika Bhalerao, Chinmay Tikhe, Binny Bhandari, Mannat Kalra, Savyasachi Shah, Mina He, Marisa Booth, Aishwarya Iyer, Matthew Panicker, Heather Braeuniger, Andrew Schoenberger, and Nicole Mendonsa- thank you for being the best support system I could have ever hoped for and for bringing so much joy and happiness in my life. Through your love, words and actions, you all have helped me become a better and kinder person. To the Hardenbrook family- Jodie, Jim and Bethany- thank you for always welcoming me into your home and lives during the holidays, and especially during the pandemic. Words will never be enough to describe how much you all mean to me.

I am forever grateful to my high school friends and undergraduate friends for their guidance and friendship from across the miles- Nafisa Jassani, Manali Karoor, Vicky Matani, Shivangi Shinari, Nazia Sheikh, Dr. Priyanka Amonkar, and Dr. Manish Gore- there's not a single day that I do not miss you all.

While none of my grandparents lived long enough to see this day, I know that they are watching me from the beyond. Their life, achievements and sacrifices will forever remain the cornerstones of my moral compass. Finally, to the most important people in my life- my parents, Dr. Uday Hegdekar and Nandita Hegdekar, and my sister, Namita Hegdekar- everything I am today, am I because of you. Without your blessings, love, and encouragement, I would not have been here today. Your support means a lot more than I can express in words.

TABLE OF CONTENTS

Dedication.....	iii
Acknowledgements.....	iv
List of Table.....	xii
List of Figures.....	xiii
List of Abbreviations	xvi
CHAPTER 1: Introduction.....	1
1.1. Traumatic Brain Injury	1
1.1.1. Overview of TBI	4
1.1.2. Pathophysiology of TBI	4
1.1. 3. Neuroinflammation	8
1.1.3.1. Microglia	8
1.1.3.2. Infiltrating Myeloid Cells.....	11
1.2. Innate Immunity	14
1.2.1. Overview of Innate Immunity	14
1.2.2. Toll-like Receptor (TLR) Signaling Pathway	16
1.2.3. NOD-like Receptor (NLR) Signaling Pathway.....	19
1.2.4. Cytosolic DNA Sensors (CDS) and the cGAS-STING Pathway.....	23
1.3. Autophagy	26
1.3.1. Overview of Autophagy	26
1.3.2. Autophagy Pathway (in detail).....	29
1.3.3. Autophagy Flux	31
1.3.4. Role of Autophagy in TBI.....	34

1.3.5. Role of Autophagy in Innate Immunity and Inflammation	36
1.4. Scope of Research	42
CHAPTER 2: Inhibition of autophagy is associated with increased expression of pro-inflammatory markers and defects in phagocytosis.....	44
2.1. Introduction	44
2.2. Results	46
2.2.1. Autophagy flux is inhibited in activated microglia and macrophages after TBI	46
2.2.2. Inhibition of autophagy is associated with increased expression of pro-inflammatory markers and functional defects in phagocytosis	47
2.2.3. Modulation of autophagy in macrophages and microglia alters inflammatory responses <i>in vitro</i>	56
2.3. Discussion	57
2.4. Methods.....	62
CHAPTER 3: Inhibition of Autophagy in Microglia and Monocytes/Macrophages Exacerbates Innate Immune Responses, Neuroinflammation, and Functional Defects following TBI.....	69
3.1. Introduction	69
3.2. Results.....	72
3.3.1. LysM-Cre expression is present in both monocytes/macrophages and resident microglia	72
3.3.2. Inhibition of autophagy is associated with increased expression of pro-inflammatory markers and functional defects in phagocytosis	75

3.2.3. <i>Becn1</i> deficiency in microglia and infiltrating monocytes/macrophages increases innate immunity gene expression in mice brain cortices.....	77
3.2.4. <i>Becn1</i> deficiency in microglia and infiltrating monocytes/ macrophages increases protein expression of markers involved in innate immunity and inflammation	80
3.2.5. <i>Becn1</i> deficiency in microglia and infiltrating monocytes/ macrophages does not alter fine motor coordination deficits in TBI and Sham- injured mice	85
3.2.6. <i>Becn1</i> deficiency in microglia and infiltrating monocytes/ macrophages exacerbates TBI-associated deficits in spatial learning and declarative memory.	87
3.2.7. <i>Becn1</i> deficiency in microglia and infiltrating monocytes/ macrophages exacerbates hippocampal neurodegeneration but does not significantly exacerbate overall cortical lesion volume after injury	90
3.2.7. Gene expression of inflammation and innate immunity remains higher, but not statistically significant, at 28 days post-TBI.....	92
3.3. Summary and Future Directions.....	93
3.4. Methods.....	99
CHAPTER 4: N-acetyl-L-leucine improves functional recovery and attenuates cortical cell death and neuroinflammation after traumatic brain injury in mice	110
4.1. Introduction.....	110
4.2. Results.....	113

4.2.1. NALL treatment does not negatively affect food intake and body weight of mice after TBI	113
4.2.2. NALL treatment attenuates cortical cell death after TBI	113
4.2.3. NALL treatment restores autophagy flux after TBI	117
4.2.4. NALL reduces expression of inflammatory cytokines in TBI mouse Brain	119
4.2.5. NALL treatment improves motor and cognitive function in mice after TBI	119
4.3. Summary	125
4.4. Methods	129
CHAPTER FIVE: Discussions	135
5.1. Role of Autophagy in Neuroinflammation	135
5.2. Role of Autophagy in Innate Immunity	136
5.3. Role of Autophagy in TBI: expansion of existing paradigm	137
5.4. Autophagy, TBI & Aging	138
5.5. Future Directions	140
5.6. Final Thoughts on Project	142
References	143

LIST OF TABLES

Table 1-1. List of recognized DAMPs in injury.....16

Table 1-2. Role of autophagy in immunologic responses.37

LIST OF FIGURES

Figure 1-1. Report of TBI-related emergency department visits, hospitalizations, and deaths (EDHD) from 2001-2010	3
Figure 1-2. Pathophysiological mechanisms of primary injury in TBI	5
Figure 1-3. General timeline of TBI pathophysiology.....	7
Figure 1-4. Morphological changes of microglia	9
Figure 1-5. Temporal inflammatory response following TBI	12
Figure 1-6. TLR signaling receptors.....	18
Figure 1-7. Formation of the NLRP3 inflammasome.....	21
Figure 1-8. cGAS-STING signaling	25
Figure 1-9. Schematic diagram of the steps of autophagy	28
Figure 1-10. Autophagy flux under normal and pathological conditions	33
Figure 2-1. Autophagy is inhibited in activated microglia and infiltrating monocytes after TBI	48
Figure 2-2. Microglia and infiltrating myeloid cells accumulate markers of autophagy after TBI	49
Figure 2-3. Inhibition of autophagy flux is associated with increased expression of pro-inflammatory markers after TBI	52
Figure 2-4. Inhibition of autophagy flux is associated with increased expression of the pro-inflammatory cytokines IL-1 β and TNF- α	54
Figure 2-6. Inhibition of autophagy flux is associated with decreased phagocytic function of microglia and infiltrating monocytes	55

Figure 2-7. Inhibition of autophagy results in increased expression of pro-inflammatory markers <i>in vitro</i>	63
Figure 3-1. Characterization of the <i>LysM-Cre</i> line in the microglia and infiltrating Myeloid cells	73
Figure 3-2. <i>Becn1</i> knockout in <i>Beclin^{flox/flox}</i> , <i>LysM^{Cre/Cre}</i> (<i>Becn1</i> cKO) mice results in decreased <i>Beclin1</i> mRNA and protein levels in bone marrow-derived macrophages (BMDM) compared to <i>LysM^{Cre/Cre}</i> (Control) mice	74
Figure 3-3. <i>Becn1</i> deficiency in microglia and infiltrating monocytes/macrophages alters gene expression clustering of various groups, based on the NanoString nCounter® Neuroinflammation panel, in mice brain cortices	76
Figure 3-4. <i>Becn1</i> deficiency in microglia and infiltrating monocytes/macrophages alters transcription levels of neuroinflammatory genes in mice brain cortices.	78
Figure 3-5. <i>Becn1</i> deficiency in microglia and infiltrating monocytes/macrophages increases expression of genes involved in innate immunity in mice brain cortices post-TBI	79
Figure. 3-6. <i>Becn1</i> deficiency in microglia and infiltrating monocytes/macrophages increases expression of pro-inflammatory genes and innate immune gene expression in mice brain cortices post-TBI.....	81
Figure 3-7. <i>Becn1</i> deficiency in microglia and monocytes/macrophages exacerbates neuroinflammation and innate immune gene pathways in mice brain cortices post-TBI.....	82

Figure 3-8.	The effects of <i>Becn1</i> knockout on inflammatory responses in microglia and monocytes from mice brain cortices post-TBI.....	84
Figure 3-9.	<i>Becn1</i> deficiency does not exacerbate impairments in fine motor coordination post-TBI.....	86
Figure 3-10.	Deficits in declarative memory spatial and learning and memory are exacerbated in <i>Becn1</i> cKO mice after TBI.....	88
Figure 3-11.	<i>Becn1</i> deficiency in microglia and monocytes/macrophage exacerbates hippocampus neurodegeneration but not overall cortical neurodegeneration.....	91
Figure. 3-12.	Increased expression levels of pro-inflammatory and innate immune gene expression due to <i>Becn1</i> deficiency in microglia and infiltrating monocytes/macrophages in brain cortices persists at 28 days post-TBI gene expression and innate immune gene expression after TBI.....	92
Figure 4-1.	NALL does not affect food intake and body weight in mice.....	114
Figure 4-2.	NALL attenuates cortical cell death after TBI.....	116
Figure 4-3.	NALL restores autophagy flux after TBI.....	118
Figure 4-4.	NALL reduces pro-inflammatory markers in injured mouse cortices ...	120
Figure 4-5.	NALL alters the levels of anti-inflammatory markers in the injured Mouse.....	121
Figure 4-6.	NALL attenuates motor and cognitive deficits and cortical tissue loss in mice after injury.....	123

List of Abbreviations

3-MA	3-Methyladenine
ACTB	β -actin
AD	Alzheimer's disease
ALS	Amyotrophic lateral sclerosis
AMBRA1	Autophagy and Beclin-1 regulator 1
AMPK	Adenosine monophosphate-activated protein kinase
APC	Antigen presenting cells
AIM2	Absent in melanoma 2
ASC	Apoptosis-associated speck-like protein containing a CARD
ATG	Autophagy related
ANOVA	Analysis of variance
BafA	Bafilomycin A1
BBB	Blood-brain barrier
BECN1	Beclin 1
BMDM	Bone marrow-derived macrophages
BW	Beam walk
CARD	Caspase activation and recruitment domain
CCI	Controlled cortical impact
CDS	Cytosolic DNA sensor
CCL2	C-C motif chemokine ligand 2
CCR2	C-C motif chemokine receptor 2

cGAS	Cyclic GMP-AMP synthase
CNS	Central nervous system
cPLA2	Cytosolic phospholipase A2
DAMPs	Damage-associated molecular patterns
DC	Dendritic cells
dsDNA	Double-stranded DNA
dsRNA	Double-stranded RNA
ER	Endoplasmic Reticulum
FACS	Fluorescence activated cell sorting
FDA	Food and Drug Administration
GAPDH	Glyceraldehyde-3-phosphate dehydrogenase
GFP	Green fluorescent protein
HMGB1	High mobility group box 1
HD	Huntington's disease
IF	Immunofluorescence
IFN	Interferon
IL	Interleukin
iNOS	Inducible nitric oxide synthase
KO	Knockout
LAMP1	Lysosomal-associated membrane protein 1
LAP	LC3- associated phagocytosis
LC3	Light chain 3
LPS	Lipopolysaccharide

LLR	Leucine-rich repeats
MFI	Mean fluorescence intensity
MTOR	Mechanistic target of rapamycin kinase
MTORC1	MTOR complex 1
MWM	Morris Water maze
NALL	N-acetyl-L-leucine L-enantiomer
NBR1	next to BRCA1 gene 1
NLR	NOD-like receptor
NLRP3	NLR Family Pyrin Domain Containing 3
NPC	Niemann-Pick disease type C
NO	Novel object
NOX2	NADPH oxidase 2
NOR	Novel object recognition
PD	Parkinson's disease
PE	Phosphatidylethanolamine
PI	Preference index
PAMPs	Pathogen-associated molecular patterns
PCA	Principal component analysis
PRRs	Pattern recognition receptors
PRP	Pattern recognition patterns
PtdIns3K/PI3K	Phosphatidylinositol 3-kinase
PtdIns3P	Phosphatidylinositol 3-phosphate
qRT-PCR	Quantitative Real-Time Polymerase Chain Reaction

RAGE	Receptor for advanced glycation end products
ROS	Reactive oxygen species
RFP	Red fluorescent protein
ssRNA	Single-stranded RNA
SCI	Spinal cord injury
SQSTM1	Sequestosome-1
STING	Stimulator of interferon genes
TBI	Traumatic brain injury
TGF- β	Transforming growth factor- β
TLR	Toll-like receptor
TNF- α	Tumor necrosis factor- α
TRIM	Tripartite motif
TUNEL	Terminal deoxynucleotidyl transferase (TdT) dUTP Nick-End Labeling
ULK1	Unc-51 like autophagy activating kinase 1

Abbreviations, other than those in common usage, are also defined at the first point of occurrence in the text.

CHAPTER 1: Introduction

1.1 Traumatic Brain Injury

1.1.1 Overview

Traumatic brain injury (TBI) is defined as a sudden, external, physical blow to the head that disrupts normal brain function. It is a form of an acquired brain injury (i.e., it occurs after birth) and is a major cause of disability and mortality in the United States (US). Epidemiological data suggest that 2.8 million Americans sustain a TBI every year, and approximately 56,000 people die every year from TBI-related complications. (Langlois et al., 2006; McKinlay et al., 2008). TBI is a growing socioeconomic concern in the US, with estimated healthcare costs of over \$76.5 billion in 2010 (CDC website). Major causes of TBI include falls, motor vehicle accidents, gunshots, sports-related injuries, being struck by an object, explosive blasts, and other military injuries (CDC Stacks, 2020). While the risk of having a TBI is substantial among all age groups, this risk is highest among adolescents, young adults, and persons older than 75 years. Moreover, the risk of TBI among males is twice the risk among females, most likely due to the increased overall probability of injury in males (Tiret et al., 1990; Egea-Guerrero et al., 2013; Leitgeb et al., 2011).

TBI is a complex, heterogeneous injury. It is characterized as mild, moderate, or severe, based upon the Glasgow Coma Scale, which assigns scores from 3 to 15 (severe: 3-8; moderate: 9-12; mild: 13-15) based on clinical assessments, including eye opening (E), motor response (M), and verbal response (V) (Iankova, 2006; G. Teasdale & Jennett, 1976; Teasdale & Jennett, 1974). It is estimated that the majority of TBIs diagnosed are

mild, comprising approximately 70% of cases (Faul et al., 2010). Although total incidences of TBI are increasing, the associated death rate has decreased, highlighting that TBI patients are increasingly surviving the initial injury (**Figure. 1-1**). Symptoms of mild to moderate TBI include headaches, dizziness, nausea; these injuries usually resolve within days to weeks of the insult. However, moderate to severe TBI and even repeated mild TBI results in long-term effects such as aphasia, seizures, amnesia, impairments in motor and cognitive function, social behavior, sensation, development of mood disorders, alteration of sleep patterns, and changes in personality, and coma (in severe TBI); these can persist up to months and years after injury (Bruns & Hauser, 2003; Andriessen et al., 2010).

In addition, post-traumatic stress disorder has a high occurrence rate in TBI survivors (Risvall & Menon, 2011). Thus, more severe TBI results in poor prognosis, long-term disability, and long-lasting adverse effects on patient quality of life and overall life expectancy (Aungst et al., 2014; Dijkstra-Kersten et al., 2020; Dams-O'Connor et al., 2013; Faul & Coronado, 2015; Finkelstein et al., 2006). Reports estimate that 3.17 to 5 million people in the US (approximately 1-2% of the US population) live with a TBI-related disability (Selassie et al., 2008; Thurman et al., 1999; Zaloshnja et al., 2008). Furthermore, there is evidence that moderate to severe TBI, and repeat mild TBI, may be associated with increased risk of neurodegenerative diseases such as late-onset dementias (Mortimer et al., 1985; Salib and Hillier, 1997; Plassman et al., 2000), Alzheimer's Disease (AD) (Lye & Shores, 2000), and Parkinson's Disease (PD) (Hutson et al., 2011).

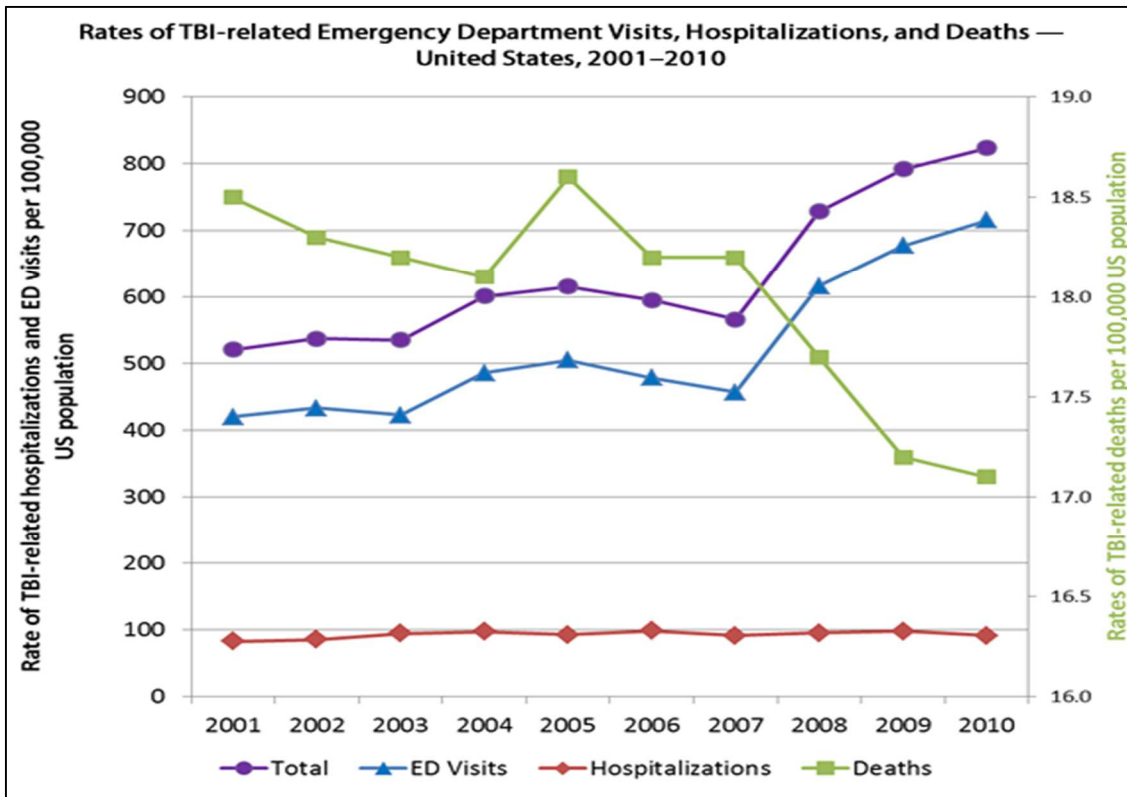


Fig 1-1. Report of TBI-related emergency department visits, hospitalizations, and deaths (EDHD) from 2001-2010. Between 2001 to 2010, the total number of TBI-related hospitalization increased by 54% (purple line), from approximately 521 visits per 100,000 US population in 2001 to approximately 824 visits per 100,000 US population in 2010, while the number of emergency department (ED) visits increased by 54% (blue line), from approximately 420 visits per 100,000 US population in 2001 to approximately 716 visits per 100,000 US population in 2010. On the other hand, the rate of TBI-related deaths decreased from 18.5 per 100,000 US population in 2001 to 17.1 per 100,000 US population, indicating that more people are likely to survive a TBI-related injury. (Centers for Disease Control and Prevention, National Center for Injury Prevention and Control).

TBI treatment is complicated by a lack of FDA-approved treatment interventions and failure of clinical trials (Loane & Faden, 2010; Gruenbaum et al., 2016). Current treatments majorly rely on alleviating the TBI-associated symptoms and improving patient quality of life rather than preventing TBI disease progression. Given the heavy socioeconomic burden of TBI on the US healthcare system, there is a pressing need to identify and develop effective therapeutic interventions for TBI patients.

1.1.2 Overall Pathophysiology

TBI pathophysiology is complex, and its time course and resulting neurological consequences vary significantly from individual to individual based on factors such as sex, age, overall health, injury severity, injury location, genetic predisposition, and the development of co-morbidities (Bennett et al., 2016; Chan et al., 2017; Gupte et al., 2019; Cortes et al., 2021). It includes both the mechanical damage resulting from the injury impact itself and the delayed molecular cascades that follow the injury. These phases, distinguished as primary and secondary injury, contribute to temporary or permanent neurological deficits after TBI (**Figure. 1-2**).

Primary injury, directly resulting from the primary external impact to the brain, occurs within seconds or minutes after the impact. It is characterized by the displacement of and mechanical damage to brain tissue, including contusion, vasculature damage, hemorrhages, increased blood-brain barrier (BBB) permeability, axonal shearing, and irreversible neuronal and glial cell death (Frati et al., 2017; Gyoneva & Ransohoff, 2015; Tehse et al., 2018; Tehse & Taghibiglou, 2019; Khaksari et al., 2018). Additionally, primary injury results in a disruption of metabolic processes, rapid accumulation of intercellular ions (Ca^+ , K^+ , Na^+), and excitotoxicity (Loane & Faden, 2010; Algattas & Huang, 2014).

The events of primary injury lead to the development of secondary brain injury, which can begin within minutes of the primary mechanical injury and persist for days, months, and years following the primary insult. It comprises molecular, biochemical, and inflammatory cascades that exacerbate secondary neuronal cell damage, death, and neuroinflammation, leading to neurological deficits (Loane et al., 2015). Secondary injury

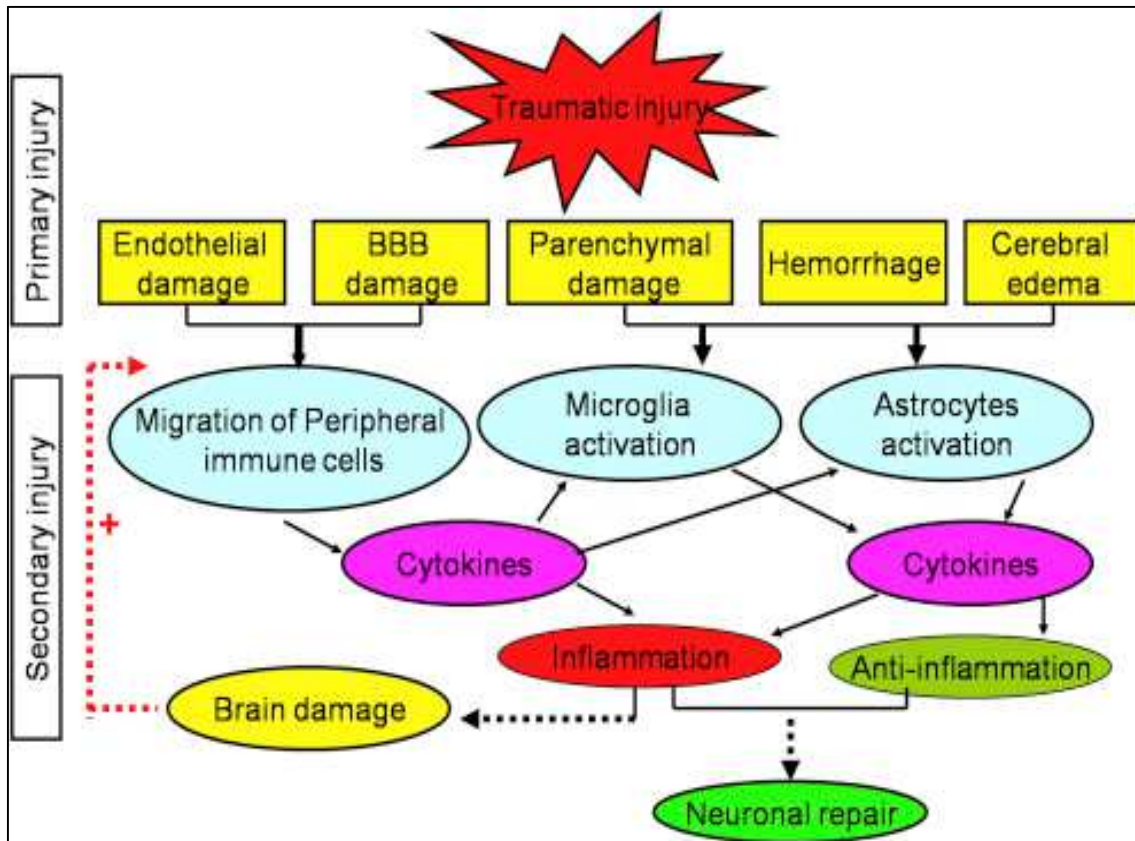


Figure. 1-2. Pathophysiological mechanisms of primary injury in TBI. Mechanisms involved in primary injury associated with TBI. Primary injury eventually results in the development of secondary injury. Secondary injury includes molecular pathways that aid in neuroinflammation, brain damage and neuronal repair (Adapted with permission from Hongjuan et al., 2018)

processes include the continued flux of intracellular ions (Ca^{2+} , Na^{+} , K^{+}) and the release of excitotoxic neurotransmitters such as glutamate. In addition, cytoplasmic and nuclear proteins and genetic material are released from cells into the microenvironment (Fрати et al., 2017; Tehse & Taghibiglou, 2019).

Damaged and dying cells release mediators and danger signals, such as damage-associated molecular patterns (DAMPs) (Roth et al., 2014; Yang et al., 2017; Liesz et al., 2015). Microglia, the intrinsic immune cells in the brain, are the first responders to these danger

signals. Disruption of the BBB causes infiltration of peripheral immune cells, including leukocytes (monocytes/macrophages, neutrophils, and lymphocytes), to the site of brain injury. Together, resident microglia and infiltrating cells secrete multiple inflammatory mediators (e.g., pro-inflammatory cytokines, anti-inflammatory cytokines and chemokines) that regulate robust interactions among the cells, resulting in neuroinflammation (role of microglia and peripheral cells, and overall neuroinflammation, covered in detail in Chapter 1.2).

Proliferating astrocytes, also activated in response to injury, form a glial scar surrounding the injury site and secrete trophic factors and immune mediators that promote tissue remodeling and neurogenesis. While in mild TBI, the secondary injury events generally subside within days or weeks, some can persist into the chronic phase (**Figure. 1-3**). The chronic phase of TBI also includes a restorative phase during which the brain remodels itself to counter tissue damage and death resulting from secondary injury (Schoch et al., 2012). This restoration phase includes repair mechanisms such as proliferation and differentiation of endogenous neural precursors and stimulation of neurite outgrowth and re-myelination. Depending on the severity of TBI, these restorative mechanisms may or may not be able to compensate for neuronal tissue loss and neuroinflammation in chronic TBI.

The evidence for chronic TBI progression is supported by clinical and experimental data. Clinical studies utilizing structural imaging has found progressive atrophy and demyelination in the brain of TBI patients one-year post-injury (J. H. Cole et al., 2018; Green et al., 2014), up to 18 years post-injury (Johnson et al., 2013). Similar findings have

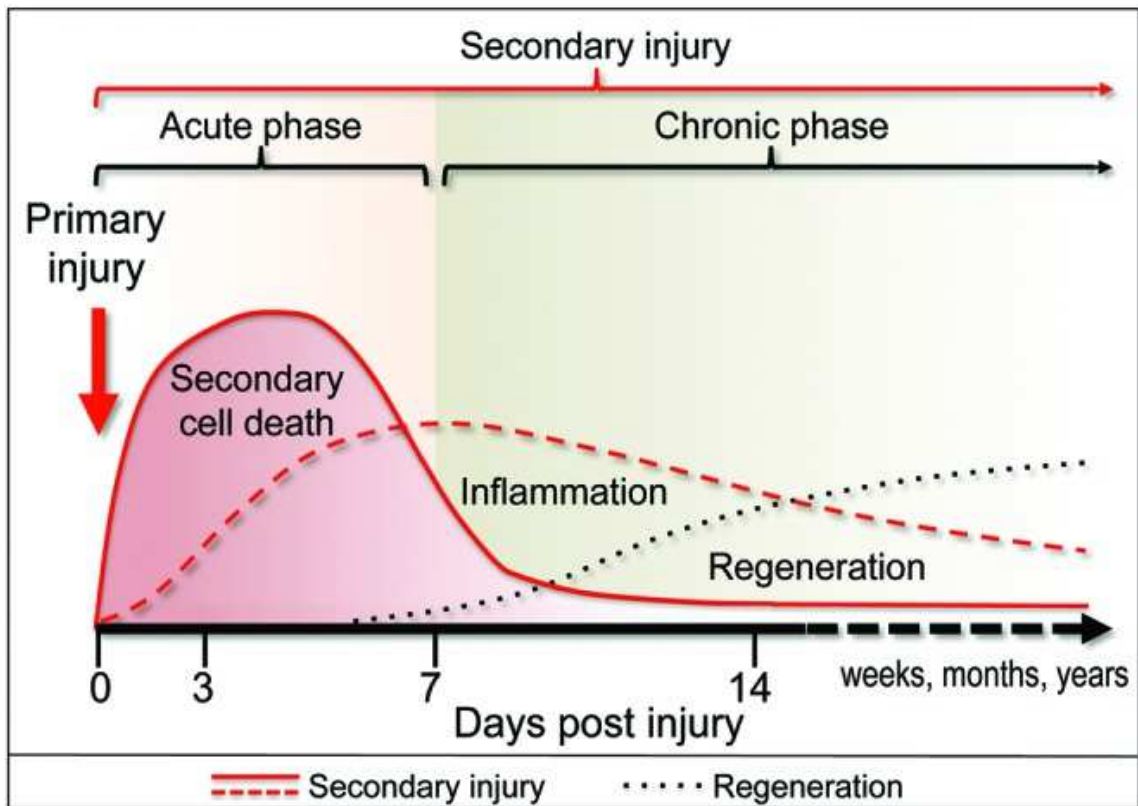


Figure. 1-3. General Timeline of TBI Pathophysiology. The initial mechanical impact (primary injury—red arrow) disrupts the structure of the brain and leads to complex secondary changes that collectively spread the damage to the intact neighboring tissue (secondary injury—red lines). The secondary injury includes secondary neuronal cell death as well as long-term inflammatory changes, which further tissue damage. Cell damage and death resulting from secondary injury are followed by a restorative phase (regeneration—black dotted line) during which the brain or the spinal cord remodels itself to compensate for the tissue damage. CNS, central nervous system. (Adapted with permission from *Lipinski et al, 2015*).

been found in experimental models of severe TBI, were the injured brain lesion doubles in volume one year from the time of initial injury (Loane et al., 2014). Mouse cortical neurons continue to die following TBI, and by one-year post-injury, the hippocampus contains half the number of neurons as an age-matched uninjured mouse (Loane et al., 2014). Moreover, there are emerging findings that TBI also contributes to acute and chronic dysfunction of numerous peripheral organ systems, including the adrenal glands,

bladder, bone, gastrointestinal tract, heart, lung, kidney, and spleen (Hanscom et al., 2021; Doran et al., 2020).

1.1.3 Neuroinflammation

Neuroinflammation is a major consequence of TBI and is primarily driven by infiltrating immune cells from peripheral circulation (during the acute phase of TBI), astrocytes, and resident brain microglia (during both acute and chronic phases on TBI) (**Figure. 1-4**). The delicate balance between production and release of pro- and anti-inflammatory cytokines drives neuroinflammation after TBI. While immune cells in the injured brain have mixed pro- and anti-inflammatory polarization in the acute phases following injury, the anti-inflammatory responses become dysfunctional over time, resulting in the development of pathological pro-inflammatory responses (Kumar et al., 2015).

1.1.3.1. Microglia

Microglia constitute the highly versatile resident immune cells in the brain, comprising 5% to 10% of the total glial cell population (Lawson et al., 1990). Microglia were first thought to be identical to macrophages, however later studies established that they have a distinctive lineage and molecular signature as compared with macrophages (Ginhoux et al., 2010; Hickman et al., 2013). Adult microglia are derived from distinct myeloid precursor that leave the yolk sac on E8.5–E9.0, enter the primitive blood stream, and journey to the CNS where they gain lineage specific gene expression and differentiate into mature microglia (Ginhoux et al., 2010). The identification of microglia-specific markers

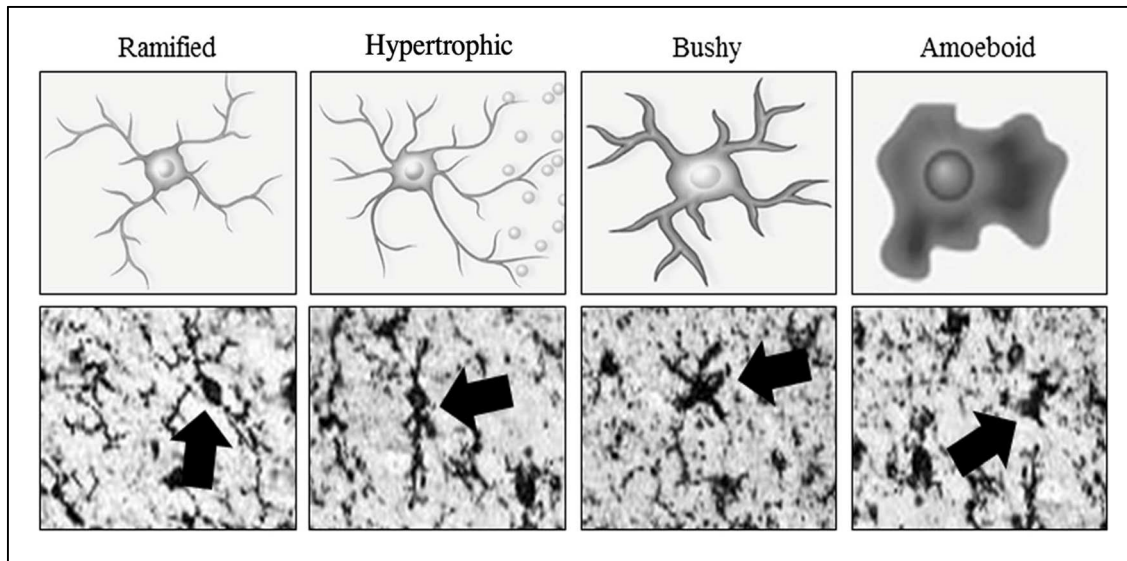


Figure. 1-4. Morphological changes of microglia. Above- representative schematics; Below- photomicrographs of human brain microglia (Iba-1 immunohistochemistry) depicting morphological stages of microglial activation. Ramified microglia are characterized by small bodies and long, branched processes. Mildly activated hypertrophic microglia are characterized by increased branching of processes as well as lengthening of processes. Bushy morphology is intermediate activation and is characterized by swollen, truncated processes, and enlarged cell bodies. Amoeboid microglia are characterized rounded macrophage-like morphology with no or few processes. (Adapted from *Crews et al., 2015*)

and the use of flow cytometry have made it possible for researchers to discriminate between microglia and macrophages in the injured brain (Tanaka et al., 2020).

Microglia have numerous functions in the brain, including synaptic pruning, CNS repair, mediating the immune responses against peripheral infection (Salter & Beggs, 2014). In a healthy CNS, microglia have a ramified morphology characterized by a small cell body and extended branches which allow microglia to survey the surrounding environment. The primary injury phase of TBI induces instantaneous neuronal and glial cell death that cells release DAMPs, which serve as ‘danger signals’ to other residents and infiltrating cells

via pattern recognition receptors (PPR). These damaged cells also secrete cytokines and chemokines that recruit more microglia and astrocytes at the site of injury (Gyoneva & Ransohoff, 2015; Loane & Byrnes, 2010; Nakamura et al., 2002; Woodcock & Morganti-Kossmann, 2013). Activated microglia then undergo gene expression changes and distinct morphological changes, including increased cell body size and decreased branching. The microglial morphology switches from their ramified shape (small cell body with long, branched projections) to hypertrophic, “bushy” (large cell body with swollen, truncated processes), or amoeboid morphologies (macrophage-like morphology with few or no processes) (**Figure. 1-4**). These highly activated microglia phagocytose cellular debris and produce various pro-inflammatory cytokines (TNF- α , IL-1 β , iNOS, IL-6, IL-8), anti-inflammatory cytokines (IL-10, IL-1ra), chemokines, and reactive oxygen species (ROS) at the site of injury. Phagocytosis and the release of neurotrophic factors and anti-inflammatory cytokines prevent further neuronal injury and are believed to restore tissue integrity in the injured brain. Microglia have a mixed pro- and anti-inflammatory polarization in the acute phases following injury; however, this transitions predominantly to a pro-inflammatory response over time that persists into the chronic phase of TBI (Kumar et al., 2015). Chronic activation of microglia results in the prolonged production of neurotoxic and pro-inflammatory cytokines and ROS (Loane et al., 2014; Izzy et al., 2019). This persisting microglial activation has been confirmed in autopsy results in TBI patients and football players who suffered repeated, mild TBI (Johnson et al., 2013; Coughlin et al., 2015; Coughlin et al., 2017; Bendlin et al., 2008). Furthermore, there is increasing evidence that chronic inflammation after TBI is associated with cognitive decline and can lead to the development of sleep disorders, neurodegenerative diseases,

and psychiatric diseases (Masel & DeWitt, 2010; Faden et al., 2016; Ramlackhansigh et al., 2011; Wilson et al., 2017; Kumar et al., 2016; Henry et al., 2019).

1.1.3.2 Peripheral Immune Cells

The blood-brain barrier (BBB) is a highly selective semipermeable membrane comprising endothelial cells, sealed by tight junction proteins that restrict solutes in the circulating blood from non-selectively crossing into the brain. However, during the primary phase of TBI, the mechanical impact to the brain results in the damage to the endothelial cells of the BBB, leading to loss of blood flow followed by disrupted tight junctional proteins and the basal membrane. This results in a loss of BBB integrity and subsequently elevated membrane permeability. BBB disruption is commonly observed in both mild TBI patients and experimental animal models (Sandsmark et al., 2019). In the injured brain, damaged neuronal tissue releases chemokines which recruit peripheral immune cells to the area of injury through the disrupted BBB (Cardona et al., 2003; Wilson et al., 2010). Preclinical studies have established a general time course of inflammatory response after TBI (Simon et al., 2017) (**Figure. 1-5**).

The first peripheral immune cells to infiltrate the CNS after trauma are neutrophils, bone-marrow-derived cells that function to phagocytose cellular debris and bacteria (Schloz et al., 2007). In response to TBI, these are the first immune cells to cross the BBB and enter the sites of injury, though this response is short-lived, with a peak at 24–48 hours after injury and a resolution in neutrophil numbers by seven days (Clark et al., 1994; Semple et al., 2010).

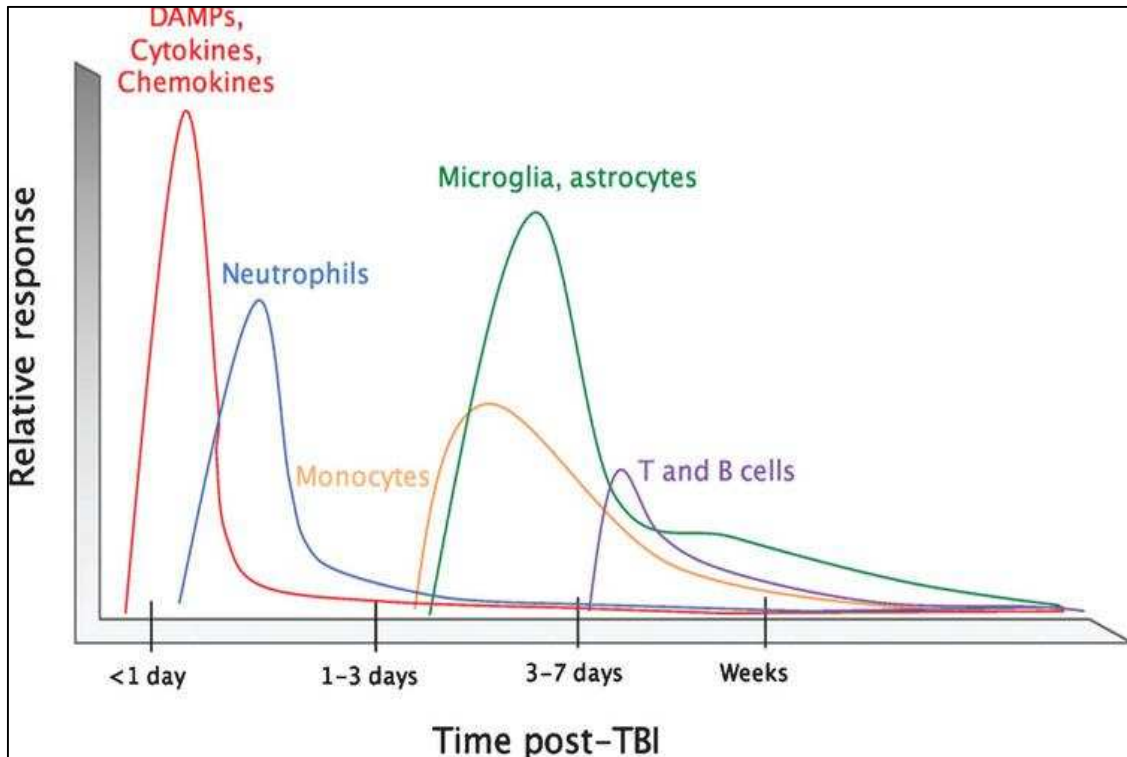


Figure. 1-5. Temporal Inflammatory response following TBI. The number of activated astrocytes and microglia increase and peak within 3-7 days post-TBI. The inflammatory response is mostly resolved by 10 days post-injury. Representation of the injury site at an acute (minutes/hours) time point post-TBI. The focal injury site is characterized by tissue damage due to the impact and the secretion of chemokine/cytokines by damaged cells (Adapted from *McKee & Lukens, 2016*).

Monocytes/macrophages are also bone marrow-derived and contribute to neuroprotection and recovery after CNS injury by phagocytosing cellular debris and preserving healthy tissue. They infiltrate the injured brain in the early days following TBI via the CC motif chemokine receptor 2, CCR2 (Gyoneva et al., 2015). Acutely after injury, infiltrating macrophages produce growth factors and neurotrophins, and anti-inflammatory cytokines such as interleukin IL-10 and transforming growth factor- β (TGF β). On the other hand, they also secrete pro-inflammatory cytokines (TNF- α , IL-1 β , iNOS, IL-6, IL-8), chemokines, and ROS (Makinde et al., 2017). While macrophages are thought to play a

beneficial role by clearing debris more efficiently than microglia, they may also negatively impact the latter following injury. For example, in a model of peripheral induced inflammation, mice injected with LPS showed enhanced microglial activation and increased levels of pro-inflammatory cytokines IL-1 β and TNF- α in the cortical brain as early as two days post-injection (Gyoneva et al., 2014). Anti-CCR2 neutralizing antibodies that prevent infiltration of peripheral macrophages into the brain following injury have been shown to better neurological outcomes and smaller brain lesion volumes in mice following TBI (Hsieh et al., 2014; Morganti et al., 2015).

Lymphocytes extravasate the brain following TBI, and peak infiltration occurs one week or later following injury (Bai et al., 2017a). These lymphocytes, most of which are T cells, are highly suggestive of a transition to an adaptive immune response following a TBI. However, studies in TBI and ischemic stroke models suggest that infiltrating T cells might also contribute to neurological impairment following injury (Daglas et al., 2019).

In recent years, there has been mounting evidence from both clinical and experimental models that implicate neuroinflammation and dysregulated immune responses in the exacerbation of neurological dysfunction after TBI. (Das et al., 2012; Giunta et al., 2012; Woodcock et al., 2013; Walsh et al., 2014; Corps et al., 2015; Gadani et al., 2015). Clinically, elevated cytokine production is one of the strongest prognostic indicators of poor clinical outcomes in TBI patients (Woiciechowsky et al., 2002; Arand et al., 2001; Chiaretti et al., 2005). Inhibition of IL-1 β receptor in experimental TBI preclinical models confers neuroprotection and improves functional recovery in mice (Jones et al., 2005; Sanderson et al., 1999). In addition, global deletion of TNF- α in mice results in

improvements in long-term neurological deficits after TBI (Scherbel et al., 1999; Sullivan et al., 1999). Finally, pharmacological depletion of microglia in mice following TBI results in the repopulation of ‘newer’ microglia with decreased pro-inflammatory phenotypes and improved long-term neurological outcomes (Henry et al., 2020, Witcher et al., 2020).

There are currently no FDA-approved therapeutics to effectively slow the TBI-related disease progression. Most phase II/III clinical trials have failed to show consistent outcomes for TBI patients. Hence current treatments primarily focus on rehabilitation and alleviation of TBI-associated symptoms. The prolonged secondary injury process in TBI pathophysiology provides a wide therapeutic window for clinical intervention. As TBI pathogenesis is complex, better understanding the molecular mechanisms underlying TBI-related secondary injury is necessary to develop effective therapeutics, particularly those targeting neuroprotection, after TBI.

1.2. Innate Immunity

1.2.1. Overview of Innate Immunity.

Innate immunity provides the first line of defense against invading pathogens and is defined by the body’s ability to rapidly respond to foreign antigens in a non-specific manner. The innate immune system includes anatomical barriers, such as the skin and mucus membranes, soluble immune proteins, and innate immune cells. In the periphery, this includes neutrophils, monocytes/macrophages, mast cells, natural killer (NK) cells,

and dendritic cells (DCs), and microglia in the brain. Within the brain, microglia can be activated during systemic infections (without the integrity of the BBB being compromised), brain injury, and chronic diseases. In general, immune cells respond to specific pathogen-derived molecular moieties (e.g., peptides, lipopeptides, carbohydrates, DNA, RNA, others), collectively known as pathogen-associated molecular patterns (PAMPs), or damage-associated molecular patterns (DAMPs), which are released from injured cells (Santoni et al., 2015). Numerous DAMPs are significantly released in the brain during conditions of trauma, including TBI (Sharma et al., 2016) (**Table 1-1**).

PAMPs and DAMPs are recognized by immune cells via germ-line-encoded pattern recognition receptors (PRRs), which include membrane-bound Toll-like receptors (TLRs), NOD-like receptors (NLR) and cytosolic DNA sensors (CDS), C-type lectin receptors (CLR), retinoic acid-inducible gene I (RIG-I)-like receptors (RLR). TLRs detect ligands from the extracellular and endosomal milieu, whereas NLRs, ALRs, and RIG-I-like receptors provide immune surveillance in the cytoplasm. Together, these receptors facilitate innate immune responses by activating key signaling pathways and producing essential cytokines and chemokines to mediate the immunological response. For this thesis, only TLR, NLR, and CDS will be discussed in detail.

Intracellular location	DAMPs	Receptors
Nucleus	Histones	TLR 2, 4, 9
	Genomic DNA	TLR 9
	HMGB 1	TLR 2, 4, RAGE, TIM3
	IL-1 α	IL-1R
	IL-33	ST2
Cytosol	ATP	P2Y2, P2X7
	F-actin	DNGR 1
	Cyclophilin A	CD147
	HSPs	CD91, TLR 2, 4, SREC 1, FEEL 1
	Uric acid crystals	NLRP3
Mitochondria	S100s	TLR 2, 4, RAGE
	Mitochondrial DNA	TLR 9
	Mitochondrial transcriptional factor A	RAGE, TLR 9
Endoplasmic reticulum	Calreticulin	CD91

Table 1-1. List of recognized DAMPs in injury. DAMPs are released by damaged or dying cells during conditions of trauma, including TBI. They are recognized by different pathogen recognition receptors (PPR) located on immune cells (Adapted from *Sharma et al., 2016*).

1.2.2. Toll-like Receptor (TLR) Signaling Pathway.

Toll-like receptors (TLRs) are a conserved transmembrane receptor family that can recognize the specific PAMPS and DAMPs released from damaged cells and recruit a set of adaptors leading to the activation of downstream kinases and nuclear factors which regulate the expression of inflammatory genes. They a variable number of LRR motifs, a transmembrane region, and a Toll/IL-1 receptor (TIR) domain. TLRs are classified into two subfamilies based on their localization: those expressed at the plasma membrane, encompassing TLR1, TLR2, TLR4, TLR5, TLR6, and TLR10, and the intracellular ones

expressed on endosomes, including TLR3, TLR7, TLR8, TLR9, TLR11, TLR12, and TLR13.

Each TLR interacts with a specific PAMP/DAMP through its extracellular leucine-rich-repeat (LRR) (**Figure 1-6**). Plasma membrane TLRs mainly recognize microbial membrane components such as lipids, lipoproteins, and proteins. For example, TLR4 recognizes bacterial lipopolysaccharide (LPS). TLR1, 2, and 6 recognize a wide variety of PAMPs including lipoproteins, peptidoglycans, and lipotechoic acids (Kawai & Akira, 2010), TLR5 recognizes bacterial flagellin (Akira et al., 2006). On the other hand, intracellular TLRs recognize nucleic acids derived from bacteria and viruses and recognize self-nucleic acids in disease conditions such as autoimmunity. For example, TLR3 recognizes viral double-stranded RNA (dsRNA), small interfering RNAs, and self-RNAs derived from damaged cells (Zhang et al., 2013; Takemura et al., 2014), and TLR7 recognizes single-stranded (ss)RNA from viruses and bacteria.

Upon ligand binding, TLRs dimerize and undergo conformation changes, which lead to the recruitment of TLR domain-containing adaptor proteins. To date, five adaptors with TLR domains have been identified: Myeloid differentiation primary-response protein 88 (MyD88), TIR domain-containing adaptor protein (TIRAP), TIR domain-containing adaptor protein inducing IFN- β (TRIF), TRIF-related adaptor molecule (TRAM), and Sterile α - and armadillo-motif-containing protein (SARM). TLR signaling is largely

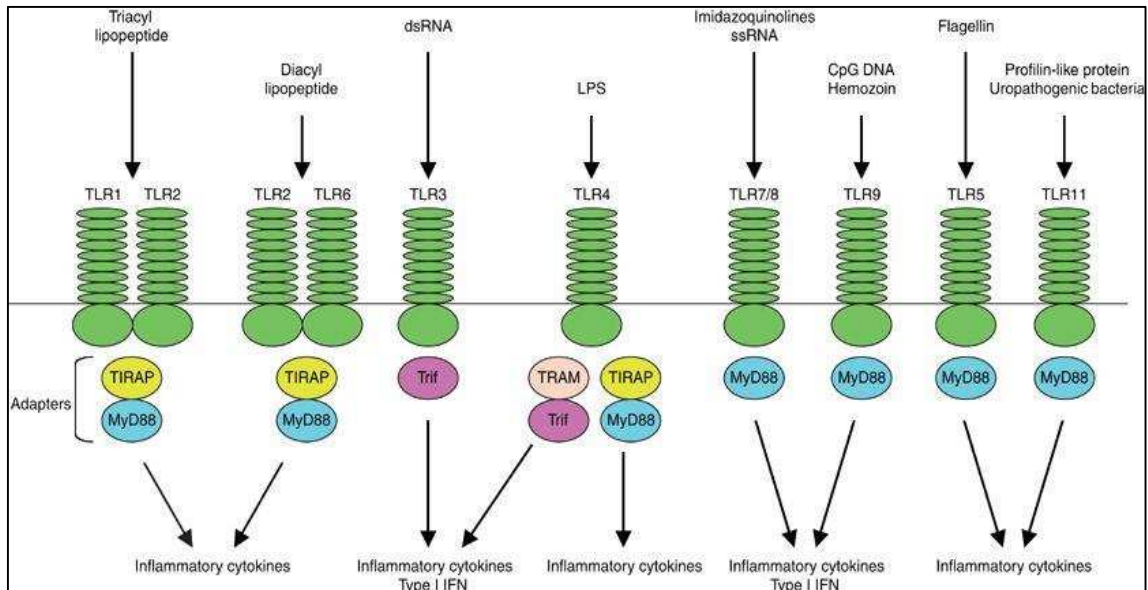


Figure 1-6. TLR Signaling Receptors. Surface TLR4, TLR2/1, TLR2/6, TLR5 recognize surface bacterial molecules like LPS, triacylated lipoproteins, diacylated lipoproteins, and flagellin, respectively. Endosomal TLRs such as TLR7, TLR8, and TLR9 respond to nucleic acids like dsRNA, ssRNA, and DNA. (Adapted from Kawai *et al*)

divided into two pathways: the MyD88-dependent and TRIF-dependent pathways. The differential utilization of distinct these two adaptor molecules by TLRs results in activation of different transcription factors that, in turn, induce different subsets of genes.

MyD88-dependent signaling: All TLRs, except TLR3, associate with MyD88. TIRAP, associated with the interior cell membrane, facilitates recruitment of cytosolic MyD88 to the TIR domain of the intracellular region of the TLR through TIR-TIR interactions. MyD88 then forms a signaling platform to which enzymatic proteins such as Interleukin-1 receptor associated kinase-4 (IRAK-4), IRAK-1, TANK-binding kinase 1 (TBK1), and others are recruited. This results in the formation of a large multimeric structure that initiates a signaling cascade and ultimately triggers NF- κ B activation and its nuclear translocation, leading to NF- κ B-mediated transcription.

TRIF-dependent signaling: TLR3 and TLR4 also can recruit TRIF as an adaptor. The TRIF pathway leads to the activation of Interferon Response Factor-3 (IRF-3), a transcription factor that mediates expression of a different subset of genes, including IFN- β and IFN- γ -inducible protein-10 (IP-10). In the case of TRIF signaling, IFN- β can, in turn, act back on the Type I IFN receptor in an autocrine or paracrine fashion to activate a second signaling pathway leading to the induction of hundreds of interferon response genes (IRGs).

TLR activation may be beneficial or detrimental to the cell. While the main function of TLRs is to mediate pro-inflammatory cytokine production as a protective response against pathogens in the CNS, they may be activated in the absence of microbial invaders. TLRs have been found to be upregulated in brains of patients with AD (Liu et al., 2005), PD (van Noort & Bsibsi, 2009; De Paola et al., 2012; Lee et al., 2015) and amyotrophic lateral sclerosis (ALS). While TLRs, particularly TLR2 and TLR4, are significantly upregulated following TBI, they are believed to play a more detrimental role in TBI pathophysiology. For example, the absence of TLR4 is shown to attenuate neuroinflammation and brain damage in mice after TBI (Ahmad et al, 2013; Hongsheng et al., 2018).

1.2.3. NOD-like Receptors (NLRs) and the Inflammasome Pathway

NOD-like receptors (NLRs) are cytoplasmic PRRs that respond to intracellular PAMPs, such as parts of the Type 3 Secretion System (T3SS), as well as DAMPs such as ATP and potassium (K⁺) (Davis et al., 2011). NLRs consist of three domains: nucleotide binding domain (NOD or NBD), Leucine-Rich Repeats (LRRs), and an N-terminal interaction

domain. The N-terminal interaction domain can consist of Caspase recruitment domain (CARD) or pyrin domain (PYD) (Davis et al., 2011).

Classical NLRs such as NOD1 and NOD2 result in NF- κ B signaling (Man et al., 2016). Other NLRs participate in the formation of the inflammasome- an apoptosis-associated speck-like protein that promote immune responses and the programmed cell death in response to PAMPs and DAMPs. The term ‘inflammasome’ was first coined in 2002 by Jurg Tschopp. In addition to NLRs, the inflammasome contains adaptor proteins (for example, ASCs [apoptosis-associated speck-like proteins containing CARDs (caspase recruitment domains)]), and effector proteins (for example, caspase-1), which undergo self-cleavage and conversion of inactive zymogen into their active forms. Four key inflammasomes, namely NLRP1, NLRP3, NLRC4, and AIM2, distinguished have been best characterized. They mainly differ from each other based on their composition and activating stimulus.

1. NLRP1 interacts with ASC and caspase-1 via an N-terminal PYD and binds caspase-5 to the complex via the C-terminal CARD. Muramyl dipeptide, Bacillus anthracis lethal toxin and Toxoplasma gondii induce the activation of the NLRP1 inflammasome.
2. NLRP3 interacts with ASC through an N-terminal PYD domain, which recruits caspase-1. NLRP3 is activated by the recognition of mtDNA and cardiolipin (**Figure 1-7**).
3. NLRC4 inflammasome is activated by the NAIP family, and it can recruit caspase-1 directly via its CARD in an ASC-independent manner. However, it remains unclear how ASC interacts with the NLRC4 inflammasome complex.

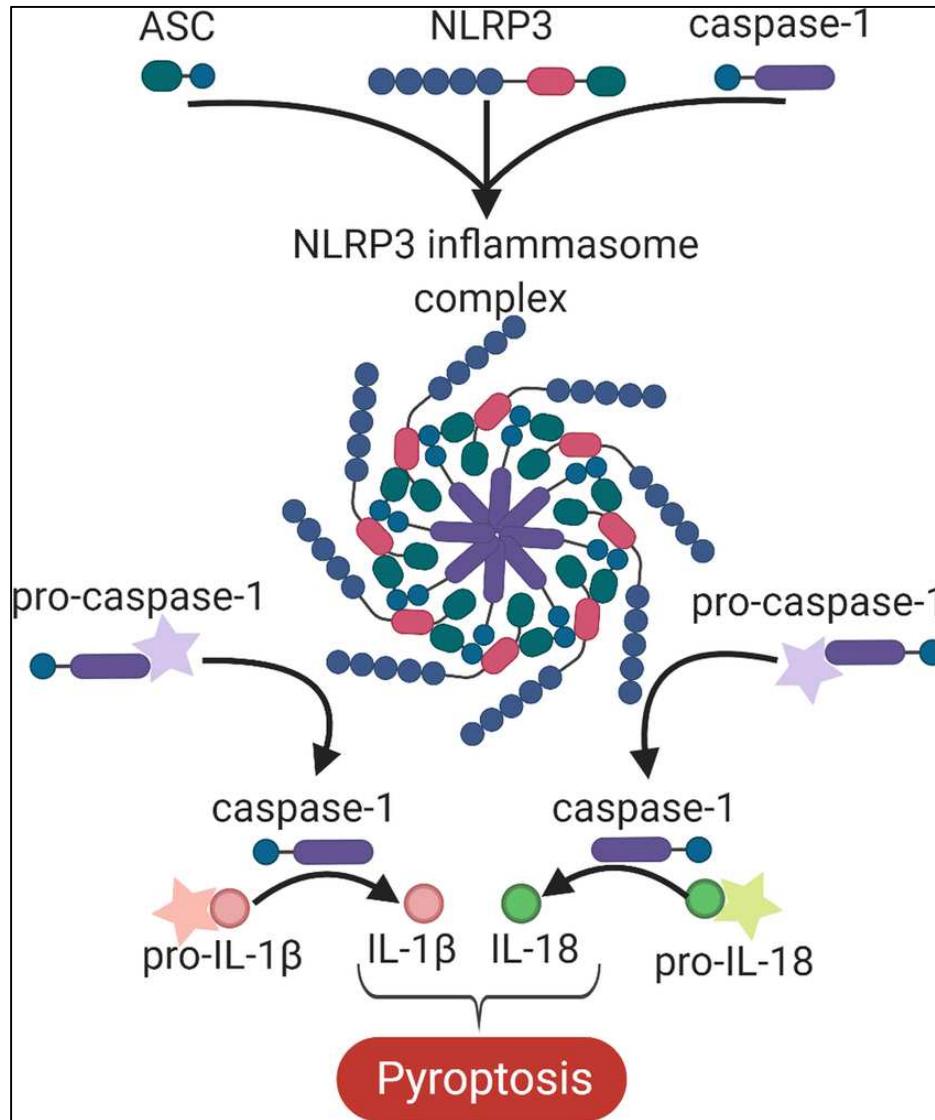


Figure. 1-7. Formation of the NLRP3 inflammasome. Activation of the NLRP3 inflammasome involves the constituent molecules of the NLRP3 inflammasome (i.e., NLRP3, ASC and caspase-1) binding to form a heptamer or octamer NLRP3 inflammasome complex. This inflammasome complex allows the cleavage of pro-caspase-1 into active caspase-1, which in turn cleaves pro-IL-1 β and pro-IL-18 to their active forms, IL-1 β and IL-18 respectively. The increase in these pro-inflammatory proteins leads to form of cell death called pyroptosis (Adapted from *O'Brien et al., 2020*)

4. AIM2 inflammasome recruits ASC and caspase-1 through its N-terminal PYD domain and is activated by direct binding with dsDNA via its HIN domain (Sutterwala et al., 2014).

Activation of these inflammasomes leads to the processing and secretion of inflammatory cytokines, including IL-1 β and IL-18, leading to an inflammatory form of cell death termed pyroptosis. In the context of CNS injury, the NLRP1 and NLRP3 inflammasomes are the most well-studied (Wallisch et al., 2017; Zendedel et al., 2017).

The functional regulation of an active NLRP3 inflammasome is a two-step process; a non-activating “priming” stimulus is firstly required to initiate expression of key inflammasome components, followed by a secondary “activating” stimulus that results in inflammasome oligomerization (Bauernfeind et al., 2009; Swanson et al., 2019). Inflammasome priming by inflammatory stimuli such as TLR4 agonists includes the transcriptional upregulation of NLRP3 and pro-IL-1 β , as well as post-translational modifications of NLRP3 that stabilize the inactive protein in a signal-component state. These molecules are inactive until a subsequent stimulus occurs. The subsequent activation from PAMPS or DAMPS induces the assembly of NLRP3 constituent proteins into the complete NLRP3 inflammasome. This process involves the oligomerization of NLRP3 proteins via homotypic interactions between two NLRP3 proteins, which recruit and bind ASC. The ASC domain of the partially assembled inflammasome then cleaves pro-caspase-1 into its active isomer, caspase-1, and subsequently binds caspase-1 to form a complete NLRP3 inflammasome. Seven NLRP3 inflammasome molecules are recruited and bound together to form a heptamer ring structure. This structure allows the self-cleavage and further activation of pro-caspase-1 proteins into caspase-1. Caspase-1 further

facilitates IL-1 β and IL-18 maturation via the cleavage of their inactive forms, pro-IL-1 β and pro-IL-18, into their active forms, IL-1 β and IL-18 respectively. (Martinon et al., 2002, Jha et al., 2010). The cell then secretes these pro-inflammatory cytokines to mediate the inflammatory response.

Under normal conditions, basal NLRP3 levels are low enough to avoid aberrant inflammasome assembly and activation. Under pathological conditions such as TBI, NLRP3 inflammasome is upregulated and is a major driver of neuroinflammation and neurobehavioral disturbances (O'Brien et al., 2020). This is supported by clinical data that reports higher CSF levels of NLRP3 in TBI patients and a positive correlation between peak NLRP3 levels of > 6.63 ng/mL in the CSF and poor outcome (Zendedel et al., 2017). The initial rise of NLRP3 may be due to necrotic cell death or traumatic lysis, whereas the late rise of NLRP3 may represent infection, cellular stress or other inflammasome activating triggers such as ion flux, mitochondrial dysfunction, ROS, and metabolic factors (Wallisch et al., 2017). Manipulation of the NLRP3 inflammasome pathways could have therapeutic efficacy in TBI. NLRP3 neutralization in mice after TBI reduces IL-1 β processing and attenuate injury-associated neuronal loss. (Simon et al., 2017). Moreover, the absence of the NLRP3 inflammasome contributes to improvement in functional recovery in mice following TBI (Irrera et al., 2017).

1.2.4. Cytosolic DNA Sensors (CDS) and the cGAS-STING Pathway.

Cytosolic DNA sensors (CDS) are DNA-binding proteins that can detect perturbations in DNA homeostasis of the cell and activate the intracellular signaling cascades of the innate

immune system as a response (Ablasser et al., 2019). One such CDS pathway is the cGAS-STING pathway, which when activated triggers a cascade that ultimately leads to the production of IFNs-I and other pro-inflammatory cytokines, allowing innate immune system to respond to injury (Nazmi et al., 2019; Peng et al., 2020; Li et al., 2020; Sun et al., 2013; Zhang et al., 2013)

When double stranded DNA (dsDNA) binds with cyclic GMP-AMP synthase (cGAS), the latter undergoes a conformational change to catalyze the formation of 2',3'-cyclic GMP-AMP (cGAMP), a cyclic dinucleotide (CDN) from ATP and GTP, containing the phosphodiester linkages of both 2'-5' and 3'-5'. cGAMP synthase activates the protein Stimulator of Interferon Genes (STING), which leads to its dimerization, re-localization, and prion-like aggregation. (Walko et al., 2014; Chin et al., 2019; Wang et al., 2019). This complex then associates with TANK binding kinase 1 (TBK1) and causes the recruitment of interferon regulatory factor 3 (IRF3). Then, IRF3 phosphorylates and translocates to the nucleus where the production of type I IFNs is induced. The NF- κ B signaling pathways can also be activated by STING (**Figure. 1-8**).

While exogenous DNA resulting from infection or efferocytosis primarily contribute to activation of the cGAS/STING-mediated pathway, 'self-DNA' leaked from the nucleus or mitochondria can also activate this pathway and trigger extensive inflammatory responses (Ma et al, 2020; Crow et al., 2006). This occurs because cGAS binds to the sugar-phosphate backbone of dsDNA, hence it is not dependent on a specific DNA sequence (Barnett et al., 2019). DNA. Chronic IFN-I production contributes the development of age-related

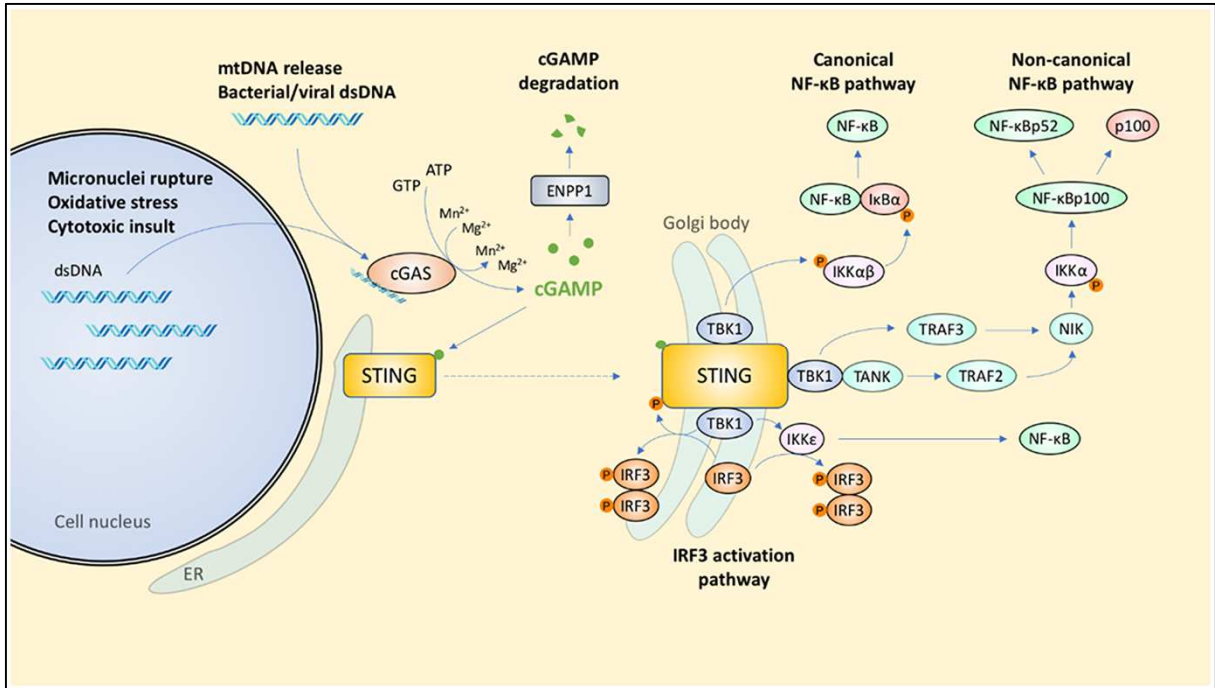


Figure. 1-8. Signal transduction coordinated by the cGAS-STING pathway. Innate immunity is triggered by exogenous or intrinsic dsDNA binds to cGAS. Upon activation, cGAS undergoes a conformational change and activates STING. This complex then associates with TANK binding kinase 1 (TBK1) and causes the activation of the IRF3 pathway as well as NF-κB signaling pathways (Adapted from *Hoong et al., 2020*)

neurodegenerative diseases (Talor et al., 2014; Deczkowska et al., 2017). There increased expression of IFN-I and IFN-related genes is observed in brain tissues across several mouse models of AD. Furthermore, disruption of the cGAS/STING signaling pathways enhances susceptibility to bacterial and viral infection (Zhang et al., 2014; Tan et al., 2020; Cheng et al., 2018) and its chronic and dysregulated activation may be detrimental (Goldman et al., 2015).

Activation of the cGAS/STING pathway and the induction of Type-I IFN/ IFN-I responses occur in response to TBI (Barrett et al., 2020). IFN-β deficiency has been found to reduce neuroinflammatory response and improve long-term motor and cognitive

function recovery in mice after TBI (Barrett et al., 2020). IFN-I have been also implicated in the progression of age- related neuroinflammation and cognitive decline after TBI (Baruch et al., 2013; Deczkowska et al., 2017). Inhibition of IFN-I signaling has been found to reduce pro-inflammatory cytokine expression in the aged brain, increase the expression of brain-derived neurotrophic factor (BDNF) and insulin-like growth factor 1 (IGF-1), reduce neurodegeneration and improve long-term motor and cognitive function recovery (Karve, et al., 2016; Barrett et al., 2020; Baruch et al., 2014).

1.3 AUTOPHAGY

1.3.1 Overview of Autophagy

Autophagy is a vital intracellular degradation pathway that delivers cytoplasmic constituents to the lysosomes for degradation. The term is derived from ancient Greek *autos*, 'self' and *phago*, 'to eat' — literally meaning 'self-eating', and was first described by Christian de Duve during his seminal work on the discovery of lysosomes (De Duve et al., 1955; Klionsky, 2007). Autophagy can occur in bulk as a response to starvation, whereby portions of the cytoplasm are digested to meet the heightened biogenesis and energy needs of the cell (Rabinowitz & White, 2010; Galluzzi et al., 2014). It plays important roles in homeostasis, acting as a quality and quantity control process by removing protein aggregates (Rubinsztein et al., 2012; Birgisdottir et al., 2013) and defunct or surplus organelles (Maejima et al., 2013; Randow & Youle, 2014), as well as invading microbes and endogenous and exogenous inflammatory agonists (Deretic et al., 2015).

Three types of general autophagy have been identified: chaperone-mediated autophagy (CMA); microautophagy; and macroautophagy. These differ from one another in how the substrates are identified and processed (Klionsky, 2005; Yang & Klionsky, 2010). Macroautophagy, referred to as autophagy from here, is the most common form of autophagy in the cell (Gatica et al., 2018). It involves the sequestration of cytoplasm into a double-membrane cytosolic vesicle referred to as an autophagosome, that subsequently fuses with a late endosome or lysosome to form an autophagolysosome (or autolysosome). Inside the autophagolysosome, the lysosomal hydrolases degrade the sequestered material, which then becomes available to the cell for recycling (**Figure. 1-9**).

Autophagy-related proteins (ATG proteins), the essential components of autophagosome formation were identified by means of yeast genetic screening in the 1990s. There are currently 38 ATG proteins identified in yeast. Of these, the core ATG proteins that are essential for the autophagy process are phylogenetically highly conserved (Longatti & Tooze, 2009; Suzuki & Ohsumi, 2007; Xie & Klionsky, 2007). The mammalian orthologs include ULK1 (mammalian ATG1), ATG3, ATG4s, ATG5, BECLIN1 (mammalian ATG6), ATG7, LC3A/B (mammalian ATG8), ATG9A, ATG10, ATG12, ATG13, ATG14, ATG16L1, FIP200 (mammalian ATG17), and WIPIs (mammalian ATG18), have been identified. The core ATG proteins are classified into several functional units, such as the ULK1/FIP200 protein kinase complex; the class III phosphoinositide 3-kinase complex; and the ATG7-mediated, ubiquitin-like conjugation system. These units induce the events responsible for isolation membrane formation and subsequent autophagosome formation.

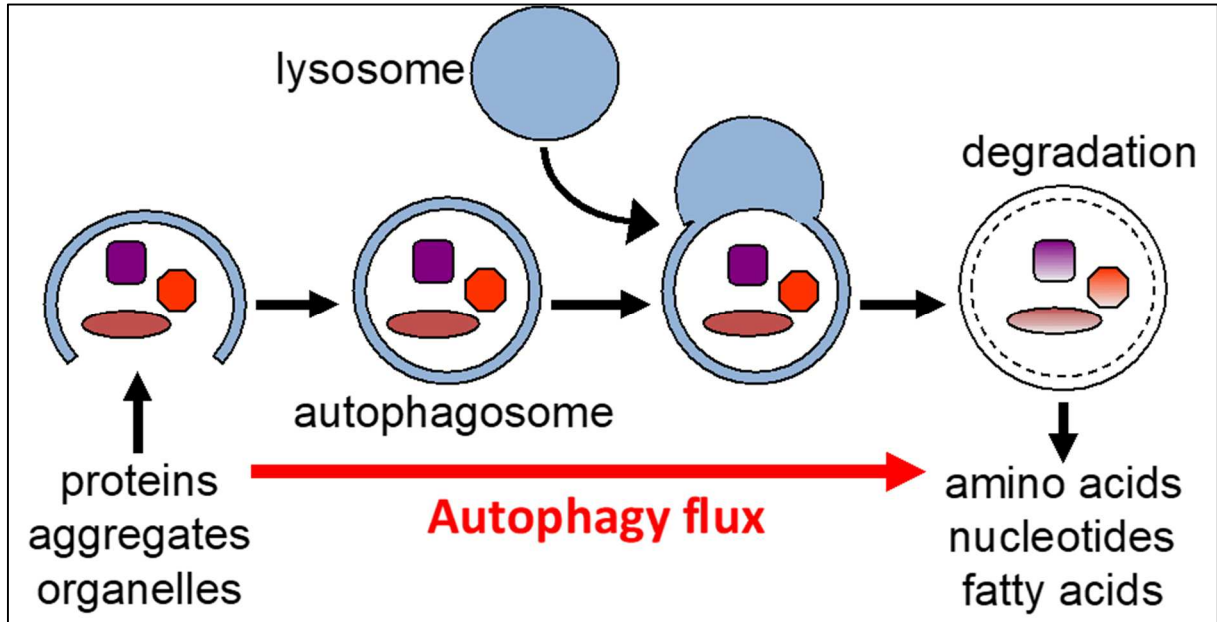


Figure 1-9. Schematic diagram of the steps of autophagy. Autophagy begins with the formation of the phagophore or isolation membrane. Phagophore elongation leads to the formation of an autophagosome, which can engulf cytoplasmic contents. When the outer membrane of the autophagosome with a lysosome it forms an autophagolysosome. This results in the sequestered material being degraded inside the autophagolysosome (vesicle breakdown and degradation). (Adapted with permission from *Lipinski et al., 2015*)

Basal levels of autophagy are important for homeostasis and in all cells. Mice lacking crucial autophagy gene such as *Atg3*, *Atg5*, *Atg7*, or *Atg6L1* have been observed to die shortly after birth due to poor nutrition and energy depletion, while mice lacking *Beclin1*, *Ambra1* and *Fip200* show early embryonic lethality (Cecconi & Levine, 2008; Mizushima & Levine, 2010). Autophagy is especially crucial in terminally differentiated cells such as neurons and oligodendrocytes; mice with neural tissue specific knockout of the essential autophagy genes *Atg5* and *Atg7* develop severe neurodegeneration, leading to abnormal motor function and reflexes (Komatsu et al., 2006). Due to this, researchers generally use tissue-specific knockout mice to study the role of autophagy in diseases.

1.3.2 Autophagy Pathway (in detail)

Autophagy is negatively regulated by the nutrient-sensing mammalian target of rapamycin (mTOR) kinase, a master regulator of cellular growth and metabolism. Under nutrient-rich conditions, mTOR inhibits autophagy by directly phosphorylating and inactivating Unc-51-like kinase 1 (ULK1) and Atg13 (Ganley et al., 2009). Phosphorylation of ULK1 by mTOR at this site prevents ULK1 from interacting with a second master regulator of metabolism, the energy-sensing AMP-activated protein kinase (AMPK) (Kim et al., 2011). AMPK induces autophagy by alleviating the negative regulation by mTOR through the phosphorylation and activation of TSC2 (Inoki et al., 2003), an upstream negative regulator of mTOR, and via direct phosphorylation of Raptor (Gwinn et al., 2008), a subunit of the mTOR complex. Additionally, AMPK induces the formation of the ULK1 complex through direct phosphorylation of ULK1 at Ser 317 and Ser 777, which result in blocking mTOR and the activation of ULK1 kinase activity (Kim et al., 2011; Joungmok et al., 2011).

Following activation, ULK1 phosphorylates several downstream targets to initiate the autophagic process (Hosokawa et al., 2009; Ganley et al., 2009). Formation of the ULK1 multi-protein complex requires ULK1-mediated phosphorylation of ATG13 and the scaffold protein family-interacting protein of 200 kD (FIP200), thus resulting in the assembly of the ULK1-ATG13-FIP200-ATG101 complex (Jung et al., 2009; Zachari and Ganley, 2017). The ULK1 complex localizes to sites of autophagosome initiation. This step is responsible for the activation of a second essential autophagy effector protein complex, the phosphatidylinositol 3-kinase (PI3K) complex. The PI3K complex is made up of the proteins VPS34, VPS15, Beclin 1, ATG14L, and AMBRA1. VPS34, a class III

PI3K, is responsible for producing the phosphatidylinositol 3-phosphate (PtdIns(3)P) that is required for autophagosome nucleation (Simonsen and Tooze, 2009).

Elongation of the autophagosome membrane is dependent on two ubiquitin-like conjugation steps (reviewed in Geng and Klionsky, 2008). The first involves the conjugation of the ubiquitin-like protein ATG12 to ATG5, which is catalyzed by ATG7 and ATG10. The ATG12-ATG5 conjugate forms a multi-protein complex with ATG16L1 and functions as an E3-like ligase (Kuma et al., 2002). The second conjugation step is mediated by ATG7 and ATG3, which together with the ATG5-ATG12:ATG16L1 complex are responsible for conjugating phosphatidyl-ethanolamine lipid to microtubule-associated protein 1 light chain 3 beta (MAP1LC3B, also known as LC3B), which has been proteolytically cleaved by ATG4 (LC3-I). Lipidated LC3B, further referred to as LC3-II, is incorporated into the both the inner and outer membrane of the autophagosome membrane during elongation (Kabeya et al., 2000; Mann et al., 1994). It plays a role in cargo degradation by interacting with the autophagy adaptor proteins (Schaaf et al., 2016) and also signals for the phagophore to seal itself off to become an autophagosome (Saha et al., 2018). When the autophagosome is completely closed, LC3-II on the outer membrane is removed by ATG4 and is recycled. LC3-II present on the inner membrane remains in the autophagosome and is eventually degraded together with its cargo (Kirisako et al., 2000; Maruyama and Noda, 2017). However, the LC3-II incorporated into the outer membrane of the autophagosome is unaffected and can be used as a marker to measure autophagosomes.

Autophagy adaptor proteins, also known as autophagy cargo receptors, are responsible for helping to recognize autophagy cargo by only binding substrates destined for autophagic degradation (Parzych & Klionsky, 2014). These include the proteins sequestosome-1 (SQSTM1 or p62), next to BRCA1 gene 1 (NBR1), and optineurin (OPTN) (Johansen & Lamark, 2011; Wild et al., 2011; Yan et al., 2013). NBR1 relies on ubiquitin to distinguish the cargo to be degraded via autophagy (Dupont et al., 2010). p62 also relies on ubiquitin tagging to recognize the targets that should be degraded (Dupont et al., 2010; Gomez-Diaz & Ikeda, 2018). Once p62 recognizes the substrates through their ubiquitin tag, it aggregates the substrates together and recruits the phagophore (Johansen & Lamark, 2011). Mature autophagosomes carrying cytoplasmic cargo are ultimately trafficked to lysosomes, resulting in the formation of the autophagolysosome, where the contents are degraded by lysosomal acidic hydrolases and are exported back to the cytoplasm to be reused for metabolic processes.

1.3.3 Autophagy Flux

The most used method to measure autophagy is by measuring the relative levels of the autophagic membrane-specific protein, LC3-II, using western blotting or fluorescence microscopy. However, sole measurements of LC3-II can lead to misinterpreted results as an increase in LC3-II levels could represent an increase in autophagy due to an increase in autophagosome formation or a decrease in functional autophagy due to blockage of downstream steps in autophagy, such as autophagosome fusion with lysosomes (resulting in a buildup of un-degraded autophagosomes and thus LC3).

Autophagy flux is a more accurate way of measuring autophagy function. The term ‘autophagic flux’ refers to the progress of cargo from the formation of the autophagosome through cargo degradation (Loos et al., 2014). When autophagy occurs, LC3-II localized to the inner autophagosomal membrane is degraded by autolysosome; thus, lysosomal degradation of LC3-II reflects the progression of autophagic flux. Flux assays compare the levels of LC3-II in the presence of lysosomal inhibitors, such as bafilomycin A1 (BafA) or in levels of autophagy cargo adaptors, such as NBR1, OPTN1, and p62. When autophagy occurs, LC3- II levels increase, and autophagy adaptor protein levels decrease. However,

when autophagy is blocked, both LC3-II and the adaptor protein levels will increase due to reduced autophagosome degradation (Yoshii & Mizushima, 2017) (**Figure. 1-10**), chloroquine, and provides a way to distinguish between increase autophagosome formation and reduced degradation. Another method to measure autophagy flux is to examine changes

Autophagic activity has been shown to decrease with age and this progressive reduction may contribute to accumulation of protein aggregates in the aging brain (Tan et al., 2014; Diskin et al, 2005). Age-related neurodegenerative diseases such as PD, AD and Huntington’s Disease (HD) are associated with autophagy defects that contribute to the accumulation of ubiquitin-positive protein aggregates and to neuronal cell dysfunction and death (Schmidt et al., 2021). In lysosomal storage diseases, defects in autophagy are secondary to deficiencies in specific lysosomal hydrolases and consequent impairment of

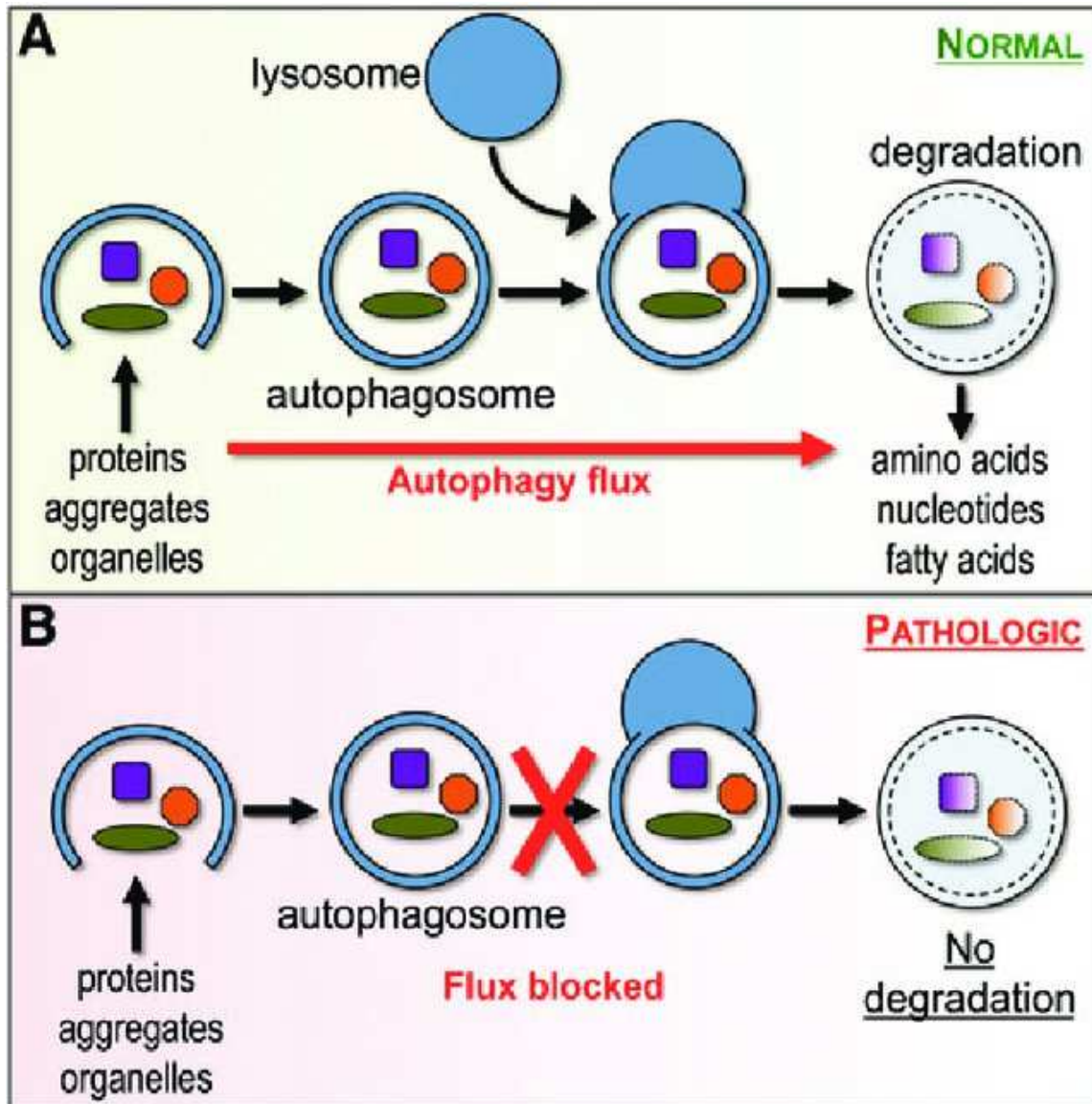


Figure. 1-10. Autophagy flux under normal and pathological conditions. (A) During homeostatic autophagy, autophagy flux processes normally- autophagosomes sequester cytoplasmic components, including damaged organelles and toxic protein aggregates, and then fuse with lysosomes to allow degradation of cargo by lysosomal proteases. (B) Under pathological conditions, autophagy flux may be blocked, for example due to lysosomal defects, resulting in accumulation of dysfunctional autophagosomes (Adapted with permission from *Lipinski et al., 2015*).

the lysosomal function (Lieberman et al., 2012). Increasing efficiency of autophagic flux has been shown to improve outcomes in animal models of neurodegenerative diseases,

making the manipulation of this pathway as a promising therapeutic approach, particularly in the early stages of these disease (Spilman et al., 2010; Majumder et al., 2011; Zhu et al., 2013; Jiang et al., 2014).

1.3.4. Role of Autophagy in TBI

Increased levels of autophagy markers, including LC3-II, beclin1, p62, and autophagosomes, have been reported in human TBI autopsy samples and cerebrospinal fluid (Chen et al., 2014; Sakai et al., 2014; Au et al., 2017). Many reports, including those referencing human samples note that markers of autophagy remain elevated for weeks to months after injury. In one study elevated levels of p62 were found in the majority of samples, with accumulation being the most pronounced in those with shortest survival times, implying more severe TBI (Sakai et al., 2014). Studies in mice indicate that impaired autophagy flux is associated with severity of trauma (Zeng et al., 2018).

Autophagy offers both beneficial and damaging roles after TBI. Autophagy upregulation in immune cells at the site of injury can provide ways for the removal damaged cells and harmful debris. Other hand, autophagosome accumulation due to decreased autophagic flux after TBI can play a detrimental role. Inhibited autophagy flux has been described in several pre-clinical models of TBI. After TBI in transgenic *GFP-Lc3* mice, inhibition of autophagy flux includes accumulation of autophagosomes and increased levels of p62 at the site of injury (Sarkar et al., 2014). Unchanged transcription levels of LC3 and p62 levels indicate autophagy flux is inhibited through decreased autophagosome degradation. Ex vivo LC3-II flux experiments using chloroquine in brain slices from control and

injured animals also confirm decrease in autophagy flux after TBI; increased LC3-II levels are observed in control but not injured mice (Sarkar et al., 2014).

Inhibition of autophagy flux is cell-type specific in the injured brain cortex after TBI; it occurs within neurons at early time points (1 day post-TBI) and within activated microglia and oligodendrocytes at later time points (3 days post-TBI and 7 days post-TBI, respectively). In neurons, this autophagy impairment is primarily driven by increased lysosomal membrane permeability, mediated through phospholipase A2, group IVA cytosolic, calcium-dependent (PLA2G4A/cPLA2), which prevents the fusion of the autophagosome with the lysosome (Sarkar et al., 2019). After TBI, neurons with impaired autophagy express markers for both apoptotic and non-apoptotic neuronal cell death. Several studies indicate that markers of inhibited autophagy flux after CNS injury correlate with the exacerbation of ER stress, implying a role for inhibited autophagy in the induction of ER stress-mediated neuronal cell death after neurotrauma (Liu et al., 2018; Sarkar et al., 2014). Similarly, autophagy flux impairment in neurons also increases necroptosis (a programmed form of necrosis, or inflammatory cell death, mediated by the RIPK1/RIPK3 complex) after SCI (Liu et al., 2018).

Much less is known about the role of autophagy in other brain cell types after TBI. Regarding oligodendrocytes, it is known that autophagy is necessary to support oligodendrocyte precursor survival and myelin development. In spinal cord injury (SCI), another form of CNS injury, oligodendrocyte-specific loss of *Atg5* in mice exacerbates the inhibition of the autophagic flux in oligodendrocytes and correlates with worse functional recovery, and greater myelin loss, which suggest that a similar outcome could

manifest after TBI. Inhibition of autophagy is also observed in activated microglia and/or infiltrating myeloid cell after TBI, however its function in these cells is not known. Additionally, the mechanisms leading to autophagy impairment in either oligodendrocytes or microglia/macrophages, after TBI is currently unclear and warrants further research.

As inhibition of autophagy is believed to play a detrimental role after TBI, upregulation of this pathway, particularly through restoration of autophagy flux, is being investigated as therapeutic approach after TBI. Rapamycin (which inhibits mTOR) and other pro-autophagy drugs (such as luteolin, ucoxanthin, tetrahydrocurcumin and melatonin) have been found successfully attenuate TBI-induced secondary brain injury and reduce inflammation after TBI. (Erlich et al., 2007; Xu et al., 2014; Ding et al., 2015; Lin et al., 2016; Gao et al., 2017; Bao et al., 2015; Zhang et al., 2017; Hegdekar et al., 2021). By inhibiting mTOR, rapamycin promotes autophagosome biogenesis and lysosomal biogenesis in the injured brain after TBI, thereby restoring autophagy flux and promoting neuroprotection. The neuroprotective role of rapamycin is directly dependent on its ability to induce autophagy; autophagy hypomorph *Beclin*^{+/-} mice are insensitive to the effects of rapamycin on neuronal cell survival and neuroprotection (Viscomi et al., 2012).

1.3.5. Role of Autophagy in Innate Immunity and Inflammation

Immunological processes are vital in eliminating damaged cells during injury or infection and initiate tissue repair. Emerging studies suggest that these processes are highly dependent on cellular autophagy for intracellular pathogen recognition and destruction, antigen presentation, lymphocyte development and effector function, and inflammatory regulation (**Table 1-2**).

Epidemiological data and experimental models demonstrate that defects in autophagy are associated with exacerbated inflammation in several autoimmune diseases. Autophagy is considered a core pathogenic contributor to the abnormal innate immunity in systemic lupus erythematosus (SLE) (Harley et al., 2008; Han et al., 2009). Insufficient autophagy due to the potential involvement of autophagic genes, such as ATG5, results in impaired LAP, increased autoantigen presentation, and excessive type I IFN production. Genome-wide association studies have linked nucleotide polymorphisms in autophagy-related genes such as ATG5 and ATG7 to susceptibility for SLE (Harley et al., 2008; Han et al., 2009; Zhou et al., 2012).

Similarly, in Crohn's disease, SNPs in the autophagic gene ATG16L1 are suspected of causing an autophagy defect that leads to failed inhibition of inflammasome activation, increased cytokine production and chronic gut inflammation. Impaired autophagy has

Pathway	Role of Autophagy
Thymic selection	Elimination of autoreactive T cells in the thymus; involved in both negative and positive selection
Programmed cell death	Mediates growth-factor withdrawal induced cell death; anti-apoptosis in CD4 T cell upon TCR stimulation
Lymphocyte homeostasis	Survival signaling and homeostasis of T and B cells
T cell activation	Autophagy-dependent T cell expansion upon TCR stimulation; altered IL-2 and IFN- γ production in helper T cells
Apoptotic corpse clearance	Removal of apoptotic bodies and damaged organelles
Oxidative stress	Clearance of dysfunctional mitochondria; increases ROS production and modulates Ca ²⁺ signaling
Antigen processing and presentation	Cross-presentation in dendritic cells; response to pathogen associated molecular patterns
Pathogen degradation	Xenophagy and phagolysosomal maturation
Cytokines production	Biogenesis and secretion of proinflammatory cytokines (IL-1 β , IL-18), adipocytokines, type I IFN, TNF, IL-7R α chain, etc
Inflammasome activation	Limits inflammasome activity
Antimicrobial peptides	Mediates CD40-induced antimicrobial activity in macrophages

Table 1-2. Role of autophagy in immunologic responses. Immune cells rely on autophagy for intracellular pathogen recognition and destruction, antigen presentation, lymphocyte development and effector function, and inflammatory regulation

been also linked to adaptive immunity in multiple sclerosis (MS) and experimental autoimmune encephalomyelitis (EAE). Intensified autophagy through high ATG5 levels supports the survival of autoreactive T cells and results in CNS inflammation (Alirezaei et al., 2009).

Autophagy can affect the immune responses through several mechanisms. In general, high levels of autophagy flux are associated with anti-inflammatory properties and the inhibition of flux, with pro-inflammatory phenotypes. For example, autophagy can modulate inflammatory polarization through its influence on NF- κ B activity by directly targeting the RELA/p65 protein and by affecting the availability of the p62 protein, which is needed for NF- κ B activation (Duran et al., 2008; Lee et al., 2011; Chang et al., 2013). NF- κ B can also restrict its own inflammation-promoting activity in macrophages by promoting p62-mediated removal of damaged mitochondria (Zhong et al., 2016). Conversely, a pro-inflammatory environment may also regulate levels of autophagy, as in primary cultured mouse microglia, where increased IL-1 β induced the accumulation of many acidic vesicles loaded with autophagic markers (p62 and LC3). Autophagy can also affect the secretion of cytokines. Loss of autophagy in macrophages or dendritic cells, either through knock down of *Atg7*, *Atg16L1* or *Beclin1* or treatment with autophagy inhibitor 3-MA (that targets Type III PI3K), stimulates the processing and secretion of IL-1 β in response to TLR agonists, independent of inflammasome activation (Crisan et al., 2011). Conversely, induction of autophagy with rapamycin inhibits the secretion of IL-1 β in murine dendritic cells in response to LPS with ATP or alum.

The role of autophagy in the innate immunity has also been studied in context of its role in removal of pathogens and apoptotic cells, which is important for immune response and resolution of inflammation. Autophagy aids in the removal of intracellular microbial pathogens and apoptotic cells by two major processes. One is called xenophagy, which eliminates pathogens (mainly bacteria and parasites) by engulfing them in double-membrane autophagosomes and is activated during infection by TLRs. The other way is mediated by a non-canonical autophagy pathway called LC3- associated phagocytosis (LAP). Pathogens and dying/apoptotic cells trigger LAP via surface markers (TLR1/2, TLR2/6, TLR4, TIM4) resulting in the recruitment of a subset of the ATG proteins (including ATG5, ATG7 and Class III PI3K complex) to conjugate LC3 to the cytoplasmic surface of the single-membrane phagosome called the LAPosome. This is followed by rapid LAPosome maturation and lysosomal degradation of the engulfed pathogens, cellular debris and DAMPs. It is important to point out that LAP is autophagosome-independent and proceeds independently of the pre-initiation ULK1 complex, which is required in canonical autophagy. Consequences of LAP deficiency include decreased capacity to clear dying cells and the establishment of a lupus-like autoimmune disease in mice (Heckmann et al., 2017).

As part of its role in regulation of innate immunity, autophagy plays a crucial role in the removal of intracellular DAMPS and damaged mitochondria that can activate pro-inflammatory pathways after TBI. It can downregulate the activation of NLRP3 inflammasomes to reduce inflammation. It does this directly by either digesting the interleukin precursors (e.g., pro-IL-1B) produced by inflammasomes or recycling of the inflammasome components, such as NLRP3 or ASC (Harris et al., 2017) with the help of

the autophagy adaptor protein p62 (Shi et al., 2012). Loss of autophagy has been shown to result in the accumulation of ROS-producing mitochondria and subsequently enhanced activation of NLRP3 inflammasome in response to NLRP3 agonist ATP, monosodium urate crystals, palmitic acid or influenza A virus (Zhou et al., 201; Nakahira et al., 2011; Wen et al., 2011; Lupfer et al., 2013). Interestingly, the induction of NLRP3-containing inflammasomes in macrophages induces formation of autophagosomes. Inflammasome activation appears to create a negative-feedback loop by activating autophagy, which controls inflammation by eliminating active inflammasomes. This loop is disrupted if autophagy is impaired. Autophagy can also degrade STING and cGAS to regulate inflammatory response (Chen et al., 2016; Prabakaran et al., 2016). Autophagy proteins ATG9L1 and LC3 co-localizes with STING after dsDNA stimulation to regulate trafficking and activation. The loss of ATG9L1 enhances the assembly of STING after stimulation, leading to aberrant activation of the pathway after TBI (Saitoh et al, 2009). These data suggest that autophagy plays a significant role in the regulation of inflammatory signaling pathways.

In recent years, there is growing evidence that autophagy directly targets cytoplasmic regulators of innate immunity through a receptor-regulated form of autophagy, called precision autophagy (Kimura et al., 2015). In precision autophagy, certain receptors can guide autophagic machinery to targets, obviating the need for ubiquitin or galectins tags. Proteins such as members of the tripartite motif (TRIM) family act as both receptors and platforms for assembly of autophagosome machinery by two means. Firstly, TRIMs recognize their targets (Mandell et al., 2014; Kimura et al., 2015) by finding their cognate cargo (e.g. viral core, inflammasome components) through direct protein–protein binding

without a need for ubiquitin or galectin intermediates. Secondly, the same TRIMs that function as receptors then also act as platforms for the assembly of the core regulators of autophagy, such as ULK1, Beclin1, ATG16L1 (Mandell et al., 2014; Kimura et al., 2015).

Precision autophagy through TRIM proteins has been shown to target cytoplasmic regulators of innate immune pathways. For example, TRIM21 targets IRF3 for autophagic degradation (Kimura et al., 2015). Another TRIM protein, TRIM20, targets inflammasome components, including NLRP3, NLRP1, and pro-caspase 1, for autophagic degradation, thereby modulating their activity, and also serves as the platform for the assembly of ULK1, Beclin1, and ATG16L1. This suggests that TRIM20 acts as an autophagy receptor for delivery of the NLRP3 inflammasome components for autophagic degradation. Overall, the precision autophagy broadens the concept of the role of autophagy as a mediator of innate immunity responses, and might play a crucial role in diseases where innate immune responses govern disease outcomes.

1.4. Scope of Research and Specific Aims

As highlighted in Chapter 1.3, neuroinflammation is a prominent consequence of TBI. CD68 expressing immune cells (which includes activated microglia and infiltrating macrophages) accumulate autophagy markers LC3 and p62 around the injured lesion after TBI, demonstrating inhibition of autophagy flux in these cells in the acute phases following TBI (Sarkar et al., 2014). As these immune cells play important roles in mediating neuroinflammation and phagocytosis after TBI, the potential role of autophagy in mediating these responses in these cells is of significant interest.

Overarching aim of this dissertation is to determine the role of autophagy in resident microglia and myeloid cells after TBI and determine if modulation of autophagy flux levels in these cells determines neuroinflammation and outcomes. My overall hypothesis is that **“inhibition of autophagy flux in microglia and infiltrating monocytes/macrophages exacerbates neuroinflammation and functional defects after TBI”**

Sub-aims:

- 1. To evaluate autophagy flux levels in microglia and infiltrating myeloid cells following TBI and determine association with inflammation and phagocytic function (Chapter 2)**

Hypothesis #1: Inhibition of autophagy flux occurs in microglia and infiltrating myeloid cells following TBI, and this inhibition of autophagy flux is associated with increased proinflammatory cytokine expression.

Hypothesis #2: Inhibition of autophagy flux occurs in microglia and infiltrating myeloid cells after TBI is associated with decreased phagocytic function after TBI.

2. To determine the effect of autophagy dysregulation in microglia and infiltrating monocytes/macrophages on neuroinflammation and functional outcomes following TBI, and elucidate the molecular pathways are impacted (Chapter 3)

Hypothesis #1: Autophagy dysregulation in microglia and infiltrating myeloid cells exacerbates of neuroinflammation and innate immune responses following TBI.

Hypothesis #2: Autophagy dysregulation in microglia and infiltrating myeloid cells worsens neurological outcomes, and motor and cognitive behavior following TBI.

Chapter 4 of this thesis assess the role that a therapeutic agent- N-acetyl-L-Leucine (NALL) plays in reducing neuronal cell death, neuroinflammation and improving functional recover after TBI. It also demonstrates that NALL increases autophagy flux in the brain after TBI, which is likely a contributing factor to its beneficial effects. This paper features in Chapter 4 and is cited as follows: Hegdekar, N., Lipinski, M. M., & Sarkar, C. (2021). N-Acetyl-L-leucine improves functional recovery and attenuates cortical cell death and neuroinflammation after traumatic brain injury in mice. *Scientific reports*, 11(1), 9249. <https://doi.org/10.1038/s41598-021-88693-8>.

CHAPTER 2: Inhibition of Autophagy in Microglia and Monocytes/Macrophages is Associated with Increased Expression of Pro-inflammatory Markers and Defects in Phagocytosis after TBI.

2.1. Introduction

Autophagy is a well-known conserved lysosome-dependent cellular degradative process by which cells remove damaged organelles and toxic macromolecules. It is essential for cellular homeostasis (including protein degradation for energy needs and removal of damaged substrates for recycling) and the survival of terminally differentiated cells such as neurons. Autophagy is upregulated under physiological stress, for example, during conditions of nutrient starvation or ER stress (Mirushima et al., 2008). Although under certain pathological circumstances, increased autophagy is implicated in cell death, autophagy is largely considered to be a cytoprotective mechanism. (Moreau et al., 2010).

TBI is a complex disease, whose pathophysiology is characterized by neuronal cell death and secondary injury. Given the crucial role that autophagy regulation plays in homeostasis and cellular recycling, researchers have investigated the role of autophagy in mediating post-TBI molecular and neurological outcomes (Zhang et al., 2018). Whether autophagy plays a protective or detrimental role mainly depends on the extent of injury severity; following mild TBI, an initiation of autophagy is observed. On the other hand, following moderate and severe TBI, autophagosome accumulation of autophagosomes and inhibition of autophagy flux occurs within the injured brain, with little to no alterations to levels of autophagy initiation (Zeng et al., 2018).

Given the heterogenous populations of cells present within the brain, it is important to determine cell-type specific nature of autophagy following TBI. We previously showed that autophagic flux is inhibited in neurons following moderate controlled cortical impact (CCI) in C57Bl6 and transgenic *GFP-Lc3* autophagy reporter mice, and overall autophagosomal accumulation occurs primarily around the ipsilateral injured lesion following-injury (Sarkar et al., 2014). Within neurons, LC3-associated autophagosomal accumulation occurs within hours after injury and remains elevated for at least 1 week following injury. We showed that this accumulation of autophagosomes after TBI is not due to increased initiation of autophagy, but rather a temporary impairment of autophagic clearance associated with decreased lysosomal function after TBI. Inhibition of autophagy flux also occurs in other cell types in the brain after injury. For instance, inhibition of autophagy flux peaks in CD68⁺ immune cells by 3 days post-injury.

Our previous work shows that inhibition of autophagy within neurons results in increased neuronal cells death, however the consequence of autophagy inhibition in the immune cells was not investigated. Research studying peripheral macrophages in cancer and other autoimmune disease suggest that inhibition of autophagy flux, particularly through block of autophagosome clearance, can increase inflammation by activating inflammatory pathways such as the NF-kB pathway (Tracoli et al., 2011). The neuroinflammatory responses after TBI are mediated by the production of cytokines, chemokines, reactive oxygen species, and secondary messengers by resident CNS glia (primarily microglia) and peripherally derived myeloid immune cells. The degree of neuroinflammation varies based on the context, duration, and severity of the brain insult.

In this study, we used immunohistochemistry and flow cytometry to investigate phenotypic and functional responses in microglia and infiltrating myeloid cells based on autophagy levels, following moderate-controlled cortical impact (CCI) in young adult mice. We employed C57Bl6 mice and lineage-specific transgenic reporter mice to gain novel insight into the inflammatory status of these immune cells based on their levels of autophagy flux. Our data showed that both microglia and infiltrating myeloid cells (specifically monocytes/macrophages) have inhibited autophagy flux following TBI as early as 1 day post-TBI, and this inhibition is associated with increased production of pro-inflammatory cytokines and decreased phagocytic function. Furthermore, our *in vitro* data using murine microglia and macrophages demonstrate that autophagy modulation can directly impact neuroinflammatory responses, with inhibition of autophagy directly increasing the production of pro-inflammatory cytokines.

2.2. Results

2.2.1. Autophagy flux is inhibited in activated microglia and macrophages after TBI.

As mentioned earlier, cell-type specific inhibition of autophagy flux within the injured brain cortex occurs at different time points following TBI (Sarkar et al., 2014). Autophagosome accumulation in CD68+ immune cells peaks at 3 days post-injury, with 59% of these activated microglia/monocytes positive for autophagosome accumulation. This increase in autophagosome accumulation in immune cells is transient, and levels eventually decrease by 7 days post-injury. While this data supports that inhibition of autophagy occurs in activated immune cells, the CD68 marker does not distinguish between activated microglia and infiltrating monocytes within the injured brain.

In this study, our first goal was to determine whether resident microglia or infiltrating monocytes/macrophages are preferentially impacted by inhibition of autophagy. To address this, we performed moderate CCI on Cx3Cr1-GFP mice, a transgenic mouse line with a green fluorescent protein (GFP) that marks cells positive for Cx3Cr1 (a known as the fractalkine receptor, specifically present on brain-resident microglia and infiltrating monocytes/macrophage cells). Using immunofluorescence, we co-stained mice cortical brain sections with antibodies against F4/80, to selectively label infiltrating monocytes/macrophages, and the autophagy adaptor protein, which increases in cells with inhibited autophagy flux (**Figure 2-1A**). While p62 accumulation occurred in both microglia (F4/80^{low}Cx3Cr1⁺) and infiltrating monocytes (F4/80^{high}Cx3Cr1⁺) following injury, it accumulates more predominantly within the infiltrating cell population (**Figure 2-1B**). At 3 days post-injury, 13% of all quantified CX3CR1⁺ cells are positive for p62; however, 65% of all quantified CX3CR1⁺F4/80⁺ cells are positive for p62, which indicates that the majority of cells with inhibited autophagy at 3 days post-injury are the infiltrating monocytes/macrophages (**Figure 2-1C**). Across all indicated time points, p62 accumulates more predominantly in CX3CR1⁺F4/80⁺ monocytes. Consistent with published data, the overall levels of the infiltrating monocytes/macrophages reduce by day 7 following injury (Sarkar et al., 2014).

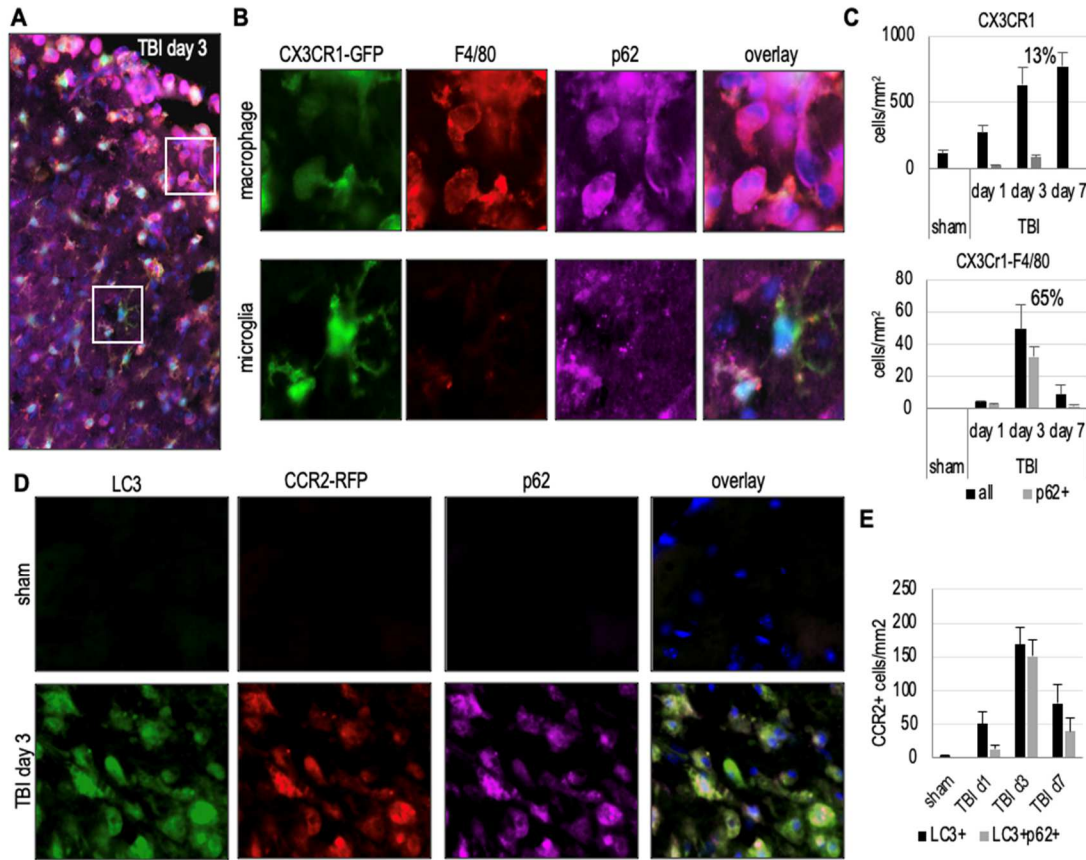


Figure 2-1. Autophagy is inhibited in activated microglia and infiltrating monocytes after TBI. (A) 20X immunofluorescences (IF) images of Cx3Cr1-GFP mouse cortical brain sections co-stained with antibodies against infiltrating monocyte/macrophage marker F4/80 and autophagy adaptor protein p62; (B) close-up images of microglia (F4/80^{low}) and infiltrating macrophage (F4/80^{high}) and accumulation of p62 in the injured perilesional cortex at 3 days post-TBI. (C) Corresponding quantification of numbers of Cx3Cr1+ cells (black bar) and Cx3Cr1+/F4/80+ cells (grey bars) positive for p62 (grey bars), normalized to area images (mm²) indicated that autophagy inhibition occurs predominantly within the infiltrating cell population over the resident microglia. (D) 20X IF images of CCR2-RFP mouse cortical brain sections co-stained with antibodies for autophagosome marker LC3 and autophagy adaptor protein p62, and (E) corresponding quantification of numbers of CCR2+ cells which are positive for LC3 (black bar) and double positive for LC3 and p62 (grey bar), normalized to area imaged (mm²). Data are presented as mean \pm SEM; n=5/group; at least 1,000 cells were quantified per mouse.

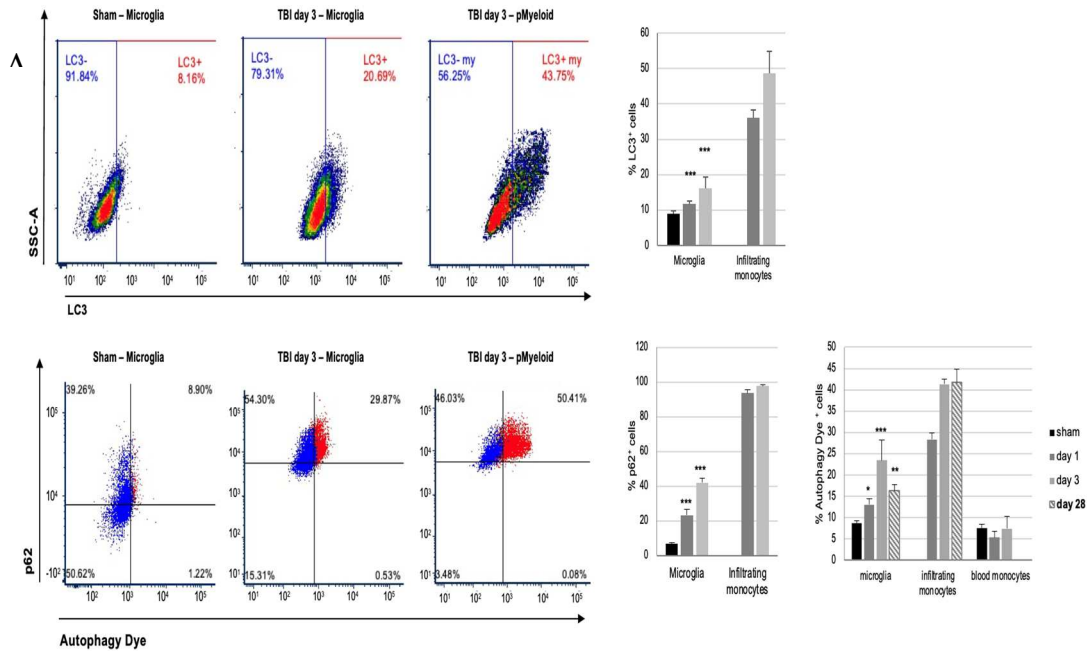


Figure 2-2. Microglia and infiltrating myeloid cells show inhibition of autophagy after TBI. Flow cytometry analysis of resident microglia ($CD45^{int} CD11b^{+}$) and infiltrating myeloid cells ($CD45^{high} CD11b^{+}$) from Sham and TBI mice. **(A)** A representative dot plot showing gating strategy for expression of LC3 in the microglia and infiltrating myeloid cells in Sham and injured mice at 3 days post-TBI. **(B)** Quantification of the % of LC3+ microglia and infiltrating monocytes. **(C)** Representative dot plots showing gating strategy for expression of LC3 in the microglia and infiltrating myeloid cells in Sham and injured mice at 3 days post-TBI. **(D)** Quantification of the % of LC3+ microglia and infiltrating monocytes. Data are presented as mean \pm SEM; $n=5-7$ /group. * $p < 0.05$, ** $p < 0.01$, *** $p < 0.005$ vs Sham; Ordinary One-Way ANOVA with Tukey's test for multiple comparisons).

Autophagy flux inhibition in infiltrating monocytes was confirmed by performing CCI on CCR2-RFP reporter mice. CCR2 is the main chemokine receptor inducing macrophage and monocyte recruitment to sites of inflammation and is useful to mark this infiltrating cell population in the injured cortex post-TBI. Using immunofluorescence on mice cortical brain sections, we observed accumulation of autophagy markers LC3 and p62 in 89% of the $CCR2^{+}$ cells at 3 days post-TBI, confirming inhibition of autophagy flux within these infiltrating cells (**Figure 2-2D-E**). Collectively, these findings suggest that

while autophagy inhibition occurs in both microglia and infiltrating monocytes following TBI, it predominately occurs in the infiltrating monocyte/macrophage population.

We used flow cytometry as a complementary technique to gain novel insight into the phenotypic and functional dynamics of resident microglia ($CD45^{int} CD11b^{+}$) and infiltrating myeloid cells ($CD45^{hi} CD11b^{+}$) in the injured brain post-TBI. We observed increase in the number of $LC3^{+}$ and $p62^{+}$ microglia and infiltrating myeloid cells after injury, with levels peaking at 3 days post-injury. (**Figure 2-2A-B**). We further assessed autophagy flux levels in our flow cytometry-sorted cells using Enzo Cyto-ID Autophagy dye, a pH-sensitive autophagy dye that fluorescently labels autophagosomes in lysosomally inhibited live cells Guo et al., 2015). Following TBI, there is an increase in the percentage of autophagy dye⁺ microglia and infiltrating monocytes within the injured brain (**Figure 2-2E**).

Furthermore, we noted an interesting observation when comparing the infiltrating monocytes/macrophages ($CD45^{hi} CD11b^{+} Ly6C^{+}$) in the brain versus the system circulation. While the percentage of autophagy dye⁺ monocytes increases from 27% at day 1-post TBI to 43% at day 3-post TBI, corresponding increases are not reflected in the circulating blood monocytes; in fact, the percentage of autophagy dye⁺ circulating blood monocytes remains relatively after TBI. This suggests that autophagy impairment within the monocytes is restricted to those that cross the impaired BBB following TBI. We hypothesize that molecular processes that occur at the injured brain microenvironment are

responsible for impairment of autophagy flux within the monocytes/macrophages that cross the BBB

2.2.2. Inhibition of autophagy is associated with increased expression of pro-inflammatory markers and defects in phagocytic function.

Next, we determined the inflammatory status of the activated microglia and infiltrating monocytes/macrophages showing inhibited autophagy flux after TBI. We performed immunofluorescence staining using antibodies against p62 and various pro-inflammatory markers on Cx3Cr1-GFP mice cortical brain sections at one day, three days, and seven days post-TBI. We observed significant accumulation of pro-inflammatory markers iNOS, NLRP3, and NOX2 in CX3CR1⁺ positive cells in the injured cortex post-TBI, with levels peaking at 3 days post TBI (**Figure 2-3 A-F**). These findings are consistent with published work assessing pro-inflammatory cytokine production in the acute phase post-TBI (Kumar et al., 2014). Additionally, most of these pro-inflammatory microglia and macrophages also accumulated high levels of p62, indicating inhibition of autophagy flux in these cells. At three days post-injury, 69% of the Cx3Cr1⁺iNOS⁺ cells were positive for p62, 89% of the Cx3Cr1⁺NOX2⁺ cells were positive for p62, and 81% of the Cx3Cr1⁺NLRP3⁺ cells were positive for p62. This strong overlap between p62 level and pro-inflammatory cytokine expression persisted through seven days post-TBI. Based on these findings, we predicted that inhibition of autophagy flux in microglia and infiltrating monocytes/macrophages is associated with increased levels of pro-inflammatory cytokine production compared to cells with higher autophagy flux.

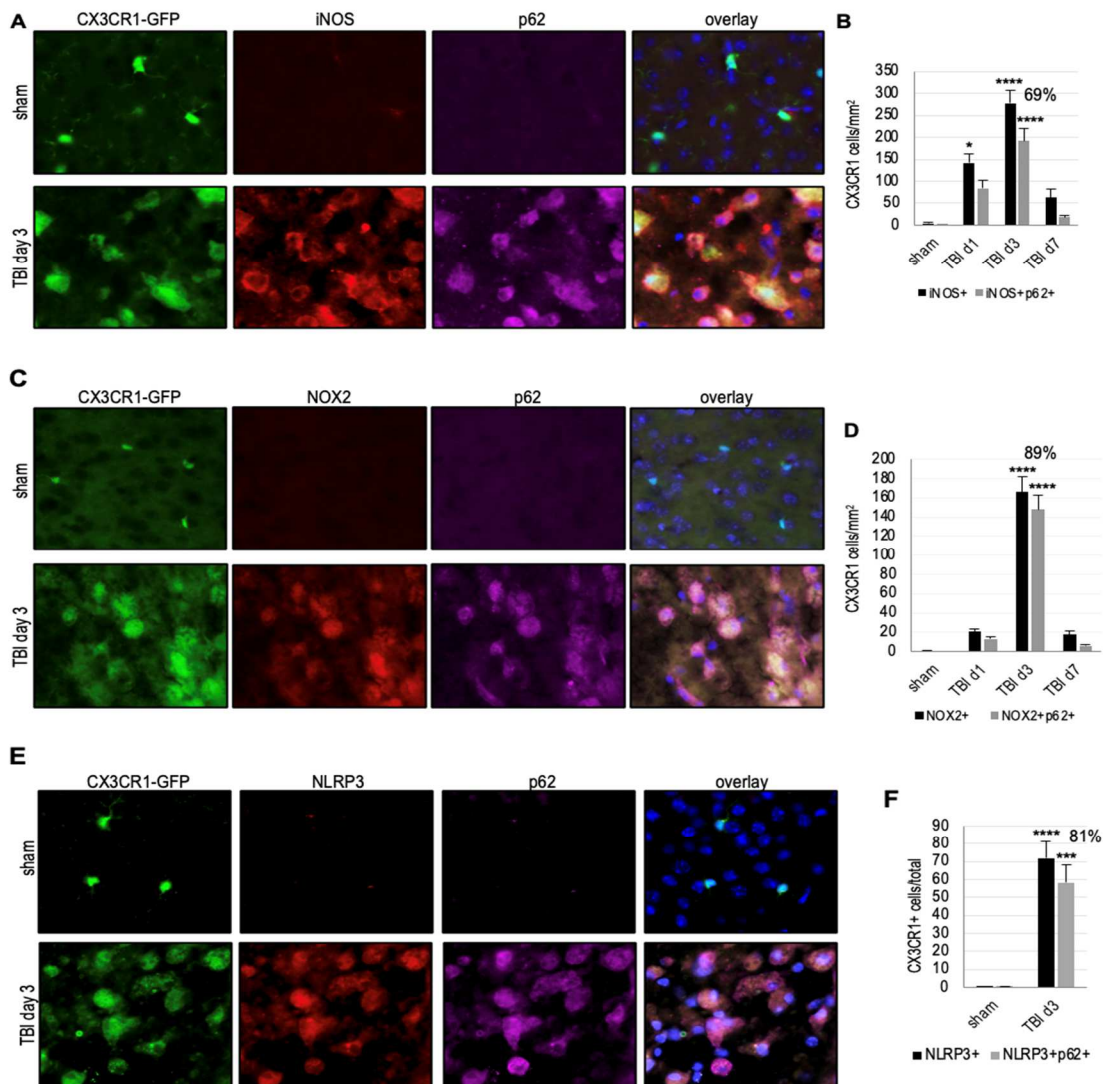


Figure 2-3. Inhibition of autophagy flux is associated with increased expression of pro-inflammatory markers after TBI. 20X immunofluorescence (IF) images of Cx3Cr1-GFP mouse cortical brain sections co-stained with antibodies against autophagy adaptor protein p62 and pro-inflammatory markers (A) iNOS, (C) NOX2 and (E) NLRP3. The percentages of double-positive versus single-positive cells are indicated at the 3-day time post-injury. Corresponding quantifications normalized to total Cx3Cr1⁺ cell numbers show that (B) 69% of the Cx3Cr1⁺iNOS⁺ cells were also positive for p62, (D) 89% of the Cx3Cr1⁺NOX2⁺ cells were also positive for p62, and (F) 81% of the Cx3Cr1⁺NLRP3⁺ cells were also positive for p62 (**p<0.005, ****p<0.001 vs corresponding sham levels; Ordinary One-Way ANOVA with Tukey's test for multiple comparisons). Data are presented as mean ± SEM; n=5/group; at least 1,000 cells were quantified per mouse per experiment.

To test this prediction, we used flow cytometry to distinguish between microglia and infiltrating myeloid cells with high and low levels of autophagy flux. Because Cyto-ID autophagy dye levels correspond to autophagosome accumulation, we defined cells with low levels of autophagy flux/inhibited autophagy flux as Autophagy dye⁺ (dye⁺) cells and cells with high levels of autophagy flux as Autophagy dye⁻ (dye⁻) cells (**Figure 2-4A**). We then evaluated the corresponding levels of pro-inflammatory cytokines production (TNF α , IL-1 β) in these cell populations isolated from sham or CCI-injured mice.

Starting at one day post-TBI, dye⁺ microglia expressed higher levels of the pro-inflammatory cytokines TNF- α and IL-1 β compared to dye⁻ microglia at the same time points. This higher production of IL-1 β in dye⁺ microglia compared to dye⁻ microglia was statically significant up to 28 days post-TBI (**p<0.01 at the day 28 post-TBI), while the higher levels of TNF- α in the dye⁺ microglia compared to the dye⁻ microglia remained statistically higher in the acute time points post-TBI, but not at day 28 post-TBI (p=0.062 compared to dye⁻ microglia at day 28 post-TBI). Conversely, within the infiltrating myeloid cells we observed significantly higher levels of both TNF- α and IL-1 β in the dye⁺ cells only at the later time points after TBI (for IL-1 β ,* p<0.05 at day 7 post-TBI and **p<0.01 at day 28 post-TBI; for TNF- α , ****p<0.001 at days 7 and 28 post-TBI). These findings suggest that inhibition of autophagy in microglia and infiltrating myeloid cells is associated with higher levels of proinflammatory cytokine production.

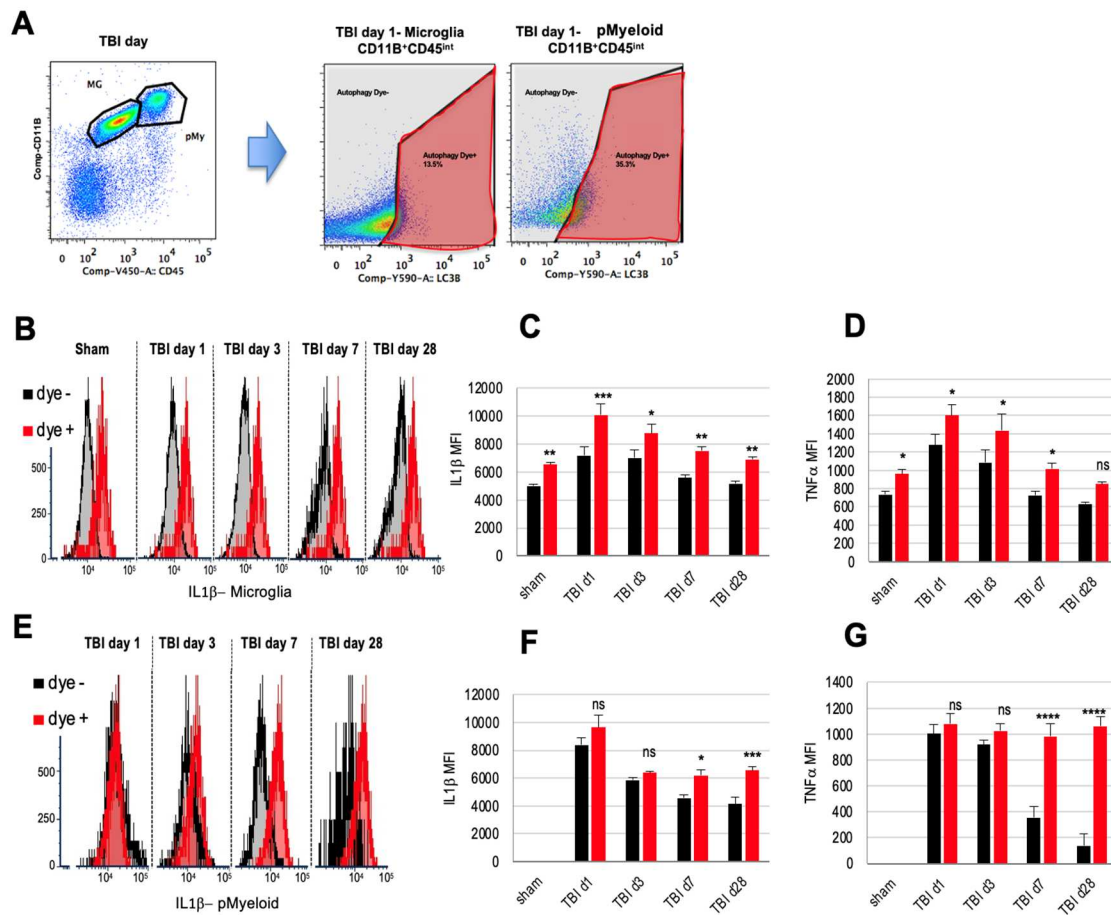


Figure 2-4. Inhibition of autophagy is associated with increased expression of the pro-inflammatory cytokines IL-1 β and TNF- α after TBI. (A) Representative gating strategy for distinguishing between Autophagy dye⁺ (dye⁺) and Autophagy dye⁻ (dye⁻) microglia and peripheral myeloid cells post-injury. (B). Representative histogram shows higher levels of IL-1 β +cells is dye⁺ microglia compared to dye⁻microglia up to 28 days post-TBI. Mean fluorescence intensity (MFI) of (C) IL-1 β levels and (D) TNF- α levels shows statistically higher levels in dye⁺ microglia vs dye⁻ microglia after TBI. Similar trends were observed in the infiltrating myeloid cells after TBI (E). Representative histogram shows higher levels of IL-1 β +cells is dye⁺ myeloid cells compared to dye⁻myeloid cells. significance only at the day 7 and day 28 time points after TBI. (MFI) of (F) IL-1 β levels and (G) TNF- α levels shows higher levels in dye⁺ myeloid cells compared to the dye⁻ myeloid cells after TBI, however, this showed significance only at the day 7 and day 28 timepoints post-TBI. n = 5/ group. Data are presented as mean \pm SEM; *p < .05, **p < 0.01, ***p < .005, ****p < .001 vs corresponding Dye- time point; two-way ANOVA using Tukey's test for multiple comparison.

Phagocytosis of dying cells and injury-associated DAMPs is another important function of activated microglia and infiltrating immune cells following TBI. Flow cytometry was used to evaluate the phagocytic function of dye⁺ and dye⁻ microglia and myeloid cells after TBI by measuring uptake of red fluorescently labelled beads (**Figure 2-5**). In both microglia and myeloid cells, phagocytic bead uptake was higher in the dye⁻ cells compared to corresponding the dye⁺ cells. This finding suggests that inhibition of autophagy flux in immune cells after TBI might be the cause of their decreased phagocytic function.

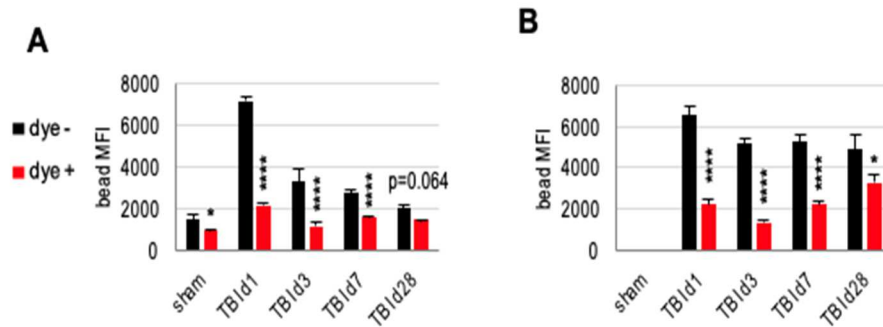


Figure 2-5. Inhibition of autophagy flux in microglia and myeloid cells is associated with decreased phagocytic function. Mean fluorescence intensity (MFI) of red latex bead uptake (phagocytosis) in (A) microglia and (B) infiltrating myeloid cells. Across all time points, Autophagy dye⁺ cells have decreased phagocytic bead uptake compared to dye⁻ cells. n = 5/ group. Data are presented as mean ± SEM; *p < .05, ***p < .005 vs corresponding Dye⁻ time point; two-way ANOVA using Tukey's test for multiple comparison.

2.2.3. Inhibition of autophagy results in increased expression of pro-inflammatory markers *in vitro*.

Our *in vivo* findings demonstrate that inhibition of autophagy flux (i.e., decreased autophagy levels) in microglia and monocytes/macrophages is associated with increased pro-inflammatory cytokine production. However, it is not clear whether this decrease in autophagy flux contributes to the exacerbated inflammatory phenotype, or whether this is a mere correlation. To understand this further, we performed *in vitro* studies using murine microglia (IMG cells) and murine macrophages (RAW 246.7 cells) (**Figure 2-6**). We treated these cell lines with various inhibitors of autophagy for 6 hours (reflecting an acute time point). The inhibitors targeted different components of the autophagy machinery: Bafilomycin A1 (BafA) inhibits autophagosome-lysosome fusion, 3-MA inhibits the Type III PI3K complex, thus preventing autophagosome formation, MRT68921 inhibits ULK1, thus preventing autophagy initiation. Following treatment with the autophagy inhibitors, we determined corresponding changes in the expression of pro-inflammatory markers iNOS and NLRP3 by western blotting. We observed that IMG and RAW cells treated with autophagy inhibitors had increased inflammation as assessed by elevated expression of iNOS and NLRP3. This was true under baseline conditions, as well as in cells pre-treated with lipopolysaccharide (LPS) to simulate pro-inflammatory conditions present in the brain after TBI. It is important to note that all three inhibitors caused increased levels of the pro-inflammatory markers, which demonstrates that modulation of autophagy (rather

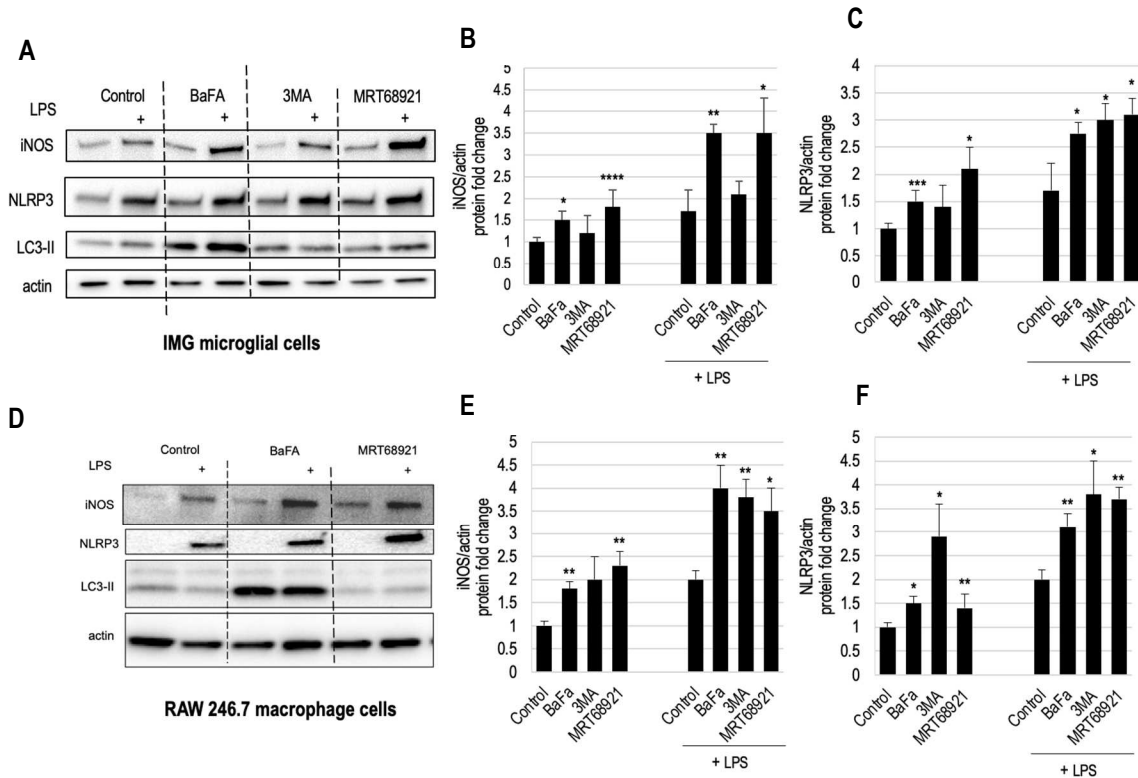


Figure 2-6. Inhibition of autophagy in macrophage and microglial cell lines alters inflammatory responses *in vitro*. (A) Western blot of murine IMG microglial cells treated with autophagy inhibitors bafilomycin A1 (BafA), 3-methyladenine (3-MA), or MRT68921 for 6 hours in the absence or presence of LPS pre-treatment (3 hours) and corresponding quantifications of iNOS protein fold change (B) and NLRP3 protein fold change (C). (D) Western blot of murine RAW 246.7 macrophage cells receiving the same treatments as IMG microglia. (E) iNOS protein fold change. (F) NLRP3 protein fold change. * $p < .05$, ** $p < 0.01$, *** $p < .005$, **** $p < 0.001$, vs corresponding control; Ordinary One-way ANOVA using Tukey's test for multiple comparison. Data are presented as mean \pm SEM; $n=3$ independent experiments/group.

than of only one specific component of the pathway) in macrophages & microglia can directly alter inflammatory responses *in vitro*. We extrapolate these findings to suggest that following TBI, autophagy inhibition in microglia and macrophages within the injured brain increases pro-inflammatory cytokine production.

2.3. Summary

Given the roles that autophagy plays in regulating homeostasis and cellular recycling, understanding its regulation in pathological conditions such as TBI is important. Our previous studies demonstrate transient inhibition of autophagic flux in various brain cell types following TBI, with activated CD68⁺ immune cells accumulating autophagosomes and markers of autophagy inhibition (LC3 and p62) beginning at one day post-injury. (Sarkar et al., 2014).

Neuroinflammation, characterized by increased production of pro-inflammatory cytokines in the brain, is a classic hallmark of both the acute and chronic phases of TBI. It is mediated by microglia and infiltrating myeloid cells, which are primarily monocytes/macrophages. The purpose of this study was to determine whether there is an association between autophagy flux levels in microglia or infiltrating monocytes/macrophages and levels of neuroinflammation following moderate CCI in young adult mice. Studies of peripheral macrophages in cancer and autoimmune diseases found that increased levels of autophagic flux are associated with anti-inflammatory properties, while impaired flux is associated with pro-inflammatory phenotypes; we expected the same trends to hold true for immune cells in the brain after TBI. In this study, we attempted to understand the role of autophagy in inflammation. Through our studies, we found that inhibition of autophagy flux in both microglia and infiltrating macrophages starting at one day post-TBI, with levels peaking at three days post-TBI, followed by decreased levels at seven days post-TBI.

Differentiating the contribution of resident microglia from infiltrating macrophages can be difficult, particularly in the context of TBI. This is because once peripheral monocytes differentiate into brain macrophages, they are nearly indistinguishable from microglia by histology due to similarities in the expression of many cell surface markers. To tease out these differences, we used transgenic lineage specific mouse lines and flow cytometry-based cell surface markers to distinguish between resident microglia and infiltrating monocytes/macrophages. We initially used Cx3Cr1-GFP mice, as we believed them to mark just microglia and not the infiltrating monocytes/macrophages; however, we discovered that Cx3Cr1 marks both resident microglia and infiltrating monocytes/macrophage cell populations. To overcome this, we co-stained mice brain sections with antibodies against F4/80, which selectively labels the infiltrating monocytes/macrophages over the resident microglia. We observed that the infiltrating monocytes/macrophages are impacted by autophagy impairment to a higher extent than the resident microglia at all timepoints. The reason for this preferential inhibition is currently unknown and warrants future investigation.

Furthermore, we observed that these microglia and infiltrating monocytes/macrophages with impaired autophagic flux show increased expression of pro-inflammatory markers such as NLRP3, iNOS, and NOX2. Immunofluorescence staining showed a positive correlation between pro-inflammatory cytokine production and levels of the autophagy adaptor protein, p62. Using flow cytometry, we presented a practical approach to study microglia and infiltrating myeloid cell subpopulations in the brain based on their levels of autophagy flux after TBI. Cyto-ID Enzo autophagy dye is a pH-sensitive dye that fluorescently labels autophagosomes in lysosomally-inhibited live cells and can thus be

used as a marker to infer autophagic flux rate. Based on our flow cytometry gating strategies, we distinguished microglia and infiltrating myeloid cells into dye+ (cells with low autophagy flux) and dye- cells (cells with high autophagy flux) across a time course ranging from one day to 28 days post-TBI. The dye+ versus dye- cell populations showed significantly different inflammatory statuses at all time points after TBI.

Although the present study highlights important differences between neuroinflammatory dynamics in autophagy flux following TBI, there are several caveats to note. First, for our time-course FACS experiment (**Figure 2-4 and 2-5**), we did not distinguish between neutrophils and monocytes when analyzing $CD45^{high}CD11b^{+}$ myeloid cells after TBI. $CD11b^{+}CD45^{high}$ cells include monocytes $CD11b^{+}CD45^{high}Ly6C^{+}$ and neutrophils $CD11b^{+}CD45^{high}Ly6G^{+}$. However, as most infiltrating cells disappear by seven days post-TBI in the injured brain, it is difficult to distinguish between monocytes and neutrophil populations at the later time points. As we wanted to characterize the entire time course collectively, we focused on a combined $CD11b^{+}CD45^{high}$ infiltrating myeloid cell population. Future work should focus on more specific populations within the $CD45^{high}CD11b^{+}$ myeloid cells as monocytes and neutrophils have different functions.

Another caveat to this study is that we included only male mice in our experiments. At baseline, male and female microglia have different functional activation states during homeostasis, showing differences in cell morphology, cytokine and ROS production, and phagocytosis (Doran et al., 2019). Following moderate-to-severe TBI, sex-specific differences in microglial functional responses and motor function recovery are noticed between male and female mice. Infiltrating myeloid cells produce higher levels of pro-

inflammatory cytokines compared to resident microglia following TBI, indicating that peripherally derived immune cells dictate sex-dependent post-traumatic neuroinflammatory responses that impair neurological outcomes acutely after TBI. Interestingly, our data demonstrates that infiltrating cells, which are primarily monocytes/macrophages, show a greater extent autophagy flux inhibition than the resident microglia (**Figures 2-1 and 2-2**). Future work should test whether sex-specific changes in autophagy flux occur following TBI.

We demonstrated through our *in vitro* experiments that inhibition of autophagy flux in murine microglia and macrophages directly results in increased pro-inflammatory cytokine production upon challenge with the pro-inflammatory stimulus LPS. We accomplished this by utilizing drugs that inhibit different components of the autophagy machinery: MRT68921 is an ULK1 inhibitor, 3-MA is a Type III PI3K inhibitor, and BafA prevents fusion of the autophagosome with the lysosome, thereby decreasing autophagy flux. This result is consistent with the hypothesis that general inhibition of autophagy contributes to the increase in pro-inflammatory cytokine levels in microglia and infiltrating monocytes/macrophages that was seen for several days after CCI. We did not investigate the molecular mechanism(s) that mediate the increased pro-inflammatory cytokine production by autophagy inhibitors; it is plausible that more than one molecular pathway contribute.

2.4 Methods

2.4.1. Animals

All experiments were performed according to NIH guidelines for the care and use of animals in research and under protocol approved by IUCAC at the University of Maryland, Baltimore. All experiments were performed on young adult male mice (9–11 weeks old, 21–27 g). The following mouse lines were purchased from The Jackson Laboratory (Bar Harbor, ME) - CX₃CR1-GFP (Strain #005582; Jung et al., 2020), CCR2-RFP (Strain #017586), and C57Bl/6 mice (Strain #000664).

2.4.2. Controlled Cortical Impact (CCI)

TBI was performed on mice using a custom-designed controlled cortical impact (CCI) injury device consists of a microprocessor-controlled pneumatic impactor with a 3.5 mm diameter tip. Mice were anesthetized with an inducing concentration of 3% isoflurane evaporated in a gas mixture containing 70% N₂O and 30% O₂ and administered through a nose mask. Once the mice were heavily anesthetized, as measured by loss of toe-pinch reflex, gaseous isoflurane concentration was reduced to 1-1.5% to maintain the mice in an anesthetized state. Fur on the head was removed using shearing razors. Mice were placed on a heated pad and core body temperature was maintained at 37°C. The head was mounted in a stereotaxic frame, a 10 mm midline incision was made over the skull, and the skin and fascia were retracted. A 5 mm craniectomy was made on the central aspect of the left parietal bone using a handheld micro-drill (**Figure 2-7**). The impounder tip of the injury device was then extended to its full stroke distance (44 mm), positioned to the surface of the exposed dura, and reset to impact the cortical surface. Moderate-to-severe level CCI injury was induced on the exposed dura using an impactor velocity of 6 m/s and

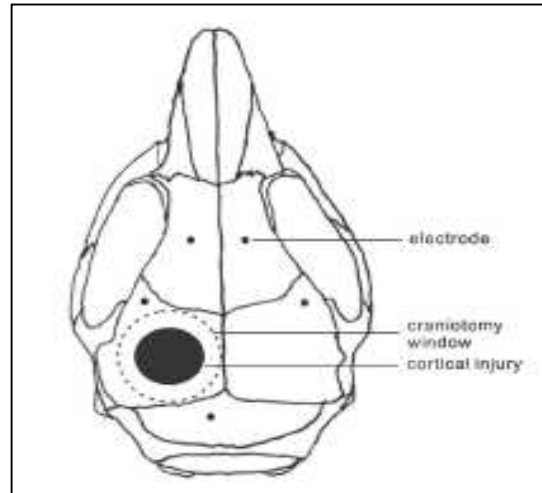


Figure 2-7. Controlled Cortical Impact (CCI) injury in mice. Mice under anesthesia underwent a midline head incision of 10 mm. The fascia on the skull was removed and a craniectomy at the indicated site (craniotomy window) was performed, with care not to disturb the dura. The impounder was then extended to its full length such that it touched the exposed dura. Then the impounder was retracted and set to impact 2 mm in depth at a speed of 6 m/s, which then results in moderate-to-severe injury (black circle indicating infarct).
 (Image source: <https://www.creative-biolabs.com/drug-discovery/therapeutics/rodent-controlled-cortical-impact-injury-cci-model-of-traumatic-brain-injury.htm>)

a deformation depth of 2 mm. After performing injury, the incision was closed with interrupted 6-0 silk black sutures, anesthesia was terminated, and the mouse was placed into a heated cage to maintain normal core temperature for 60 minutes post-injury. Sham animals were subjected to the same procedure as CCI mice except for craniectomy and cortical impact.

2.4.3. Immunofluorescence

At 1 day, 3 days and 7 days post-TBI, mice were anesthetized with 5% isoflurane and transcardially perfused with ice-cold saline followed by 4% paraformaldehyde (pH 7.4).

Brains were removed and post-fixed in 4% paraformaldehyde for 24 hours, 20% sucrose for 24 hours, and then protected in 30% sucrose. 20 µm frozen sections were cut and mounted on glass slides for immunofluorescence. Brain sections were hydrated and washed with 1X PBS (three times), followed by blocking for one hour in goat serum containing 0.4% Triton X-100. Sections were then incubated overnight at 4°C with a combination of primary antibodies, including mouse anti-gp91^{phox} (NOX2; 1:1000; BD Biosciences, San Diego, CA), anti-NLRP3 (1:200; Cell Signaling), anti-iNOS (1:250; BD Biosciences). The following day, sections were washed with 1X PBS (three times), and incubated with appropriate Alexa Fluor-conjugated secondary antibodies (Life Technologies) for 2 hours at room temperature with minimal shaking. Sections were washed with 1X PBS (three times), counterstained with 4', 6-diamidino-2-phenylindole (DAPI; 1 µg/ml; Sigma-Aldrich), and mounted with glass coverslips using Hydromount solution (National Diagnostics).

2.4.4. Flow Cytometry

At 1 day, 3 days, 7 days and 28 days post-TBI, mice were anesthetized with 5% isoflurane and transcardially perfused with ice-cold PBS. The brains were removed, processed by mechanical disruption on a 70 µm filter screen, and resuspended in a total of 5 mL of Roswell Park Memorial Institute medium (RPMI) (Quality Biological, Gaithersburg, MD, USA). 20 Units (U) Papain (Sigma-Aldrich), 10 mg/ml DNase II (Sigma), 1 mg/ml Collagenase-Dispase (Sigma), and 1 µL of GolgiPlug containing brefeldin A (BD Biosciences) were added to the brain suspension and incubated on a shaker at 200 rotations per minute (RPM) for one hour at 37°C for further mechanical and enzymatic digestion

of the brain tissue. After incubation, leukocytes were separated from other brain cells by a Percoll density gradient (GE Healthcare, Chicago, IL, USA). Brain leukocytes were resuspended in 70% Percoll-HBSS and were slowly injected under a 30% Percoll-RPMI layer using a blunt popper pipetting needle (Sigma). This Percoll gradient was spun for 20 minutes with no braking. The myelin layer was removed from the top of the 30% Percoll layer. The leukocytes were then retrieved from the interface of the 30% and 70% Percoll layers and resuspended in RPMI as single cell suspensions. These leukocytes were then washed in fluorescence-activated cell sorter (FACS) buffer (0.1% penicillin and streptomycin with 5% fetal bovine serum in 1x HBSS) with sodium azide (NaN₃) and blocked with 1:50 mouse Fc Block (clone 93; eBioscience, San Diego, CA) for 10 minutes on ice prior to staining with primary antibody-conjugated fluorophores. Antibodies for surface staining included: from Invitrogen/eBioscience: CD45-eF450 (30-F11) and CD11b-APCeF780 (M1/70), and from Biolegend (San Diego, CA, USA): CD11c-FITC (n418), Ly6C-AF700/APC (HK1.4), and Ly6G-AF700/PE (1A8-Ly6g) at final concentration of 1:100 for each antibody. To mark autophagy flux levels, Enzo Cyto-ID Autophagy dye was added at a dilution of 1:1000, as per the manufacturer's instructions. For live/dead cell discrimination, a fixable viability dye, Zombie Aqua™ (Biolegend), was dissolved in DMSO according to the manufacturer's instructions and added to cells at a final concentration of 1:50.

After primary antibody staining, cells were washed in 100 µL of fixation/permeabilization solution (BD Biosciences) for 20 minutes. Cells were then washed twice in 500 µL Permeabilization/Wash buffer (BD Biosciences) and resuspended in an intracellular antibody cocktail of antibodies. Intracellular antibodies included: TNF-PE-Cy7 (MP6-

XT22) (Invitrogen), IL-1 β -PerCP-eF710 (NJTEN3) (Invitrogen), LC3 (FITC), and p62-AF647 (Biolegend). After antibody staining for 30 minutes at 4°C, samples were washed with Wash buffer twice (BD Biosciences) and then fixed with 2% paraformaldehyde as described above. After one more wash, these samples were resuspended in 300 μ l of FACS buffer with Sodium Azide to be analyzed on the flow cytometer.

To assess phagocytic ability, TexasRed fluorescent carboxylate-modified polystyrene latex beads (0.5 μ m mean diameter; Sigma) were added to freshly isolated cells in a final dilution of 1:500 (in RPMI). After a 45-minute incubation in a 37°C water bath, the cells were washed twice, resuspended in FACS buffer, stained for surface markers and viability, and fixed in 2% paraformaldehyde. After an additional wash, these samples were resuspended in 300 μ l of FACS buffer with 0.05% Sodium Azide to be analyzed on the flow cytometer. Data were acquired on an LSRII flow cytometer equipped with FACSDiva 6.0 (BD Biosciences, San Jose, CA) and analyzed using FlowJo (Tree Star, San Carlos, CA).

2.4.6. Cell Culture and *in vitro* Treatments

Murine microglia (IMG cells) and murine macrophages (RAW 264.7 cells) were from Sigma and ATCC (Manassas, VA, USA) respectively and cultured in DMEM media containing 10% fetal bovine serum (FBS) from Hyclone Laboratories (USA) and 1% penicillin-streptomycin from Cellgro (Manassas, VA, USA).

Twenty-four hours prior to *in vitro* experiments, cells were passaged and plated in 24-well plates at a density of 5×10^4 cells per well. Specified cells were pretreated with LPS (10

ng/ml) for three hours prior to autophagy drug treatment. The following autophagy inhibitors were used- Bafilomycin A1 (BafA) (20 nM), 3-MA (5 μ M) and MRT68921 (5 μ M). Treatment with the inhibitors was carried out for 6 hours, following which all cells were lysed and processed for western blotting. For all *in vitro* experiments, three independent experiments were performed.

2.4.7. Western Blotting

Cell lysates were prepared by lysing IMG microglia or RAW 246.7 macrophages cultured in 24-well plates with SDS-PAGE buffer. Cell lysates were resolved on 4–20% SDS-PAGE gels (Bio-Rad Laboratories, 5671095) and transferred to PVDF membrane (Millipore Sigma, IPVH00010) using semi-dry transfer (Bio-Rad Laboratories). Membranes were blocked with 5% non-fat milk in TBS-T (Tris-buffered saline with 0.05% Tween 20 [National Diagnostics, 9005–64–5]), probed with primary antibodies in 1% bovine serum albumin (BSA) in TBS-T overnight at 4°C, and incubated with horseradish peroxidase (HRP)-conjugated secondary antibodies (KPL, 474–1506, 474–1806, 14–16–06 and 14–13–06) in blocking solution at room temperature for 1 h. Protein bands were detected using SuperSignal West Dura Extended Duration Substrate (Thermo Fisher Scientific, 34076), SuperSignal West Pico Chemiluminescent Substrate (Thermo Fisher Scientific, 34080), or SuperSignal Femto Chemiluminescent Substrate (Thermo Fisher Scientific, 34080) and visualized using a Chemi-doc system (Bio-Rad Laboratories, Universal Hood II). Individual protein band intensities were analyzed using Image Lab software (Bio-Rad Laboratories) and normalized to that of a loading control (β -Actin).

Primary antibodies were: LC3 (1:1000; Novus Biologicals, NB100-2220), NLRP3 (1:1000; Cell Signaling), iNOS (1:1000; BD); β -Actin (1:10000; ThermoFisher).

**CHAPTER 3: Inhibition of Autophagy in Microglia and Monocytes/Macrophages
Exacerbates Innate Immune Responses, Neuroinflammation, and Functional
Defects following TBI in Mice**

3.1 Introduction

The discovery of yeast autophagy-related (ATG) genes and subsequent identification of their mouse and human homologs have enabled researchers to investigate physiological functions of autophagy in molecular mechanisms and diseases using genetic techniques (Kuma et al., 2017). Beyond its role in maintaining cellular homeostasis and energy balance, autophagy has conserved roles in differentiation and development. Consequently, conventional systemic knockout of certain autophagy genes in mice results in embryonic or neonatal lethality. To circumvent this problem, researchers use tissue-specific *Atg* gene knockout mice to study the role of autophagy in various processes and diseases (Yoshii et al. 2016; Tsuboyama et al., 2016; Karsli-Uzunbas et al., 2014).

The Cre/lox system is one of the most powerful tools in mouse genetics because it enables generation of tissue-specific and inducible knockouts with substantial control over the location and timing of gene expression. The process involves flanking a repeating 34 base pair loxP DNA sequence on either side of a target gene of interest (resulting in a “floxed” gene) and expressing Cre recombinase in a specific cell-type. Cre expression results in cell-specific deletion of the floxed sequence (Lakso et al., 1992; Orban et al., 1992). Using tissue-specific knockout mice has particularly practical applications when studying physiological processes in the brain. As the brain comprises numerous cell types,

global gene knockouts (when not neonatally or embryonically lethal) make it difficult to attribute resulting phenotypic changes to a specific brain cell type.

The involvement of autophagy in the regulation of inflammatory responses and autoimmune diseases has only recently been studied. Most of our existing knowledge on the autophagy-inflammation link is derived from studies in peripheral macrophages and epidemiological data linking autophagy defects with the development of autoimmune and inflammatory diseases. Generally, inhibition of autophagy flux in peripheral macrophages results in increased pro-inflammatory cytokine polarization. To highlight a few recent findings, loss of the autophagy protein ATG16L1 is associated with Crohn's disease and results in enhanced pro-inflammatory cytokine production by macrophages in response to stress (Saitoh et al., 2008; Murthy et al., 2014). A conditional knockout of *Atg5* or *Atg7* in murine macrophages correlates with increased severity of uveitis (Santeford et al., 2016), liver fibrosis (Lodder et al., 2015), or colitis (Lee et al., 2016). *In vitro* data on macrophages and macrophage cell lines show that addition of the autophagy blocker 3-MA results in increased IL-1 β formation (Harris et al., 2011; Zhou et al., 2011; Shi et al., 2012; de Luca et al., 2014).

As numerous ATG proteins participate in the autophagy process, it is necessary to study one that plays a crucial role in regulating physiological processes. Beclin 1 is an essential member of the multi-protein complex that is necessary for nucleation of the autophagic vesicle during autophagy initiation and recent research underscores its importance in regulating health and disease (Zhang et al., 2016). In mouse models of AD and PD, Beclin 1 was shown to mitigate amyloidosis (the buildup of amyloid proteins in heart, liver,

kidney, and other organs) and neurodegeneration (Levine et al., 2011; Pickford et al., 2008; Spencer et al., 2009). Human AD brain sample lysates contain proteolytically cleaved forms of Beclin 1. Selective neuronal expression of these Beclin 1 cleaved products exacerbates neurodegeneration and inflammation in two models of neurodegeneration- a kainic acid-based mouse model of acute excitotoxic neurodegeneration and an hAPP-transgenic mouse model of AD (Bieri et al., 2018). Homozygous loss of the *Becn1* gene causes embryonic death between E7.5 and E8.5 (Yue et al., 2003). On the other hand, heterozygous loss of *Becn1* results in viable, hypomorphic *Becn1*^{+/-} mice with decreased autophagy levels in various cell types (Qu et al, 2003; Pickford et al, 2008), making it a useful model to study autophagy dysregulation. More recently, *Becn1*^{+/-} hypomorph mice were shown to have increased inflammatory response of microglia via NLRP3 activation (Houtman et al., 2019).

For the present study, we generated Beclin^{flox/flox}, LysM^{Cre/Cre} mice— a murine line with a cell-specific knockout of the *Becn1* gene in microglia and monocyte/macrophage cells that express Cre recombinase driven by the LysM transgene. We report a new experimental mouse model for analysis of neuroinflammation following CNS trauma. For this study, we focused on the role of autophagy dysregulation in modulating neuroinflammatory outcomes following TBI. We hypothesize that neuroinflammation and functional defects will be exacerbated in Beclin^{flox/flox}, LysM^{Cre/Cre} mice. Our collective data demonstrates that autophagy dysregulation in microglia and infiltrating monocytes/macrophages, mediated through the tissue-specific knockout of the *Becn1* gene, exacerbates innate immune responses, overall neuroinflammation, and cognitive impairments following TBI.

3.2. Results

3.2.1 LysM-Cre expression is driven in monocytes/macrophages as well as brain-resident microglia.

Our first goal was to determine whether LysM-Cre is a suitable driver to inducibly ablate *Becn1* specifically in microglia and monocytes/macrophages. For this purpose, we crossed LysM^{Cre/Cre} mice to *ROSA26 (R26)*-tdTomato reporter animals and explored the Cre-mediated recombination efficacy in microglia and infiltrating macrophages in sham- and CCI-injured mice (referred to as Sham and TBI, respectively). Microglia and infiltrating myeloid cells were gated by flow cytometry based on expression of cell surface markers CD11b and CD45, and expression of tdTomato⁺ cells was determined within these populations. tdTomato expression should be driven in cells that express LysM; thus, by quantifying tdTomato fluorescence in gated cells we can estimate the percentages of macrophages and microglia that drive expression from this promoter. In TBI mice, approximately 52% of brain-resident microglia and 80% of infiltrating monocytes were tdTomato⁺, while in Sham mice, approximately 56% of microglia were tdTomato⁺ (**Figure 3-1**). Thus LysM-is expressed in a subset of microglia and most macrophages, making it a useful driver to knockout autophagy genes and study the role of autophagy dysregulation in immune cells and neuroinflammation after TBI.

Experimental studies were carried out on age-matched Beclin^{flox/flox}, LysM^{Cre/Cre} and LysM^{Cre/Cre} mice as detailed in the methods. We first isolated bone marrow-derived macrophages (BMDM) from both strains and confirmed the knockout of Beclin 1 at the mRNA and protein levels in the Beclin^{flox/flox}, LysM^{Cre/Cre} mice. (**Figure 3-2**).

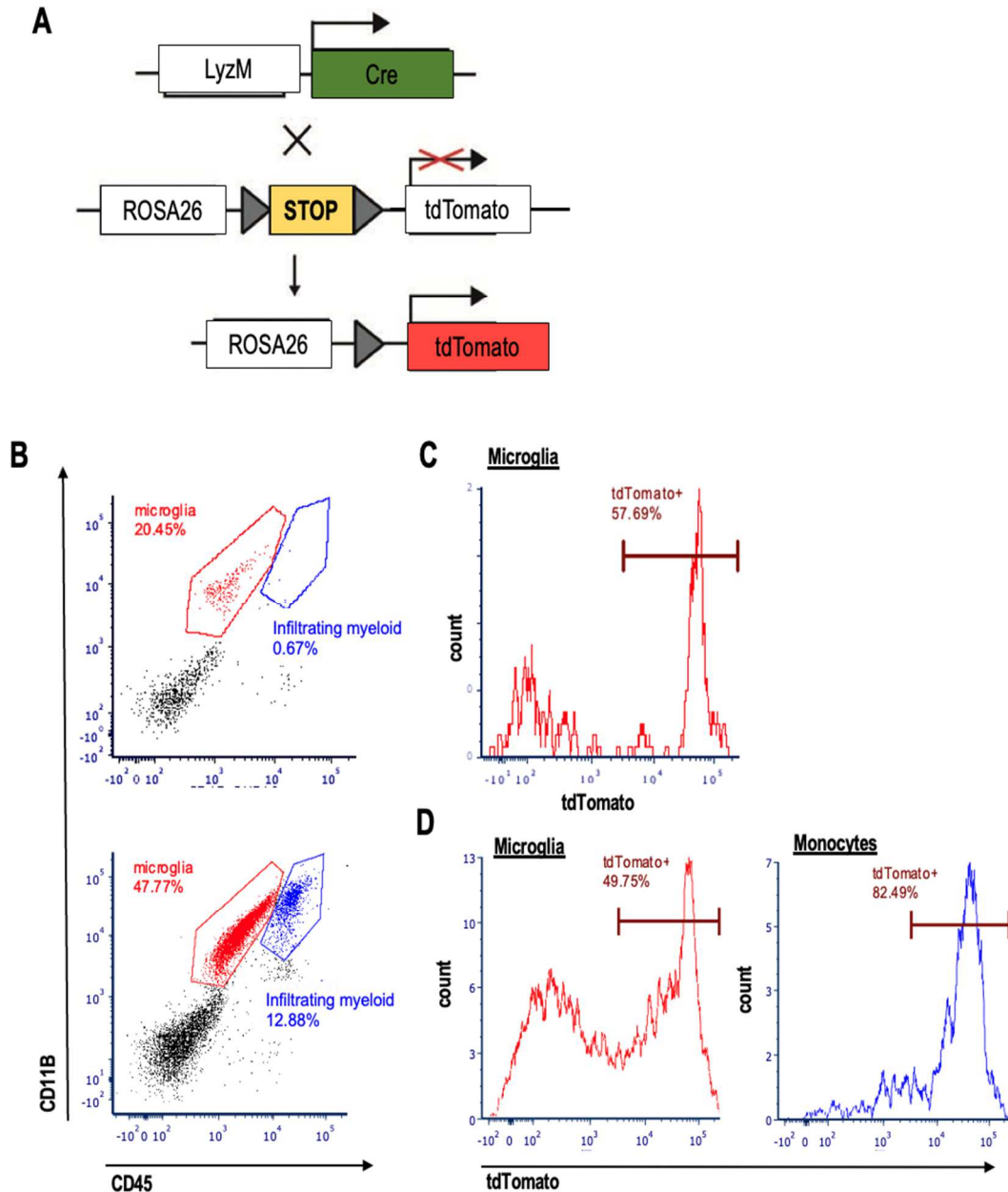


Figure 3-1. Characterization of *LysM*-Cre expression in the microglia and infiltrating monocytes/macrophages. (A) Breeding scheme of *LysM*^{Cre/Cre} mice containing the targeted *LysM*-Cre locus with *R26-tdTomato* indicator mice. (B) Representative gating strategy for microglia (CD11b⁺CD45^{int}) and infiltrating myeloid cells (CD11b⁺CD45^{high}) by flow cytometry in mice at day three in post-TBI (above) and Sham mice (below). (C) Representative histogram indicating the % of tdTomato+ microglia (in red) in Sham mice. (D) Representative histogram indicating the % of tdTomato+ microglia (in red) and tdTomato+ monocytes/macrophages (in blue) at three days post-injury. A Cre-negative littermate served as control. n=5/group.

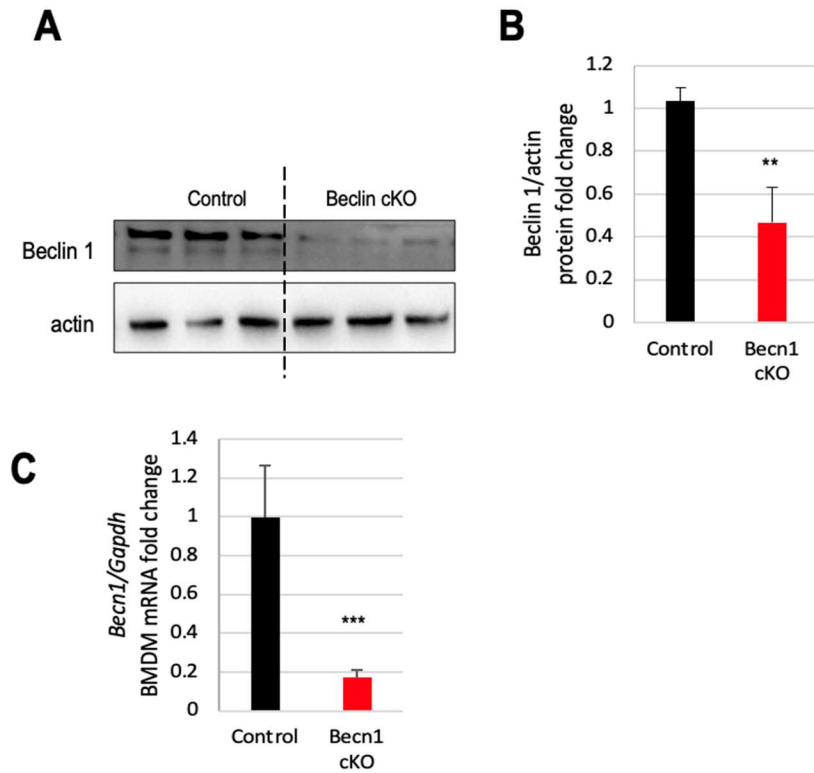


Figure 3-2. *Becn1* knockout in *Beclin*^{flx/flx}, *LysM*^{Cre/Cre} (*Becn1* cKO) mice results in decreased *Beclin1* mRNA and protein levels in bone marrow-derived macrophages (BMDM) compared to *LysM*^{Cre/Cre} (Control) mice. (A) Western blot assessing *Beclin 1* protein levels in isolated BMDM from *Becn1* cKO mice and control mice. (B) Corresponding quantification showed significant reduction in *Beclin 1* protein levels in the *Becn1* cKO mice compared to the Control mice. (C) BMDM mRNA quantification by qPCR showing that *Becn1* cKO have significantly reduced *Becn1* mRNA compared to Control mice. Data are expressed as mean \pm SEM. $n=3$ /group. ** $p < 0.01$, * $p < 0.05$ compared to Control mice; student's unpaired t test.

For the sake of convenience, *Beclin*^{flox/flox}, *LysM*^{Cre/Cre} mice, and *LysM*^{Cre/Cre} mice will henceforth be referred to as *Becn1* conditional knockout (*Becn1* cKO) mice and Control mice, respectively (**Figure 3-2**).

3.2.2. *Becn1* deficiency in microglia and monocytes/macrophages enhances global transcription changes in mice brain cortices at three days post-TBI.

To determine the inflammatory consequences of *Becn1* deficiency in microglia and infiltrating macrophages in the acute phase of TBI, we evaluated cortical brain tissue at the injury site using NanoString's nCounter technology. The Neuroinflammation panel tested a total of 757 genes and 13 internal controls within three themes: Immunity & Inflammation, Neurobiology & Neuropathology, and Metabolism & Stress. Principal component analysis (PCA) of all normalized gene counts revealed clustering of four experimental groups across the first two principal coordinates, which accounted for 75.2% and 8.5%, respectively, of the total variation across samples (**Figure 3-3A**). Injury-related effects were captured on Coordinate 1, separating the TBI groups on the right from the left; genotype differences due to *Becn1* deficiency were captured on Coordinate 2. Interestingly, the Control TBI group and the *Becn1* cKO TBI group showed greater separation than the Control/Sham and the *Becn1* cKO/Sham groups. These data suggest that the transcriptional changes observed in the TBI groups are exacerbated by genotype-dependent changes. Heatmap expression profiling showed clustering of the four groups based on injury and genotype (**Figure 3-3B**). Based on the clustering patterns, we observed some overlap between the Control Sham and *Becn1* cKO Sham groups; however, the Control TBI and *Becn1* cKO TBI groups appeared more segregated. These findings suggest that while genotype-dependent differences are minimal at baseline

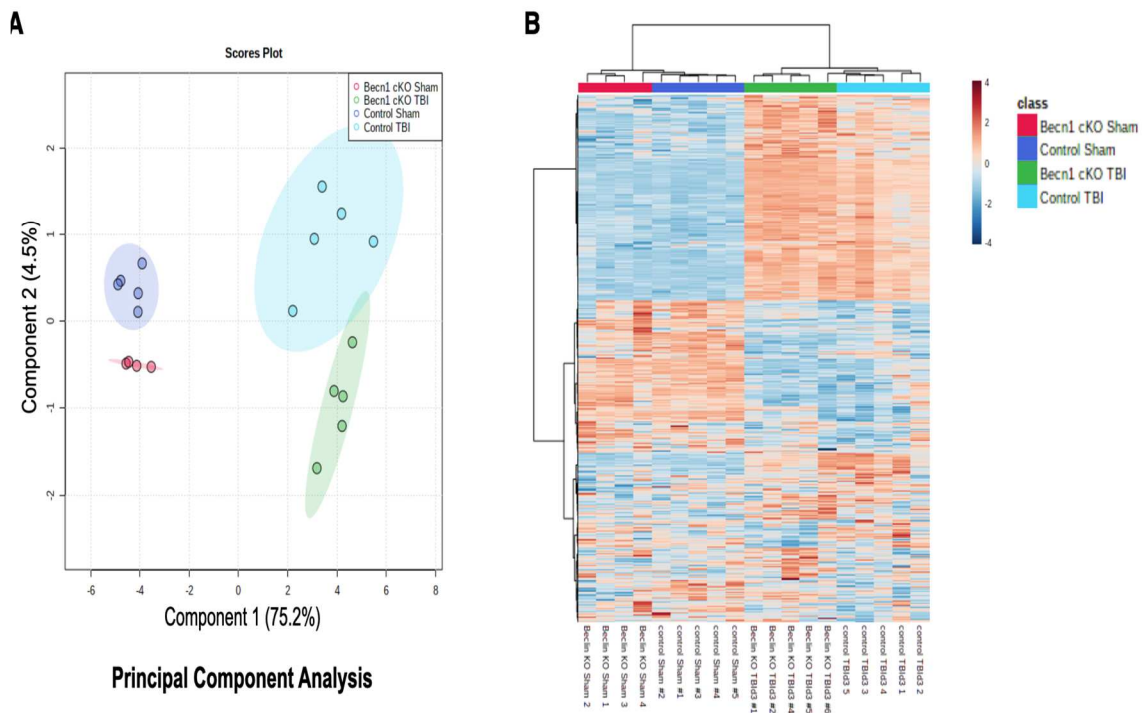


Figure 3-3. *Becn1* deficiency in microglia and infiltrating monocytes/macrophages alters clustering of various groups, based on NanoString nCounter® Neuroinflammation panel, in mice brain cortices. A NanoString nCounter® Neuroinflammation panel was used to assess transcriptional changes in the injured brain cortex at three days post-injury. **(A)** Principal component analysis (PCA) was performed using all normalized gene counts in the four sample groups: Control Sham (red), *Becn1* cKO Sham (yellow), Control TBI (green), and *Becn1* cKO TBI (blue). For PCA plots, each point represents a data set from an individual animal. The 95% confidence intervals are indicated by elliptical shaded areas per group. Data were sum normalized, log transformed, and mean centered. PCA plots generated using MetaboAnalyst. The first principal coordinate accounted for most of the variation (75.2%) across samples and separated the groups by injury, while the second principal coordinate (4.2%) separated the groups by genotype. **(B)** Heatmap expression profiling of normalized gene levels showed significant clustering of the four groups based on injury and genotype.

(hence the lack of genotype-specific clustering), injury-induced changes are exacerbated by genotype. We used volcano plots to visualize the Log_2 (fold change) and $-\text{Log}_{10}$ (p-values) of each gene in pairwise comparisons, highlighting certain genes that meet the indicated cutoff for p-value (**Figure 3-4 A-D**) and labelling ones particularly implicated in inflammation and innate immunity. Based on a threshold p value of $p < 0.05$ to define differential expression, we observed an increase in the number of differentially upregulated genes in the pairwise comparison of *Becn1* cKO TBI mice vs. *Becn1* cKO Sham mice compared to the pairwise comparison of Control TBI vs. Control Sham (**Figure 3-4E, top two lines of the table**).

3.2.3. *Becn1* deficiency in microglia and infiltrating monocytes/macrophages increases innate immunity gene expression in mice brain cortices post-TBI.

Gene ontology (GO) analysis of differentially expressed genes between *Becn1* cKO TBI mice and Control TBI groups revealed that the differentially expressed genes play key roles in multiple biological processes related to the regulation of innate immune responses. (**Figure 3-5A**). Innate immune responses after TBI are known to contribute to the pathophysiology and disease outcomes (Needham et al., 2019). A heatmap of the differentially expressed genes indicate that *Becn1* knockout in microglia and monocytes/macrophages drives increased transcription of genes involved in innate immune responses at three days post-TBI (**Figure 3-5B**). Some of these include *Irf8* (* $p < 0.05$), *Nf-kb* ($p = 0.051$), *Ly9* (* $p < 0.05$), *Csfr1* ($p = 0.060$), *Lcn2* (** $p < 0.01$), *Csfr* (**** $p < 0.001$), and *Nod1* (* $p < 0.05$) (**Figure 3-5C**).

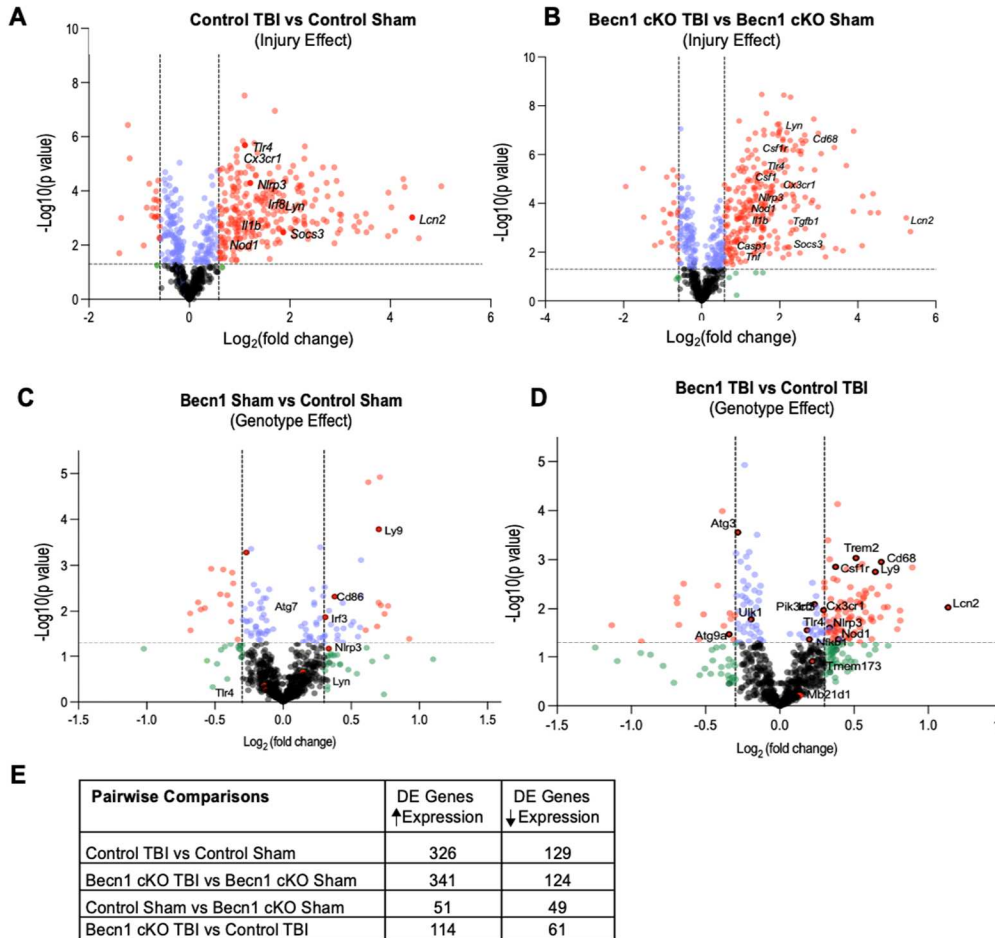


Figure 3-4. *Becn1* deficiency in microglia and infiltrating monocytes/macrophages significantly alters transcription levels of neuroinflammatory genes in mice brain cortices at three days post-TBI. Volcano plots in (A-D) depict the $-\text{Log}_{10}$ (p-values) on the x axis and \log_2 (fold change) of the indicated pairwise comparison of differential gene expression. (A) Control TBI vs. Control Sham; (B) *Becn1* cKO TBI vs. *Becn1* cKO Sham; (C) *Becn1* cKO Sham vs. Control Sham; (D) *Becn1* cKO TBI vs. Control TBI. Dotted lines on the x-axis and y-axis show the thresholds used to visualize fold change and p value benchmarks. The dotted lines at $x=-0.58$ and $x=0.58$ denote a two-fold change in gene expression in the pairwise comparison. The dotted line at $y=1.3$ denotes a p value of 0.05; genes above the line pass the significance threshold. Gray dots represent genes that did not pass any threshold criteria. Blue dots represent genes that pass the statistical threshold, but not the fold change threshold set for that comparison. Green dots show genes that pass the fold change threshold but not the statistical threshold. Red dots indicate genes that pass the statistical threshold and have fold changes greater than 2. (E) Table indicating the number of differentially expressed genes in the indicated pairwise comparisons. When determining if a gene was differentially expressed or not, a p value of < 0.05 was used as the threshold.

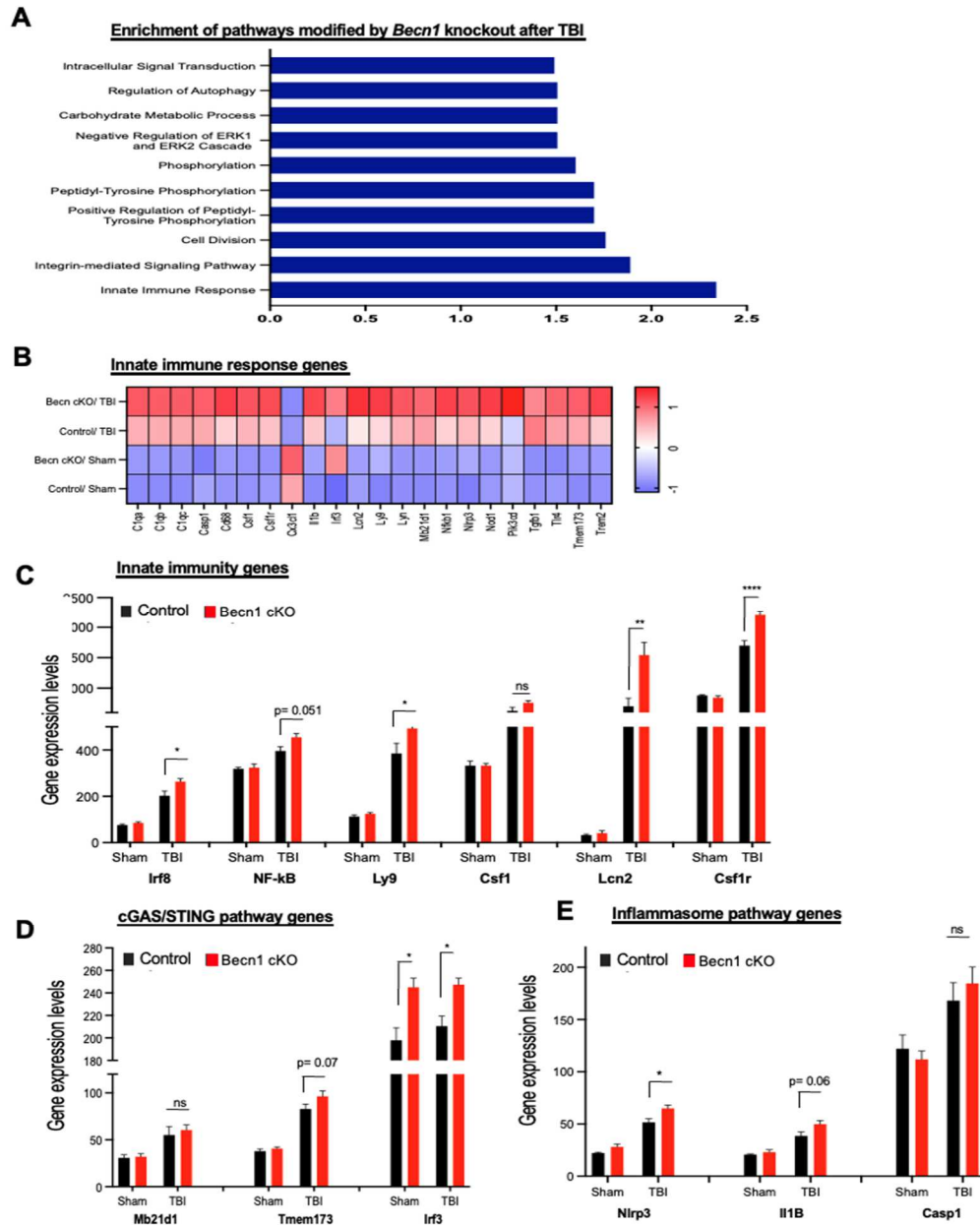


Figure 3-5. *Becn1* deficiency in microglia and infiltrating monocytes/macrophages increased expression of genes involved in innate immunity in mice brain cortices at 3 days post-TBI. (A) Gene Ontology of pathways modified by *Becn1* deficiency in microglia/macrophages after TBI, generated using David software. (B) Heatmap of genes related to innate immune response that are differentially expressed. Color coding is based on z-score scaling. (C) Normalized mRNA gene expression of genes related to innate immune response. (D) Normalized mRNA gene expression of genes related to the cGAS/STING pathway. (E) Normalized mRNA gene expression of genes related to the inflammasome pathway. Data are expressed as mean \pm SEM; n=4/5 per group. *p < 0.05, **p < 0.01, ***p < 0.005, ****p < 0.001 vs. Control TBI groups (genotype effect); ^^p < 0.01, ^^^p < 0.001 vs corresponding Sham group (injury effect).

We found significant upregulation of genes involved in the NLRP3 inflammasome signaling pathway and cGAS/STING signaling pathways in *Becn1* cKO TBI mice compared to Control TBI. **(Figure 3-5D-E)**. Activation of these pathways occurs after TBI and contributes to neuroinflammation and neurological outcomes following TBI. Within the inflammasome pathway, *Becn1* cKO mice showed increased transcriptional expression of *Nlrp3* (* $p < 0.05$) and *Il-1b* ($p = 0.06$) at three days post-TBI relative to Control mice, while *Casp1* levels were unchanged ($p = 0.1045$). The cGAS/STING pathway showed increased transcriptional levels on *Tmem173*/STING in *Becn1* cKO mice ($p = 0.05$) following TBI, while *Mb21d1*/cGAS level was unaffected by genotype in either the Sham or TBI groups. Interestingly, expression of *Ifr3*, a downstream regulator of the cGAS/STING signaling pathway, differed by genotype in both the Sham and TBI groups (* $p < 0.05$). As a complementary method to support the NanoString data, we confirmed the differential expression patterns of some of these genes and other general inflammatory markers by qRT-PCR **(Figure 3-6A-D)**.

3.2.4. *Becn1* deficiency in microglia and infiltrating monocytes/macrophages increases expression of proteins involved in innate immunity and inflammation post-TBI.

We next used cortical brain samples from Control and *Becn1* cKO Sham and TBI mice to measure protein levels of markers associated with inflammation by western blotting **(Figure 3-7)**. At three days post-TBI, we observed increased levels of pro-inflammatory markers NOX2 (* $p < 0.05$), iNOS (* $p < 0.05$), and NLRP3 (* $p < 0.05$) in *Becn1* cKO TBI mice compared to Control TBI mice. Moreover, cGAS and STING protein levels were

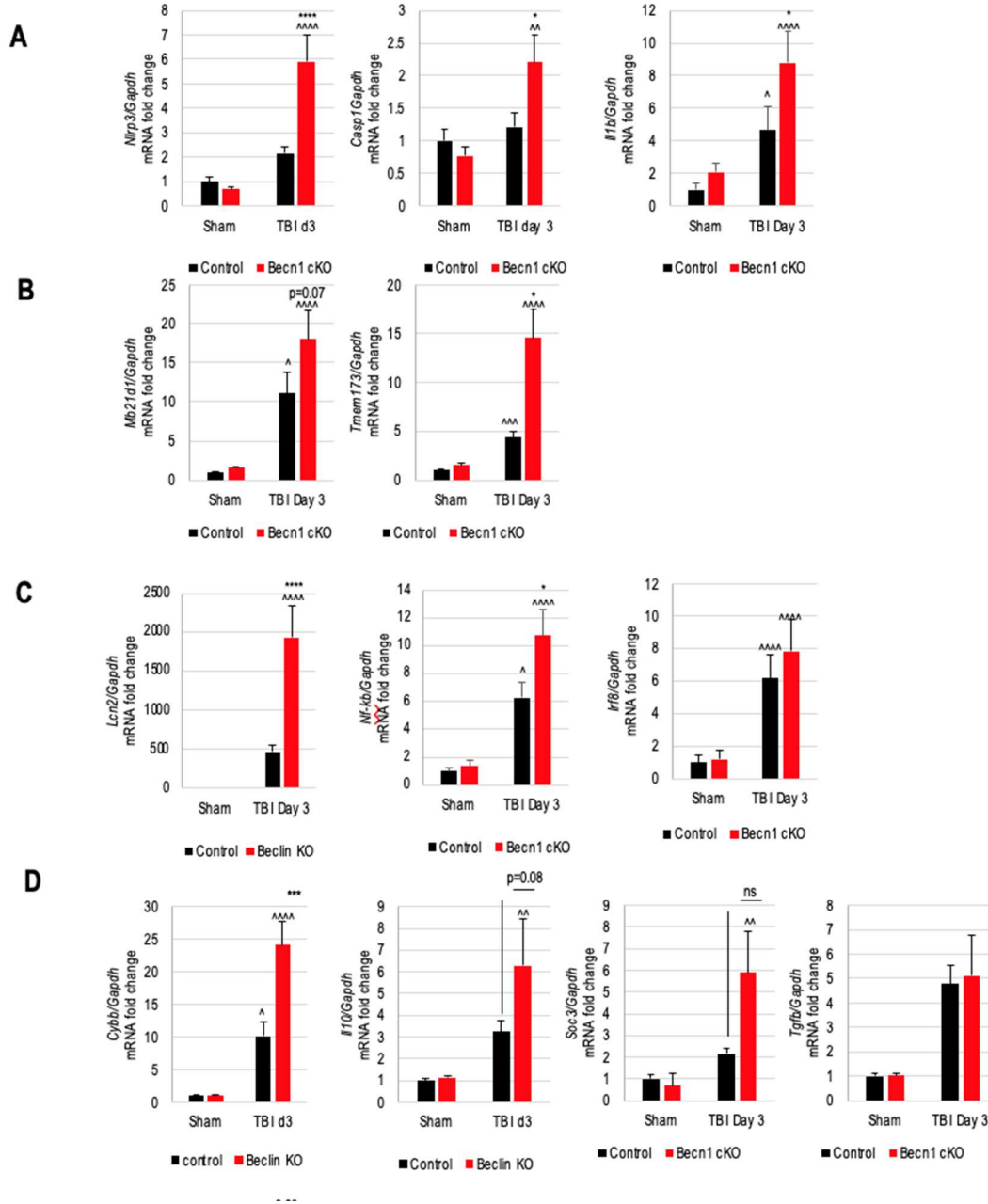


Figure 3-6. *Becn1* deficiency in microglia and infiltrating monocytes/macrophages increases expression of pro-inflammatory and innate immune genes in mice brain cortices post-TBI. We confirmed increased mRNA levels of genes in *Becn1* cKO TBI mice compared to Control TBI mice for (A) NLRP3 signaling pathway and (B) cGAS/STING signaling pathways and (C) genes involved in general innate immune responses. (D) We also saw increased gene expression of the general inflammatory marker NOX2 (*Cybb*), whereas *Il10*, *Socs3*, and *Tgfb* were not significantly different in the *Becn1* cKO mice after TBI. Data are expressed as mean \pm SEM; n = 5/group *p < 0.05, **p < 0.01, ***p < 0.005, ****p < 0.001 vs. Control TBI groups (genotype effect); ^p < 0.01, ^^^p < 0.001 (injury effect).

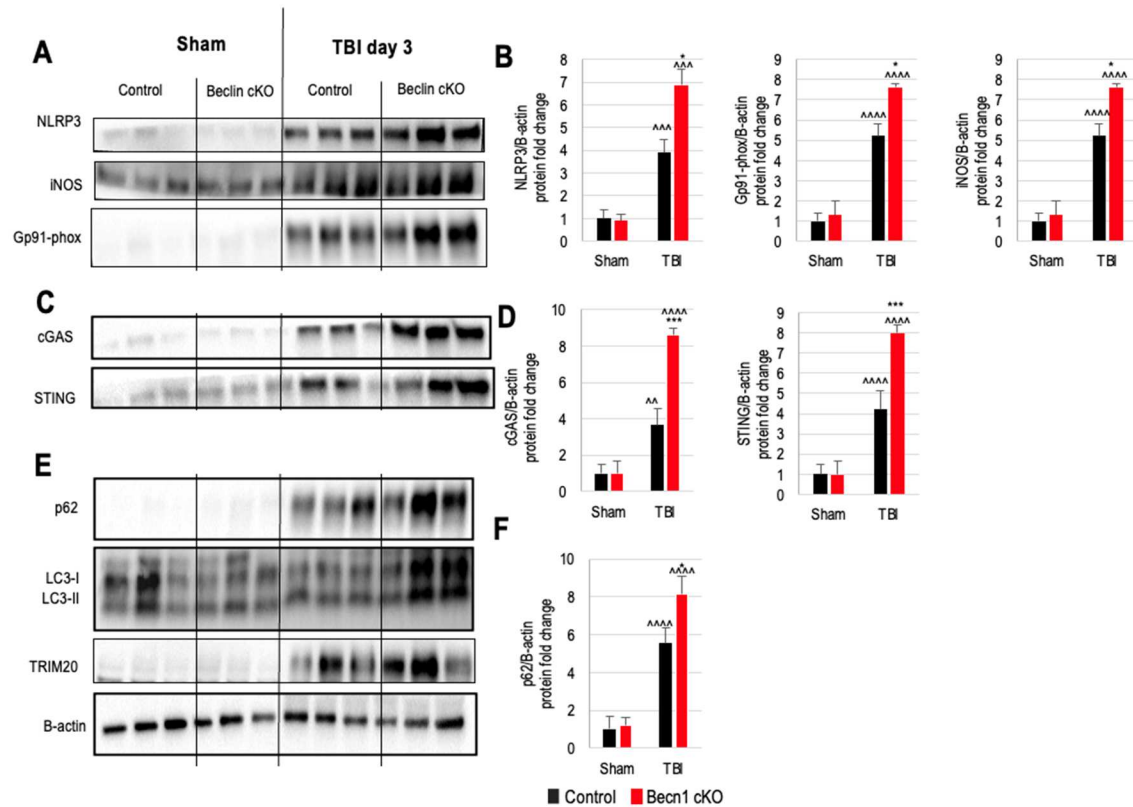


Figure 3-7. *Becn1* deficiency in microglia and monocytes/macrophages exacerbates neuroinflammation and innate immune gene pathways in mice brain cortices post-TBI. Western blotting was performed to assess changes in protein expression of pro-inflammatory markers and proteins involved in inflammasome pathways, cGAS/STING pathways, and autophagy. **(A)** *Becn1*cKO mice show increased levels of pro-inflammatory proteins NOX2, iNOS and NLRP3. **(B)** Quantification of all data for the representative blots shown in A. **(C-D)**. Representative western blots **(C)** and quantification **(D)** showing that *Becn1*cKO have increased levels of cGAS and STING proteins compared to Control TBI mice at three days post-injury. **(E)** Data are expressed as mean \pm SEM. * $p < 0.05$, *** $p < 0.005$, Control/TBI mice (genotype effect); ^^^ $p < 0.001$ vs. corresponding Sham mice (injury effect); two-way ANOVA using Tukey post-hoc tests (n=4-5/group).

also significantly higher in the *Becn1* cKO mice ($***p < 0.005$ compared to Control TBI for both markers), suggesting upregulation of cGAS/STING signaling in *Becn1* cKO mice after injury. When we analyzed markers of autophagy, we observed increased levels of the autophagosomal markers LC3-II and p62 ($*p < 0.05$) in *Becn1* cKO mice compared to the Control TBI mice, consistent with the prediction of greater autophagy impairment in these mice after injury (**Figure 3-7E-F**). No significant differences were observed in baseline levels of the autophagy markers between *Becn1* cKO Sham and Control Sham mice.

We next performed flow cytometry on mice brain cortices to determine whether microglia and infiltrating monocytes/macrophages were differentially impacted by *Becn1* deficiency (**Figure 3-8**). At three days post-TBI, we observed that *Becn1* cKO mice had a significantly higher percentage of IL-1 β ⁺ microglia compared to Control mice ($**p < 0.01$), whereas the IL-1 β level did not significantly differ between genotypes (**Figure 3-8A-B**). Infiltrating monocytes/macrophages in *Becn1* cKO mice also showed an increase in the percentage of IL-1 β ⁺ cells, as well as a strong trend toward increased IL-1 β expression ($p = 0.055$, **Figure 3-8C-D**). As IL-1 β is a downstream target of NLRP3 inflammasome activation, the observed changes complement our earlier findings that the NLRP3 signaling pathway is upregulated in *Becn1* cKO mice compared to Control mice after TBI. The data suggest that exacerbated inflammatory responses in *Becn1* cKO mice are mediated through both microglia as well as infiltrating monocytes/macrophages. The possible difference between microglia and monocytes/macrophages regarding an effect on IL-1 β expression level may be because *Becn1* is expected to be almost completely knocked out in the infiltrating monocytes/macrophages based on LysM-driven *tdTomato*

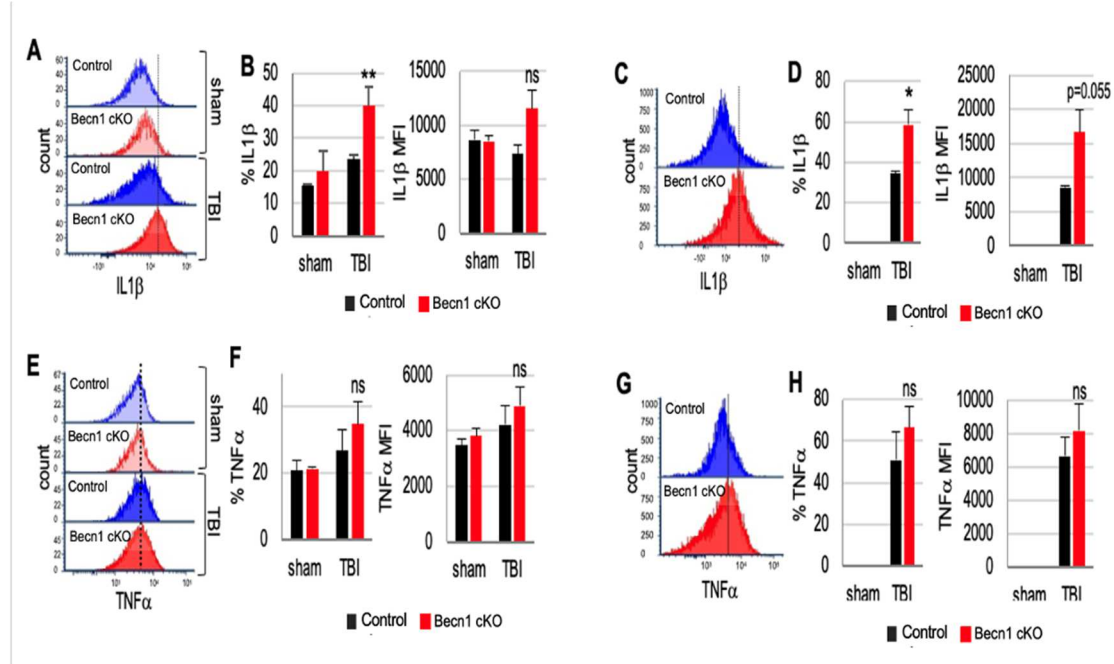


Figure 3-8. The effects of *Becn1* knockout on inflammatory responses in microglia and monocytes/macrophages from mice brain cortices post-TBI. (A) Representative histograms showing the relative mean fluorescence intensity (MFI) of IL-1 β in microglia. (B) Percentage of IL-1 β + microglia and IL-1 β MFI at three days post-TBI compared to Control mice. (C) Representative histograms showing the relative MFI of IL-1 β in infiltrating monocytes/macrophages at three days post-TBI. (D) Percentage of IL-1 β + monocytes/macrophages and IL-1 β MFI at three days post-TBI compared to Control mice. (E) Representative histograms showing the relative MFI of TNF- α in microglia at three days post-TBI and (F) percentage of TNF- α cells and TNF- α MFI levels. (G) Representative histograms showing the relative MFI of TNF- α in infiltrating monocytes/macrophages with (F) percentage of TNF- α + monocytes/macrophages and MFI levels. Data are expressed as mean \pm SEM ($n = 3/4$ group). * $p < 0.05$, *** $p < 0.005$ vs Control TBI mice; two-way ANOVA using Tukey post-hoc tests for multiple comparisons.

expression, whereas only a subset of the resident microglia are expected to show *Becn1* knockout (**Figure 3-1**). No baseline differences were detected between the *Becn1* cKO Sham mice and Control Sham mice.

On examining the expression of another pro-inflammatory marker by flow cytometry, we did not see significant changes in TNF- α expression levels between *Becn1* cKO TBI mice and Control TBI mice (**Figure 3-8E-H**), suggesting that not all inflammatory pathways are impacted by autophagy dysregulation in microglia and monocytes/macrophages.

3.2.5. *Becn1* deficiency in microglia and infiltrating monocytes/macrophages does not alter fine motor coordination in TBI or Sham-injured mice.

As *Becn1* deficiency in microglia and monocytes/macrophages resulted in increased innate immune and neuroinflammatory responses after TBI, we next wanted to assess whether these changes translate to altered behavioral outcomes in mice after injury. We performed beam walk assessment to assess changes in impairments in fine motor coordination in mice at one day, three days, seven days, 14 days, 21 days, and 28 days post-injury (**Figure 3-9A**). We observed a significant increase in the number of footfalls beginning on the first day post-injury and persisting through the 28th day post-TBI in both genotypes (Injury effect: $F(1, 49) = 1910, p < 0.001$). As no significant differences were observed between genotypes for the sham-injured groups, we infer that *Becn1* knockout does not result in any baseline difference in fine motor coordination. Moreover, no differences were observed between the TBI groups throughout the time course, indicating that *Becn1* cKO does not exacerbate motor impairment after injury (**Figure 3-9B**). This

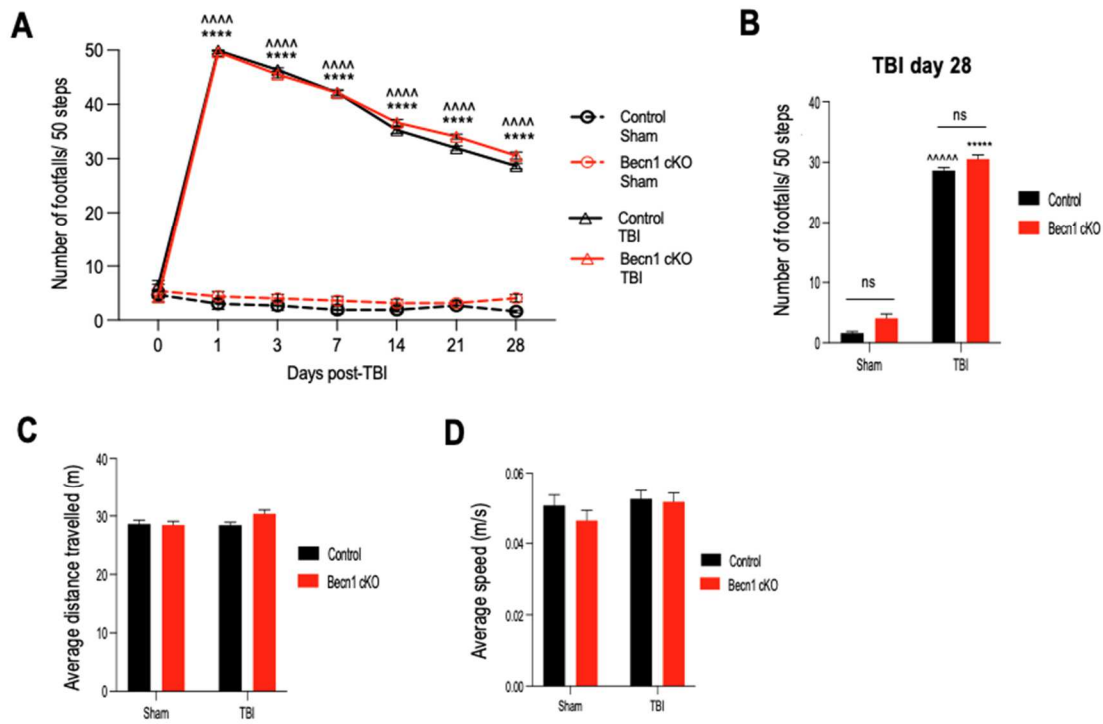


Figure 3-9. *Becn1* deficiency does not exacerbate TBI-induced impairments in fine motor coordination. (A) Number of foot faults per 50 steps across various time points after TBI. (B) Number of foot faults at 28 days post-TBI. We did not observe any significant genotype differences between Sham and TBI groups. We also measured (C) distance traveled and (D) average speed during novel object recognition habituation testing (day 15 post-TBI) and observed no genotype-dependent changes between both Sham and TBI groups. Data are expressed as mean \pm SEM ($n = 12-16/\text{group}$). $^{****}p < 0.001$ for Control TBI vs. Control Sham mice; $^{****}p < 0.001$ for Becn1 cKO TBI vs. Becn1 cKO Sham mice; analyzed by repeated two-way ANOVA using Tukey post-hoc tests for multiple comparisons.

finding was further supported by analyzing distance traveled and average speed during novel object recognition (NOR) habituation testing at day 15 post-TBI; no genotype-dependent differences were observed between *Becn1* cKO mice and Control under Sham or injury conditions (**Figure 3-9C-D**). Collectively, the data in **Figure 3-9** indicate that *Becn1* cKO does not exacerbate fine motor impairment under baseline conditions or after TBI.

3.2.6. *Becn1* deficiency in microglia and infiltrating monocytes/macrophages exacerbates TBI-associated deficits in spatial learning and declarative memory.

We tested spatial learning and memory in mice using Morris Water Maze (MWM) testing from 21-25 days post-TBI (**Figure 3-10A-D**). Both *Becn1* cKO TBI and Control TBI mice required significantly more time to locate the hidden platform during acquisition training compared to *Becn1* cKO Sham and Control Sham mice. This increased time is indicative of an injury-dependent spatial learning deficit (Injury effect: $F_{(1, 49)} = 1743$, $p < 0.001$). However, during probe trial testing, *Becn1* cKO mice spent significantly less time exploring the escape quadrant compared to the Control TBI group, indicating a relative impairment in spatial learning ($*p < 0.05$) (**Figure 3-10D**).

We also investigated the search strategies used by mice to locate the hidden platform during probe trial testing (**Figure 3-10B-C**). Sixty-seven percent of *Becn1* cKO Sham and 60% of Control Sham mice followed a spatial search strategy to find the platform during probe trial testing. On the other hand, *Becn1* cKO TBI mice and Control TBI mice showed decreased spatial search strategy usage compared to their Sham counterparts and increasingly relied on sequential and looping strategies to locate the platform. In

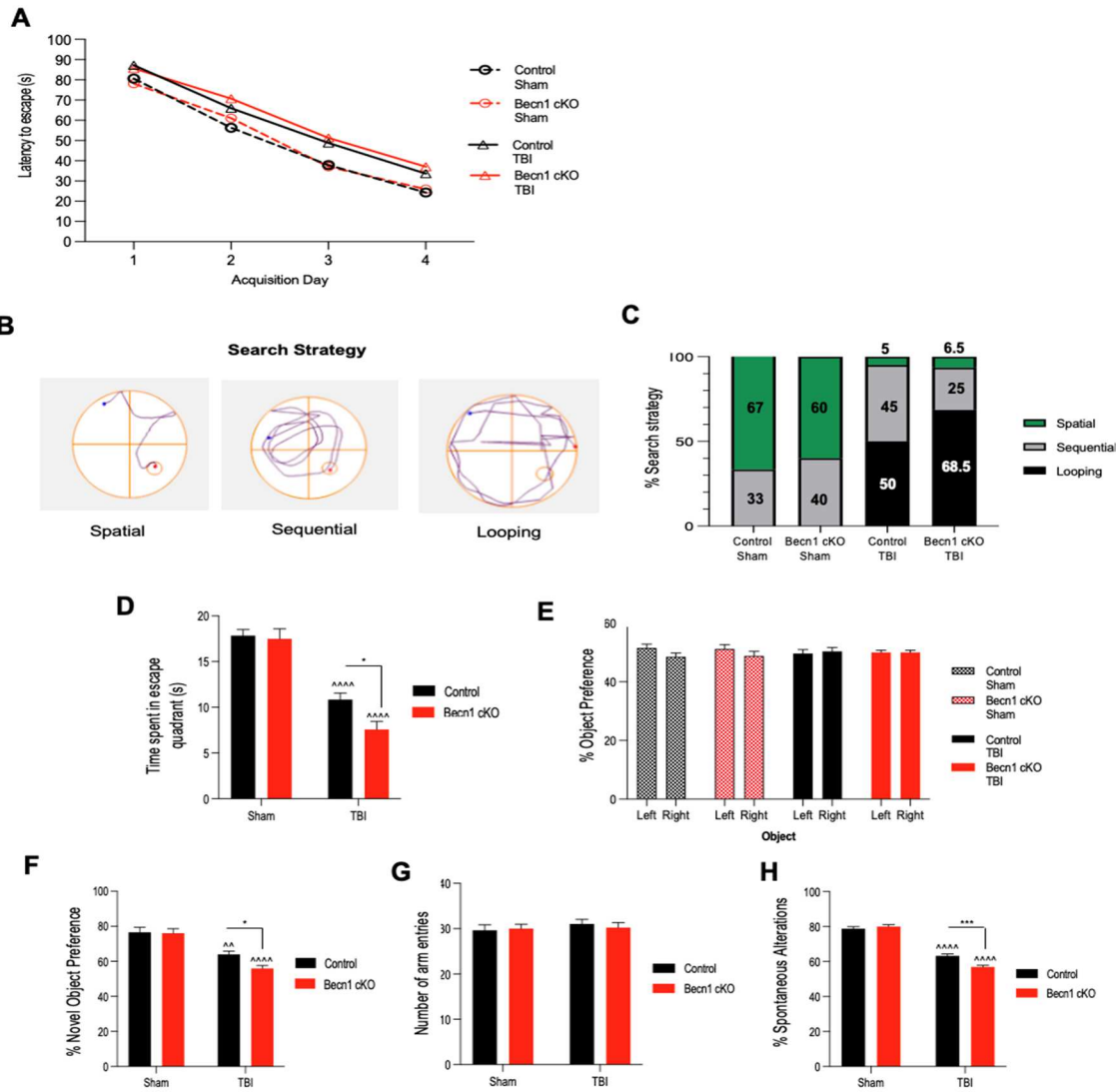


Figure 3-10. Deficits in declarative memory, spatial learning, and working memory are exacerbated in *Becn1* cKO mice after TBI. (A) Graph of latency to escape during acquisition days 1-4 of the Morris Water Maze (MWM). (B) Representative images of search strategy used during the probe trial, and (C) the percentage composition for each strategy (spatial, systematic, and looping) among the groups. (D) Time spent in the escape quadrant during MWM probe trial testing as a measure of spatial learning. (E) Object familiarization for Novel Object Recognition (NOR) testing. All groups of mice interacted equally between both the left and right objects, eliminating side bias. (F) Percentage of time spent with the novel object during the test phase as a measure of declarative memory. (G) Number of arm entries per group during Y-maze testing, showing an equal number of arm entries among the groups. (H) Percentage of spontaneous alterations in the Y-maze task as a measure of hippocampal-dependent working memory. Data are expressed as mean \pm SEM. $n=12-16/\text{group}$. $**p < 0.01$, $***p < 0.005$, vs. *Becn1* cKO TBI (genotype effect); $^{\wedge}p < 0.01$, $^{\wedge\wedge}p < 0.005$, $^{\wedge\wedge\wedge}p < 0.001$ compared to corresponding Sham group (injury effect); two-way ANOVA using Tukey post-hoc tests for multiple comparisons.

particular, the *Becn1* cKO TBI mice had greater reliance on looping compared to the Control TBI (68.5% in *Becn1* cKO TBI mice compared to 50% in Control TBI mice).

We also tested declarative memory in mice using NOR testing from 15-17 days post-TBI (**Figure 3-10E-F**). During familiar object acclimatization, there were no significant differences among all experimental groups in the amount of time that was spent with either of the two objects presented, demonstrating the absence of any side bias during testing (**Figure 3-10E**). During NOR testing, all Sham mice showed approximately 75% preference for the novel object over the familiar object and no differences were detected between the *Becn1* cKO Sham and Control Sham mice. However, both genotypes of mice showed decreased preference for the novel object after TBI. Moreover, *Becn1* cKO TBI mice spent less time exploring the novel object (NO) compared to Control TBI mice (* $p < 0.05$) (**Figure 3-10F**). These findings suggest that *Becn1* deficiency in microglia and monocytes/macrophages exacerbates declarative memory impairments after injury.

We further investigated cognitive function using the Y-maze task on day eight post-TBI to assesses hippocampal-dependent working memory. All experimental groups of mice had a relatively equal number of arm entries during testing (**Figure 3-10G**). *Becn1* cKO TBI mice showed a significant decrease in the percentage of spontaneous alterations compared to Control TBI mice (* $p < 0.05$) (**Figure 3-10H**). This finding suggests that *Becn1* deficiency in microglia and monocytes/macrophages exacerbates impairments in hippocampal-dependent working memory after injury.

3.2.7. *Becn1* deficiency in microglia and monocytes/macrophages exacerbates hippocampal neurodegeneration but does not significantly increase overall cortical lesion volume after injury.

Hippocampal neuronal cell loss and cortical lesion volume were assessed using unbiased stereology at the end of the day 28 post-TBI period to examine the effect of *Becn1* deficiency in microglia and monocytes/macrophages on TBI-associated neurodegeneration outcomes. As expected, TBI resulted in a significant loss of neurons in the dentate gyrus (DG) subregion of the ipsilateral hippocampus in both the *Becn1* cKO TBI and Control TBI mice compared to their Sham counterpart mice. No baseline difference in the ipsilateral DG neuronal count was observed between *Becn1* cKO Sham and Control sham mice, implying that autophagy dysregulation through *Becn1* knockout in microglia does not cause basal hippocampal neurodegeneration. On the other hand, we observed significantly lower ipsilateral DG neuronal counts in the *Becn1* cKO TBI mice compared to the Control TBI mice. This suggests that *Becn1* knockout exacerbates neuronal loss in the hippocampus following TBI (**Figure 3-11A**).

We also assessed cortical neurodegeneration by quantifying lesion volume. TBI resulted in a large cortical lesion in the ipsilateral cortex in both *Becn1* cKO mice and Control TBI mice. However, there was no significant difference in the measured lesion volumes in *Becn1* cKO TBI mice compared to Control TBI mice ($t_{(12)}=2.030$, $p=0.073$ vs control TBI, **Figure 3-11B**). Overall, these findings suggest that *Becn1* deficiency in microglia and monocytes/macrophages exacerbates TBI-associated neurodegeneration, at least in the hippocampal DG.

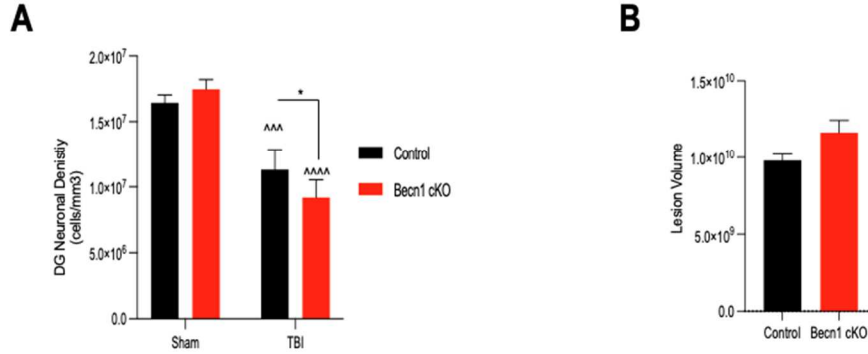


Figure 3-11. Becn1 deficiency in microglia and monocytes/macrophages exacerbates hippocampal neurodegeneration but not overall lesion volume. At day 28 post-TBI, ipsilateral hippocampal neuronal cell density and lesion volume were assessed by stereological quantification **(A)** Representative images of cresyl violet stained brains and neurons in the dentate gyrus (DG) region of the ipsilateral hippocampus (20x magnification) across all experimental groups. **(B)** Quantification of neurons in the ipsilateral DG subregion revealing TBI-induced neuronal cell loss. There was also a significant increase in neuronal cell loss in the Becn1 cKO/TBI mice compared to the compared to control/TBI mice. **(C)** Representative images of a cresyl violet stained TBI brain with missing cortical tissue, lesion, outlined in red. **(D)** Quantification of lesion volume showing no increase in the Becn1 cKO TBI mice compared to the Control TBI group (p=0.073 by Student's unpaired t-test).

3.2.8. Expression of inflammation and innate immunity genes is not significantly elevated by *Becn1* deficiency in microglia and monocytes/macrophages at 28 days post-TBI.

Lastly, as we observed functional changes in *Becn1* cKO mice at later time points following injury, we examined the expression levels of select inflammation and innate immunity genes in mice brain cortices at day 28 post-TBI. Using qPCR, we observed no differences in the expression of select genes of the NLRP3 inflammasome pathway, the cGAS-STING pathway, or general markers of inflammation in *Becn1* cKO TBI mice relative to Control TBI mice at day 28 post-TBI (**Figure 3-12**). More biochemical analysis needs to be carried out to test for long-term changes at the protein level.

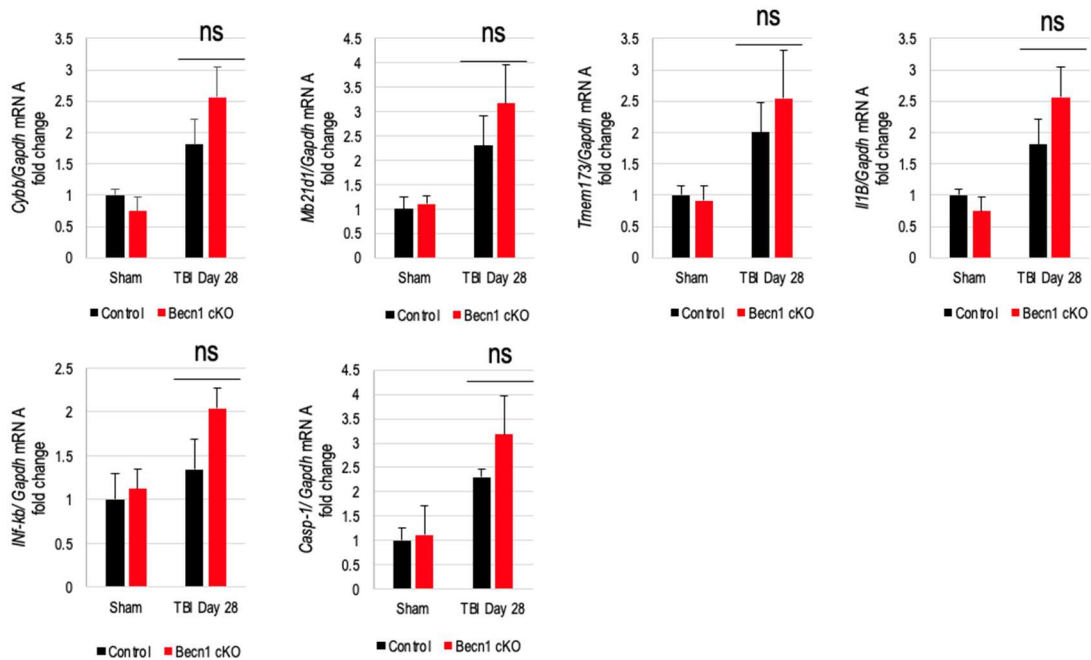


Figure 3-12. Expression levels of pro-inflammatory and innate immune genes in brain cortices at 28 days post-TBI. Data are expressed as mean \pm SEM. n=5/group; two-way ANOVA using Tukey post-hoc tests for multiple comparisons.

3.3. Summary and Future Directions

This work is among the first to evaluate the tissue-specific role of autophagy in brain-resident microglia and infiltrating monocytes/macrophages in regulating neuroinflammation and associated functional outcomes after TBI. We generated a mouse line with a cell-specific knockout of the autophagy gene *Becn1* in microglia and monocytes/macrophages and observed decreases in *Becn1* mRNA and Beclin 1 protein levels in BMDM. This makes this mouse line a suitable tool for assessing the effect of autophagy dysregulation in microglia and monocytes/macrophages on outcomes within the brain after injury or other pathological conditions. For the present study, our findings demonstrate that autophagy dysregulation in these immune cells exacerbates neuroinflammation, innate immune responses, and cognitive impairments in the acute phases following TBI. To summarize some of the significant findings:

1. Autophagy dysregulation through *Becn1* deficiency in microglia/monocytes exacerbates inflammatory responses in the brain after TBI, both at the transcriptional gene level as well as the protein level. The key pro-inflammatory proteins examined in this study were iNOS, NOX2 and TNF- α . Some of the specific innate immunity pathways impacted by *Becn1* deficiency after injury include the NLRP3 inflammasome pathway and the cGAS/STING signaling pathway. These pathways are upregulated after TBI in response to stimulation of innate immunity receptors by DAMPs released from dying and damaged cells following injury and have been associated with poorer neurological outcomes in mice after TBI. (Barrett et al., 2020; Iererra et al., 2020)
2. Autophagy dysregulation in microglia and infiltrating monocytes/macrophages increases TBI-associated hippocampal neurodegeneration after TBI. This finding

indicates that regulation of autophagy in brain immune cells impacts surrounding cells in the brain following TBI.

3. Mice with autophagy dysregulation have worse impairments in cognitive learning and memory after TBI. As this inhibition of autophagy occurs microglia/monocytes based on the cell-specific *Becn1* knockout strategy, it highlights the role that brain immune cell autophagy plays in mediating functional outcomes after TBI.

Immediate future directions for this study will include the following:

1. A more thorough assessment of biochemical changes at the day 28 time point post-TBI, looking at changes in protein levels of markers involved in inflammation and innate immunity. The goal of this experiment would be to better understand what (if any) changes in inflammation and innate immunity due to autophagy dysregulation persist at the later phases of injury.
2. Assessment of biochemical changes in ipsilateral hippocampal samples at three days post-injury. Most of our data focuses on biochemical changes in mice brain cortices. As we have observed hippocampal-dependent changes in functional outcomes, it will be useful to test for corresponding changes specifically in the hippocampus.
3. Morphological assessment of microglia at day 28 post-TBI in cortical brain sections stained with Iba1.

Our tissue-specific knockout in mice results in knockout of the *Becn1* gene in microglia and monocytes from birth, however no significant phenotypic differences were observed in these mice in terms of weight and behavioral outcomes. *Becn1* deficiency in

microglia/monocytes does result in some baseline changes, as observed from differential gene expression visualized by volcano plot in the pairwise comparison of the *Becn1* Sham mice vs. Control Sham mice (**Figure 3-4C**). However, these differences did not significantly alter baseline gene expression of innate immune response pathways or baseline outcomes in our cognitive behavior tests. It is possible that *Becn1* cKO mice develop compensatory mechanisms to maintain cellular homeostasis in of the absence of Beclin 1. Additionally, it is important to note that we performed these experiments on young adult mice (9-11 weeks old); it is possible that there are additional genotype-dependent differences that do not significantly manifest at this young age. Future work should examine how aging contributes to baseline differences between the Sham mice. As a decrease in autophagy function occurs during aging, we predict that *Becn1* knockout-mediated autophagy dysregulation further exacerbates the age-related decrease in autophagy function.

Our data demonstrates that *Becn1* deficiency results in exacerbation of innate immune responses during the acute phase of TBI (three days post-injury), which corresponds to the peak of neuroinflammation in mice after TBI. However, as seen in the **Figure 3-12** data, there are no statistically significant differences in transcriptional levels of the investigated inflammation pathway-related genes between the *Becn1* cKO TBI mice and Control mice TBI mice at day 28 post-TBI, which is considered the chronic phase. We hypothesize two possible explanations for this. Our knockout mice should have *Becn1* knockout in most of the infiltrating monocytes/macrophages and a subset, but not all, of the resident microglial cells. By day 28, there is little to no presence of infiltrating myeloid cells in the injured brain, and this could be a reason for the decline. On the other

hand, our biochemical studies at the day 28 timepoint were restricted to testing for transcriptional changes. In future experiments, we will characterize changes to inflammatory pathways in our experimental mice during the chronic phase of TBI using western blotting, flow cytometry, and immunostaining. These experiments will give us a better understanding of any long-term biochemical and molecular consequences of *Becn1* knockout in brain-resident microglia and monocyte/macrophages following TBI.

LysM-Cre is a useful driver for obtaining selective knockout of genes in microglia and monocytes/macrophages. However, other microglia/monocyte specific drivers can also be utilized. One such example is obtaining tissue-specific knockout of autophagy genes using transgenic mice with inducible Cre expression driven by the Cx3Cr1 promoter (Cx3Cr1-CreER); this could yield more efficient knockout of autophagy genes in the microglial population because Cx3Cr1 is more globally expressed by these cells. Moreover, it would be an inducible form of tissue-specific knockout, occurring only after mice are injected with tamoxifen. One could compare baseline differences before and after tamoxifen treatment, and this could more specifically tease out any baseline differences in outcome measures. We initially attempted this study using *Beclin1*^{flox/flox}, *Cx3Cr1*^{CreER/CreER} mice. However, we experienced technical challenges achieving the inducible knockout by tamoxifen, which lead us to develop the *Becn1* cKO mice used in this study.

Our study demonstrates c*Becn1* KO-induced changes in innate immune pathways and neuroinflammation following TBI on a broad level. Future work should focus on the molecular mechanisms that cause exacerbated neuroinflammatory and innate immune responses after TBI. Our work demonstrated the role of the Beclin 1 protein in regulating inflammation. However, Beclin 1 is one of the many ATGs involved in the autophagy

process. In understanding the molecular mechanisms by which autophagy regulates inflammation, studies should determine in greater detail which specific ATGs mediate inflammation. Increasing evidence has emerged that autophagy plays a more targeted and precise role in clearance of debris and components of the inflammasome pathway such as NLRP3 and DAMPs (damaged mitochondria and ROS) that activate the inflammasome pathway (Zhong et al., 2016). This process involves cooperation between target recognition and assembly of the autophagic apparatus. Recent studies demonstrate that TRIM proteins play a role in coordination between cargo recognition and the assembly and activation of the principal autophagy regulators (Kinura et al., 2016). In their autophagy roles, TRIM proteins act both as receptors and as platforms ('receptor regulators') for the assembly of the core autophagy regulators, such as ULK1 and Beclin 1 in their activated state. As autophagic receptors, TRIMs directly recognize endogenous or exogenous targets, and permit specific cargo degradation. Thus, future work should also focus on the role of precision autophagy mediated by TRIM proteins in regulating inflammation after TBI.

Overall, this study provides unique and interesting insights into the role of autophagy in regulating immune responses following TBI and offers avenues for future research direction.

3.4. Methods

3.4.1. Experimental Design

Young adult (9-11 weeks old) male $LysM^{Cre/Cre}$ mice and $Beclin^{floxed/floxed}$ mice from The Jackson Laboratory (Germantown, NY, USA) were purchased and bred in-house for two generations to produce $Beclin^{floxed/floxed}$, $LysM^{Cre/Cre}$ mice. All mice were housed on sterilized bedding in a specific pathogen-free facility (12 hours light/dark cycle).

3.4.2. Controlled Cortical Impact

CCI was done as described in Chapter 2.4.2.

3.4.3. Bone Marrow-derived Macrophage (BMDM) Isolation and Culture

BMDMs are isolated from $LysM^{Cre/Cre}$, $ROSA^{tdTomato}$ mice following euthanasia. The legs of the animals were sprayed with 70% EtOH, and the skin and muscle tissue were removed from the bones. The bones were sprayed with 70% EtOH, transferred to a sterile-flow hood, and cut at both ends. The marrow was flushed out into a sterile falcon tube in Dulbecco's Modified Eagle's Medium (DMEM; 500 ml; Invitrogen, Renfrew, UK) supplemented with heat-inactivated fetal bovine serum (FBS; 50 ml; 10%; Gibco, Paisley, UK) and penicillin-streptomycin (5 ml; 1%; Gibco, Paisley, UK). The cell suspension was triturated using a sterile Pasteur pipette, filtered through a nylon mesh filter (40 μ m; BD Biosciences, Oxford, UK) into a sterile tube, and then centrifuged (400 \times g, 5 min). The supernatant was removed, and the pellet was resuspended in red blood cell lysis buffer (Sigma-Aldrich, Gillingham, Dorset, UK). The suspension was centrifuged (400 \times g, 5 min), the supernatant was discarded, and the cells were then

washed using DMEM and centrifuged once more ($400 \times g$, 5 min). The pellet was resuspended in 20 ml of DMEM supplemented with L929-conditioned media (20%).

Cells were seeded in sterile cell culture flasks (T75 cm² flasks). On day 2, non-adherent cells were removed from the flask, the media was replaced, and the remaining adherent cells were maintained in culture for a further six days, with media being replaced on day four. On day 6, cells were transferred to 6-well plates (0.5×10^6 cells per well) and cultured for another two days, after which time they were scraped off and processed for qRT-PCR (see protocol in 3.4.4 below) or for Western blotting (see protocol in 3.4.5 below).

3.4.4. Quantitative Real-Time Polymerase Chain Reaction (qRT-PCR)

3.4.4.1. RNA isolation (for qRT-PCR and NanoString)

RNA was extracted from ipsilateral brain tissue or BMDMs using the QIAzol RNA isolation protocol. Briefly, 1 ml of Qiazol (Qiagen, Valencia, CA) was added to the samples and they were homogenized using an OMNI tissue homogenizer (OMNI-Inc, Kennesaw, GA). After homogenization, 200 μ l of chloroform was added to the samples, and the samples were shaken, and then spun at $14,000 \times g$ for 15 minutes at 4°C to separate phases. The clear top phase concentrates the RNA, and is removed from the sample and placed in a new tube. To precipitate the RNA, 500 μ l of isopropanol was added to the clear phase and allowed to sit overnight at 4°C. The RNA was then centrifuged at $10,000 \times g$ for 10 minutes at 4°C and the supernatant discarded. The pellet was washed once in ethanol, centrifuged again, and then eluted into DNase- and RNase-free water. RNA concentration was determined using a specialized plate reader (BioTek version 2.0.5;

BioTek Winooski, Vermont, USA). RNA quantity was determined by measuring optical density (OD) at 260 nm (1 OD unit at 260 nm corresponds to 40 µg/ml RNA). RNA quality was determined by measuring the OD_{260}/OD_{280} ratio. Ratios of 1.6-2.1 were deemed indicative of pure RNA. Eluted RNA samples were stored at -80°C until reverse-transcribed to cDNA for qPCR or NanoString.

3.4.4.2. Reverse Transcription of mRNA to cDNA

Complementary DNA (cDNA) synthesis was performed on 2 µg of total RNA obtained in 3.4.4.1 using a Verso cDNA RT kit (Thermo Scientific, Pittsburg, PA) using the the manufacturer's protocol. Briefly, 2 µg of RNA in RNase- and DNase-free water was prepared. In a PCR tube, 10 µl of the 1 µg RNA-water mixture was added to 10 µl of Verso Master Mix containing (in x µl of each reagent per reaction): 1 µl RNase- and DNase-free water, 1 µl Reverse transcriptase (RT) enhancer, 0.25 µl oligo nucleotides, 0.75 µl random hexamers, 4 µl synthesis buffer, 2 µl deoxyribonucleotide triphosphates (dNTPs) and 1 µl reverse transcriptase. These 20 µl reactions were then put into a thermal cycler for one cycle of 45 minutes at 50°C for synthesis and then 5 minutes at 95°C for inactivation of the reverse transcriptase. The resultant cDNA was stored at -80°C until used for mRNA quantification by qRT-PCR.

3.4.4.3. qRT-PCR for measurement of gene expression

Gene expression levels of select targets were determined using commercially available Taq-Man gene expression assays (Applied Biosystems, Foster City, CA, USA) containing specific forward and reverse target primers and 6-carboxyfluorescein (FAM)-labelled minor groove binding (MGB) probes. Glyceraldehyde 3-phosphate dehydrogenase

(GAPDH) was used as an internal control to normalize gene expression between samples. A reaction master mixture was first prepared and stored on ice for each target gene. This consisted of 1 μ l of target primers, 8 μ l of RNase- and DNase-free water, and 10 μ l of TaqMan master mix (Cat:4369016; Applied Biosystems) per sample. Nineteen μ l of the relevant reaction mixture was pipetted onto a MicroAmp® optical 384 well plate (Applied Biosystems). 1 μ l cDNA was pipetted into the reaction mixture, giving a total reaction volume of 20 μ l. Plates were then covered with optical adhesive covers and centrifuged at 1,000 x g for 5 minutes at 4°C to ensure complete mixing and elimination of bubbles. The plate was then placed in the PCR thermocycler (QuantStudio 5, Applied Biosystems) pre-set to run the following protocol: step 1: 95°C for 10 minutes, step 2: 95°C for 15 seconds, followed by one minute at 60°C. Step 2 was repeated 40 times and the fluorescence was read during the annealing and extension phase (60°C) for the duration of the program.

The following TaqMan Gene Assays were used for qRT-PCR:

Gapdh (Mm99999915_g1), *Nlrp3* (Mm00840904_m1), *Cybb* (Mm01287743_m1), *Nos2* (Mm00440502_m1), *Tnf* (Mm00443258_m1), *Ifnb1* (Mm00439552_s1), *Il1b* (Mm00434228_m1), *Arg1* (Mm00475988_m1), *Socs3* (Mm00545913_s1), *Chil3* (Mm00657889_mH), *Il4r* (Mm01275139_m1), *Mefv* (Mm00490258_m1), *Mb21d1* (Mm01147496_m1), *Tmem173* (Mm01158117_m1), *Irf8* (Mm00492567_m), *Lcn2* (Mm01324470_m1), *Nfkb1* (Mm00476361_m1), *Csf1r* (Mm01266652_m1), *Tgfb* (Mm00441724_m1), *Tlr4* (Mm00445273_m1). qRT-PCR for Beclin levels in BMDMs was performed using the following TaqMan Gene Assay: *Becn1* (Mm01265461_m1).

3.4.4.4. Analysis of qRT-PCR

Amplification plots and copy threshold (Ct) values were examined using QuantStudio5 qPCR Data Analysis Software. Ct values for each sample were analyzed after setting the threshold to the linear exponential phase of the amplification plots and exporting to Microsoft Excel for final analysis. The $2^{-\Delta\Delta CT}$ method was used to determine gene expression. This method is used to assess relative gene expression by comparing the gene expression of experimental samples to control samples after normalization of each to expression of the housekeeping gene in each sample, thereby allowing determination of the fold-change in mRNA expression between experimental groups. This method involves three steps: (1) Normalization to endogenous housekeeping control gene expression (GAPDH) where ΔCt is determined: $\Delta Ct = Ct \text{ Target gene} - Ct \text{ Endogenous control}$; (2) Normalization to control sample where $\Delta\Delta Ct$ is determined: $\Delta\Delta Ct = \Delta Ct \text{ Sample} - \text{average } \Delta Ct \text{ of Control group}$; and (3) where the fold difference is given by $2^{-\Delta\Delta Ct}$.

3.4.4.5. NanoString Analysis

RNA samples were extracted as described above from mice cortical brain samples at 3 days post-injury. Total RNA (20 ng/ μ l) was run on a NanoString nCounter® system for Mouse Neuroinflammation v1.0 panel (NanoString Technologies, Seattle, WA) to profile RNA transcript counts for 757 genes of interest and 13 housekeeping genes. All sample gene transcript counts were normalized prior to downstream analysis and pairwise differential expression analysis was performed with NanoString's nSolver software Version 4.0. Principle component analysis (PCA) and agglomerative clustering heatmap were generated using MetaboAnalyst. Subsets of differentially expressed genes displayed

as heatmaps were normalized across samples as z-scores and then averaged to a single value per group before plotting with GraphPad Prism Version 9.2.0 (San Diego, CA).

3.4.5. Western Blotting

Approximately 70 mg of ipsilateral cortical brain tissue was isolated and homogenized in 750 μ l of RIPA buffer (TekNova, Hollister, CA, USA) containing protease and phosphatase inhibitors (Sigma). Samples were then centrifuged at 13,000 x g at 4°C for 20 min. The supernatants were collected and their protein content determined by BCA assay (Pierce-ThermoFisher, Waltham, MA, USA). Samples were then diluted in ice-cold lysis buffer to give equal protein concentrations (1.5 μ g/ μ l), followed by the addition of sample buffer containing 20% 2-mercaptoethanol. Lysates were heated at 95°C for 5 min and loaded onto 4–20% gradient SDS-PAGE gels (Bio-Rad; Hercules, CA, USA). Proteins were transferred onto 0.22 μ m PVDF membranes (ThermoFisher) and then blocked for 1 h in 5% milk in 1X TBS (Bio-Rad) containing 0.05% Tween-20 (TBS-T) at room temperature. Membranes was incubated with the following antibodies:

NOX2 (1:1000; BD Biosciences, 611415), cGAS (1:1000; Cell Signaling, 15102), STING (1:1000; Cell Signaling, 13647), p62 (1:1000; BD Biosciences, 610833), LC3 (1:1000; Novus, NB100–2220), iNOS (1:1000; BD Biosciences, 610328), NLRP3 (1:1000; Cell Signaling, 15101), BECN1/Beclin 1 (1:1000; Santa Cruz Biotechnology, 11427), and ACTB/ β -actin (1:10,000; Sigma, A1978).

The next day, the membranes were washed three times with TBS-T and then incubated with anti-rabbit or anti-mouse secondary antibody conjugated to horseradish peroxidase

(HRP) (Jackson ImmunoResearch Laboratories, West Grove, PA) for 2 hours at room temperature. Membranes were washed three times in TBS-T, and proteins were visualized using SuperSignal West Femto Extended Duration Substrate (Thermo Scientific). Chemiluminescence was captured with a ChemiDoc™ XRS+ System (Bio-Rad), and protein bands were quantified by densitometric analysis using Bio-Rad Molecular Imaging Software.

3.4.6. Neurobehavioral tests

3.4.6.1. Beam Walk

Fine motor coordination was assessed using the Beam Walk test (Kabadi et al., 2012). Briefly, mice were placed at the end of a wooden beam (5 mm wide, 120 mm long) and the number of slips (foot faults) of the right hind limb were recorded over 50 steps. Mice were trained on the beam walk for three days prior to surgery and tested at 1 day, 3 days, 7 days, 14 days, 21 days, and 28 days post-TBI. Gross motor function was also assessed during the habituation stage of Novel Object Recognition testing (distance traveled, average speed) and during Morris Water Maze testing (swim speed) using Any-Maze software (Stoelting Company, Wood Dale, IL).

3.4.6.2. Open Field

The open field test was performed to assess locomotor activity post-injury. Sham and TBI mice were individually placed in a corner facing the wall of the open field chamber (22.5 x 22.5 cm) and allowed to freely explore the chamber for 7.5 minutes. The distance traveled and average speed were recorded by Any-Maze tracking software.

3.4.6.3. Y-Maze

The Y-Maze spontaneous alternation behavior test, to assess hippocampal-dependent working (short-term) memory, was performed on day eight post-injury. Briefly, the Y-maze (Stoelting Co.) consists of three identical arms with each arm at an angle of 120° with respect to the other arms, and where each arm is 35 cm long, 5 cm wide, and 10 cm high. One arm was randomly selected as the “start” arm, and the mouse was placed within and allowed to explore the maze freely for 5 minutes. Arm entries (arms A–C) were recorded by analyzing mouse activity using ANY-Maze tracking software. An arm entry was attributed when all four paws of the mouse entered the arm, and an alternation was designated when the mouse entered three different arms consecutively. The percentage of alternation was calculated as follows: $\text{total alternations} \times 100 / (\text{total arm entries} - 2)$.

3.4.6.4. Novel Object Recognition (NOR)

Non-spatial hippocampal-mediated memory in mice was assessed by performing NOR testing through days 14-17 post-TBI. Mice underwent one habituation day consisting of one 7.5-minute trial/day to acclimate to the testing arena (22.5 x 22.5 cm, black plexiglass walls). Twenty-four hours following habituation, mice underwent object familiarization in which the mice were placed into the testing arena with two similar objects positioned equidistant apart from each other and the arena walls. The mice were allowed to explore freely for 7.5 minutes or 20 seconds of total interactions with the objects. Twenty-four hours later, mice underwent novel object (NO) testing in which one familiar object was replaced with a novel object and the mice were allowed to freely explore for 7.5 minutes or until 20 seconds of total interaction between the objects was recorded. Novel/familiar objects and the side in which the novel object was positioned were balanced across all

experimental groups to control for any potential object and side biases. Testing was recorded using Any-Maze software. Object interaction included time spent sniffing or placing front paws on, while facing, the object. Time spent chewing and climbing and sitting on top of objects was not considered exploration and excluded from final scores. Because mice inherently prefer to explore novel objects, a preference for the novel object indicates intact memory for the familiar object. The analysis was represented as the ratio of the time spent with the novel object to the time spent with the familiar object.

3.4.6.5. Morris Water Maze (MWM)

Hippocampal-dependent spatial learning and memory were assessed using the MWM during days 21-25 post-TBI. The MWM protocol included two phases: (1) hidden platform training (learning acquisition) and (2) a twenty-four-hour probe test (reference memory). A circular tank (100 cm in diameter) was filled with water (23 +/- 2°C) and was surrounded by various extra-maze cues (blue square, blue diamond, blue square and blue star) on the inner walls of the testing area. A transparent platform (10 cm in diameter) was submerged 0.5 cm below the surface of the water. Mice were trained to find the hidden submerged platform located in the northeast (NE) quadrant of the tank for four consecutive days. The mice underwent four trials per day, starting from a randomly selected release point (east, south, west, and north). Each mouse was allowed a maximum of 90 s to find the hidden submerged platform. The latency to find the submerged platform was recorded using Any-Maze software. Reference memory was assessed by a probe test performed 24 hours after the final acquisition day. The platform was removed, the mice were released from the southwest position, and the time in the target quadrant was recorded. Search strategy analysis was performed, and characterized as follows: (1) a

spatial search strategy was defined as swimming directly to platform with no more than one loop or swimming directly to the correct target quadrant and searching for the platform; (2) a nonspatial systematic strategy was defined as searching the interior portion of or the entire tank without spatial bias, including searching within the incorrect target quadrant before finding platform; and (3) a repetitive looping strategy was defined as circular swimming around the tank, swimming in tight circles, or swimming around the wall of tank before finding the submerged hidden platform. Mice that remained immobile or learned to simply float throughout the 90 s trial in the MWM test were excluded from the analysis (Control Sham: 1; Becn1 cKO TBI: 1 were excluded).

3.4.7. Flow Cytometry

Flow Cytometry was performed as described in 2.4.4. Intracellular antibodies included: TNF-PE-Cy7 (MP6-XT22) (Invitrogen), IL-1 β -PerCP-eF710 (NJTEN3) (Invitrogen), NLRP3-APC (TW7-16B4) (Biolegend, San Diego, CA). Data were acquired on a Cytex Aurora flow cytometer equipped with FACsDiva 6.0 (BD Biosciences, San Jose, CA) and analyzed using FCS Express. The individual analyzing the samples and the data was blinded to treatment groups until the end of the experiment.

3.4.7. Lesion Volume

Cortical lesion volume was assessed in vehicle and TBI-treated injured mouse brains at day 28 after TBI. 60 μ m sections located approximately 240 μ m apart across the entire lesion volume were stained with cresyl violet (FD Neurotechnologies Inc) and images were acquired on Leica DM4000 B TL (BF) microscope. Quantification was based on the Cavalieri method using Stereo Investigator software (MBF Biosciences, Williston, VT)

and the lesion volume was quantified by outlining the missing tissue on the injured hemisphere using the Cavalieri estimator with a grid spacing of 0.1 mm.

3.4.7. Neuronal Count

Analysis of neuronal cell loss in ipsilateral hippocampus was performed on 60 μm fixed coronal brain sections collected at 28 days post-TBI and stained with cresyl violet. Every fourth 60 μm section between -1.34 and -2.53 mm and -2.7 to -3.16 mm from bregma, beginning at a random starting point, was analyzed (cohort 2 mice, n=8-10/group). A total of five sections per brain were analyzed. Neuronal cell loss was quantified using a Leica DM4000B microscope (Leica Microsystems, Exton, PA) with the Stereo Investigator software by counting the number of cresyl violet-stained neurons representing surviving neurons using the optical fractionator method of unbiased stereology, with fewer cresyl violet-stained neurons representing neuronal cell loss. The volume of the regions counted was determined using the Cavalieri method. Results are expressed in terms of cellular density (cells per mm^3) (Kabadi et al., 2012).

3.4.8. Statistical Analysis

Quantitative data were expressed as mean \pm standard error of the mean and statistical analysis was performed using GraphPad Prism Software v. 6.0. A $p < 0.05$ value was chosen as the minimal value for statistical significance. Animal numbers in each experiment were derived from the power calculation based on effect sizes defined by Cohen (Cohen, 1992) and variability estimated from published data.

Beam walk and MWM acquisition were analyzed by repeated measures two-way ANOVA to determine the interactions of time and injury and genotype changes, followed by *post-hoc* adjustments using a Tukey's multiple comparison test. Gene expression levels by qPCR and NanoString, protein levels by Western blotting, flow cytometry data, and behavioral outcomes (Distance traveled, mean speed, object and novel object preference, time spent in the target quadrant, swim speeds) were analyzed by Two-way ANOVA, followed by *post-hoc* adjustments using a Tukey's test for multiple comparison. The MWM search strategy was analyzed using a chi-square analysis. Neuronal cell counts were analyzed by Two-Way ANOVA, followed by Tukey's *post-hoc*. Stereological data examining lesion volume was analyzed using an unpaired, two-tailed Student *t*-test. Statistical analysis in each assay was detailed in figure legends.

CHAPTER 4: N-acetyl-L-leucine Improves Functional Recovery and Attenuates Cortical Cell Death and Neuroinflammation after Traumatic Brain Injury in Mice¹

4.1 Introduction

Repurposing of drugs that are already in clinical use for the treatment of certain medical conditions can be an effective and rapid way to develop useful therapeutic strategies for the treatment of highly devastating and intractable conditions like TBI. While the primary mechanical injury in TBI is instantaneous and cannot be altered, the subsequent secondary injury has an extended timeframe and represents a therapeutic window for a treatment aimed at restricting neuronal cell death and suppressing neuroinflammation after TBI.

In clinical and pre-clinical studies, it has been shown that N-acetyl-leucine (NAL), an acetylated derivative of leucine, improves neurological function in cerebellar ataxias (Schniepp et al, 2016; Strupp et al., 2018). The racemic mixture, N-acetyl-DL-leucine (DL-NAL) has been used as a medication for the treatment of acute vertigo and vertiginous symptoms in France since 1957; it is orally available and has a well-established safety profile (Neuzel et al., 2002). Electrophysiological studies in a guinea

¹ Hegdekar, N., Lipinski, M.M. & Sarkar, C. *N-Acetyl-L-leucine improves functional recovery and attenuates cortical cell death and neuroinflammation after traumatic brain injury in mice. *Sci Rep* 11, 9249 (2021). <https://doi.org/10.1038/s41598-021-88693-8>*

pig model of acute unilateral vestibulopathy demonstrated that DL-NAL can restore the membrane potential of abnormally polarized neurons of the medial vestibular nucleus (Vibert et al., 2003). In a rat model of an acute unilateral vestibular lesion, N-acetyl-L-leucine stereospecifically (i.e. not the D-enantiomer, see below) improved central compensation of postural symptoms in a dose-dependent manner (Gunther et al., 2015). More recent studies in the mouse model of Niemann-Pick disease type C (NPC) – a neurodegenerative lysosomal storage disorder caused by mutation in cholesterol transporting NPC 1 and 2 genes – identified that in addition to symptomatic effects, treatment with the L-enantiomer has a neuroprotective, disease-modifying effect (Kaya et al., 2020). Promising clinical outcomes following racemic NAL treatment, including improved ataxic symptoms and stabilized disease progression, were observed among small cohort of NPC patients, correlating to the pharmacological action of the drug observed in animal studies. These reports led us to predict that NAL may be useful in improving outcomes after TBI.

The enantiomers of NAL are pharmacologically different and exert distinct toxicity due to their unique pharmacokinetic properties. It has been previously observed that the L-enantiomer (NALL) is the pharmacologically active enantiomer of the racemate responsible for the long-term, neuroprotective, disease modifying effects (Kaya et al., 2020). Administration of the D-isomer of NAL was found to be ineffective compared to its L-form in reducing neuroinflammation or correcting relative lysosomal volume in Niemann-Pick disease type C, consistent with the D-isomer having no neuroprotective effect (Kaya et al., 2020). As mentioned above, the L-isomer was also reported to be the only active form of NAL that improves functional recovery after vestibular neurectomy

in the rat and cat (Gunther et al., 2015; Tighilet et al., Churchil et al., 2020). In addition, differences in the pharmacokinetics of NAL enantiomers indicate chronic administration of the racemate could have negative effects and support the isolated use of NALL (Fields et al., 2021). Based on the superiority of the L-enantiomer, three clinical trials are ongoing with NALL for the treatment of NPC, GM2 gangliosidosis, and ataxia telangiectasia (clinicaltrials.gov NCT03759639, NCT03759665, NCT03759678, and EudraCT 2018-004331-71; 018-004406-25; 2018-004407-39).

Accordingly, in this study, we assessed whether NALL is effective in preventing neurodegeneration and neuroinflammation after controlled cortical impact-induced experimental TBI in mice. Our data demonstrate that treatment with oral NALL can attenuate cell death after TBI in a CCI mouse model. This is associated with a decrease in several neuroinflammatory markers and improvement in autophagy flux. We also observed improved recovery of motor and cognitive function and reduction in lesion volume in injured mice treated with NALL. Together, these data provide further evidence of neuroprotective effect of NALL and indicate NALL as a promising novel drug candidate for the treatment of TBI.

4.2. Results

4.2.1. NALL treatment does not negatively affect food intake or body weight of mice after TBI.

To investigate if NALL treatment can attenuate secondary injury and improve recovery after TBI, we orally administered NALL to C57/BL6 mice for 1–28 days following CCI-induced experimental TBI or sham surgery as depicted in **Figure 4-1a**. Food intake was slightly higher in mice fed with NALL, particularly in the sham group ($p < 0.001$) (**Figure 4-1b**). While a slight decrease in body weight was detected among all TBI mice (both vehicle and NALL-treated) at days 1 and 3 after injury, they gradually regained the body weight and no appreciable differences in their body weight was observed at day 28 after TBI (mean weight of 26.05 ± 1.99 g in vehicle-fed TBI mouse group vs. 25.98 ± 2.27 g in NALL-fed TBI mouse group) (**Figure. 4-1c**). Body weight increased gradually in both vehicle- and NALL-fed sham mice over the course of study. These results clearly suggest that inclusion of NALL in chow does not negatively affect food intake or body weight in mice with or without TBI.

4.2.2. NALL treatment attenuates cortical cell death after TBI

CCI is associated with extensive acute cell death that peaks at 1 day after injury. We investigated whether NALL treatment can decrease overall cortical cell death after TBI by assessing the level of α -fodrin cleavage products in NALL- or vehicle-treated sham, or TBI mouse cortices by Western blot. TBI induces both calpain- and caspase-mediated cleavage of α -fodrin, generating 145-150 kDa and 120-150 kDa fragments, respectively. We observed a significantly lower level of 145-150 kDa fragments of α -fodrin in the

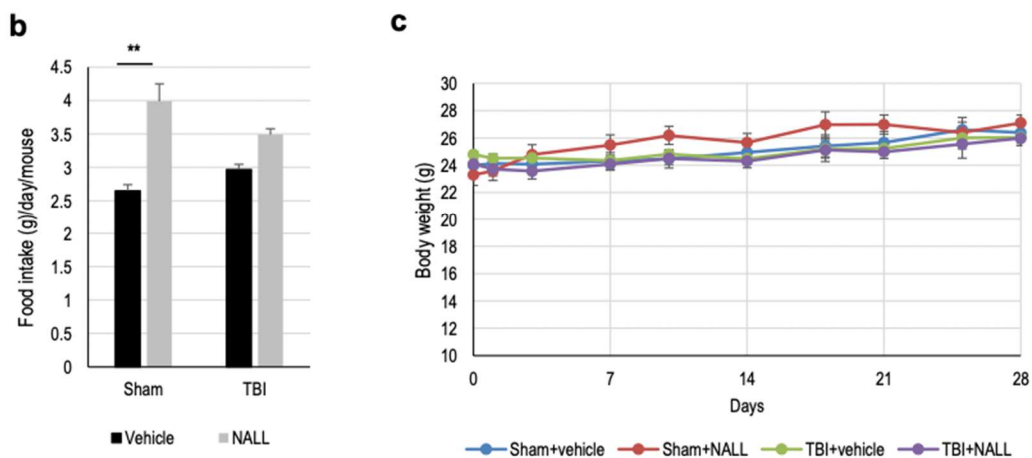
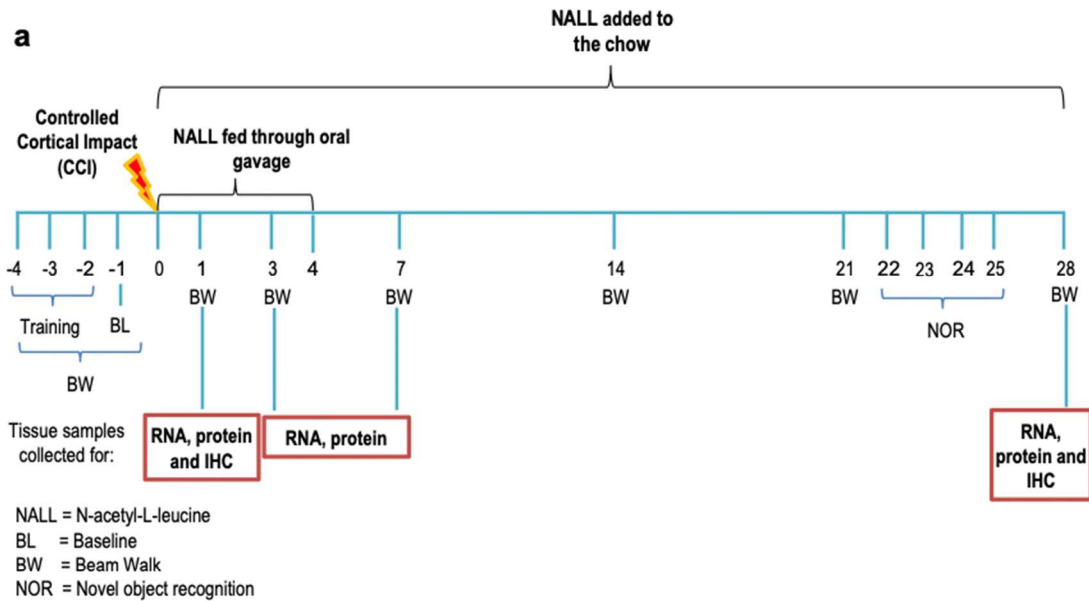
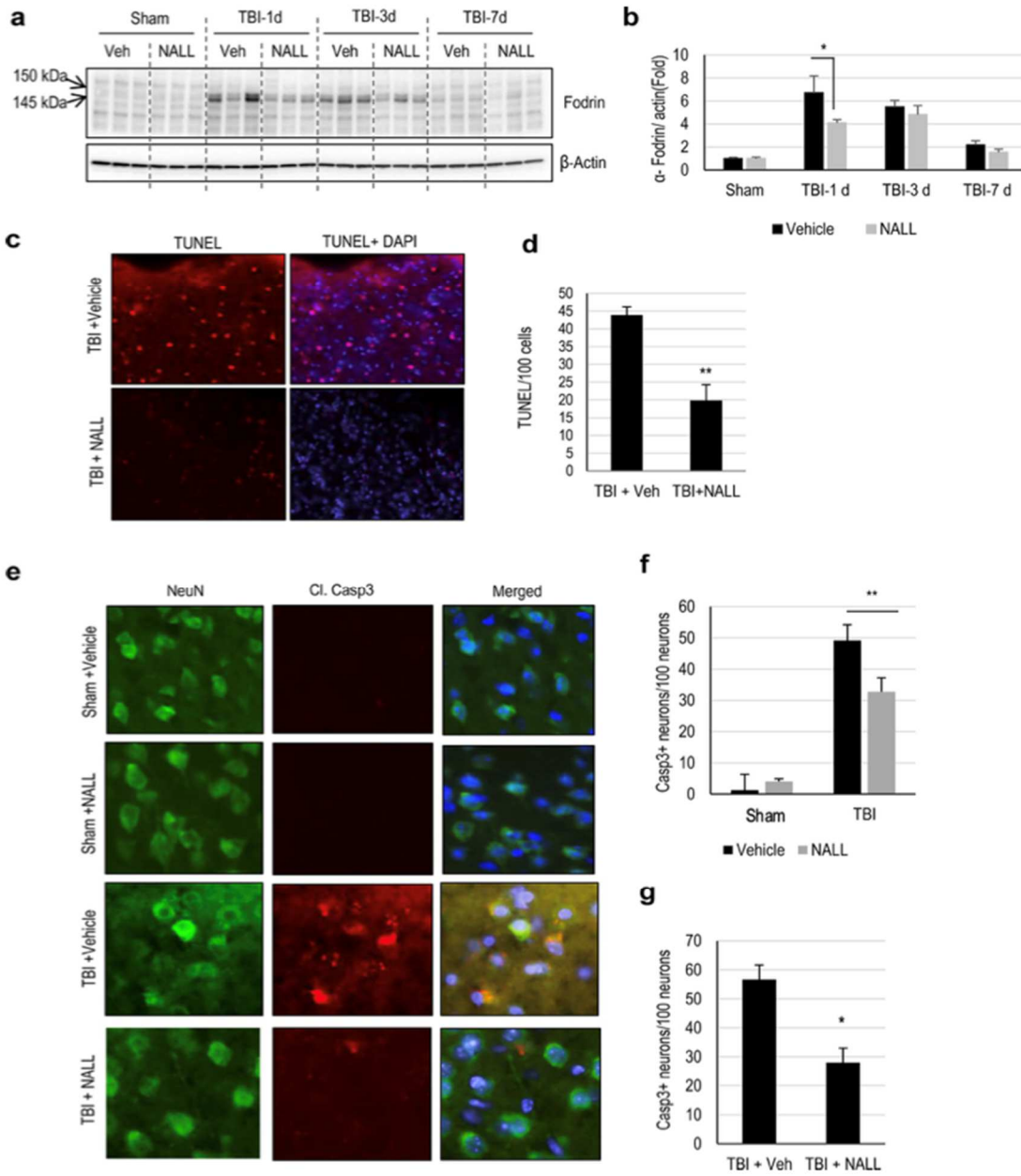


Figure 4-1. NALL does not affect food intake or body weight in mice. (a) NALL treatment strategy. Mice were orally fed with NALL and cortical tissues were collected at days 1, 3 and 7 after TBI for biochemical analyses. *BW* beam walk, *NOR* novel object recognition, *BL* Baseline. (b) Amount of NALL-containing chow eaten by the mice. (c) Body weight of sham and injured mice fed with vehicle or NALL. No significant differences were observed between corresponding vehicle and NALL groups. Data are presented as mean \pm SEM. $n = 10$ sham + vehicle, 9 sham + NALL, 20–25 TBI + vehicle and 18 TBI + NALL. $**p < 0.001$ (Two-way ANOVA with Sidak post-tests).

NALL-fed mouse cortices as compared to the cortices of mice fed with vehicle at 1 day following TBI, while the levels remained unchanged or slightly lower in the NALL-treated groups at the subsequent time points. This indicates the protective benefit of NALL in preventing cortical cell death, which peaks at early time points (e.g. day 1) after TBI (**Figure 4-2a and b**). We further investigated the effect of NALL on apoptosis-mediated cortical cell death by Terminal deoxynucleotidyl transferase (TdT) dUTP Nick-End Labeling (TUNEL) assay. We detected significantly lower numbers of TUNEL positive cells in the cortical sections of injured mice fed with NALL as compared to vehicle-fed TBI mice (**Figure 4-2c and d**). Since cortical cell death peaks in neurons early after CCI-induced TBI in mice, we determined the levels of the apoptotic cell death marker cleaved caspase-3 in the neurons (stained with NeuN) of TBI mice treated with NALL or vehicle. Our data showed significant attenuation of neuronal apoptosis in the cortices of TBI mice treated with NALL as compared to the vehicle-treated mice (**Figure 4-2e and f**).

Figure 4-2. NALL attenuates cortical cell death after TBI. (a) Western blot to detect α -fodrin breakdown products in cortical tissue lysates from sham and TBI mice fed with NALL or vehicle. (b) Corresponding densitometric analysis of cleaved bands of α -fodrin with respect to β -actin. Data are presented as mean \pm SEM. n = 5, *p<0.05 (Two-way ANOVA with Bonferroni post-tests). (c) 20X representative images of vehicle- or NALL-fed mouse cortical brain sections stained for TUNEL at 1 day post-TBI and (d) corresponding quantification. Data are presented as mean \pm SEM. n = 5, **p < 0.01 (Two-tailed Student's t-test). (e) 20X IF representative images of vehicle- or NALL-fed mouse cortical brain sections stained for cleaved caspase-3 and NeuN at 1 day post-TBI and (f) corresponding quantification, represented as number of cleaved caspase-3+ neurons/100 neurons. Data are presented as mean \pm SEM. n = 5/group, **p<0.01 (Two-way ANOVA with Sidak post-tests). (g) Quantification of cleaved caspase-3 positive neurons in hippocampal brain sections of vehicle- or NALL-fed mice at 1 day post-TBI, represented as cleaved caspase-3+ neurons/100 hippocampal neurons. Data are presented as mean \pm SEM. n = 5/group *p < 0.05 (Two-tailed Student's t-test).



We also observed a decrease in hippocampal cell death in TBI mice treated with NALL as compared to the vehicle-treated mice (**Figure 4-2g**). These data clearly indicate that NALL treatment can attenuate neuronal cell death after TBI.

4.2.3. NALL treatment restores autophagy flux after TBI

Recently, we demonstrated that autophagy, a lysosome-dependent cellular degradation process, is disrupted due to lysosomal damage after TBI (Sarkar et al., 2019). Autophagy is an important process for neuronal cells as it removes intracellular protein aggregates and damaged organelles (Klionsky et al., 2004; Klionsky et al., 2007; Mizushima et al., 2011). We reported that disruption of autophagy flux after TBI causes accumulation of autophagosomal marker LC3-II and autophagic substrate p62/SQSTM1 and is associated NALL-fed mouse cortices as compared to the cortices of mice fed with vehicle at 1 day following TBI, while Vehicle- and NALL-fed sham and TBI mice were determined by Western blot. We detected a significant decrease in the levels of LC3-II in the brains of NALL-fed mice as compared to the vehicle-treated mice at day 1 after TBI (**Figure 4-3a and b**). p62/SQSTM1 levels detected by Western blot in the cortex of mice fed with NALL or vehicle and subjected to TBI showed greater variability, potentially due to difficulties in optimizing antibody dilution (**Figure 4-3a and c**). However, we found a decrease in p62/SQSTM1 accumulation in NALL-fed TBI mouse cortices as compared to the vehicle-treated TBI controls by immunofluorescence staining (**Figure 4-3d and e**). These data demonstrate that NALL can improve autophagy flux in the mouse cortices after TBI, which may contribute to its neuroprotective function.

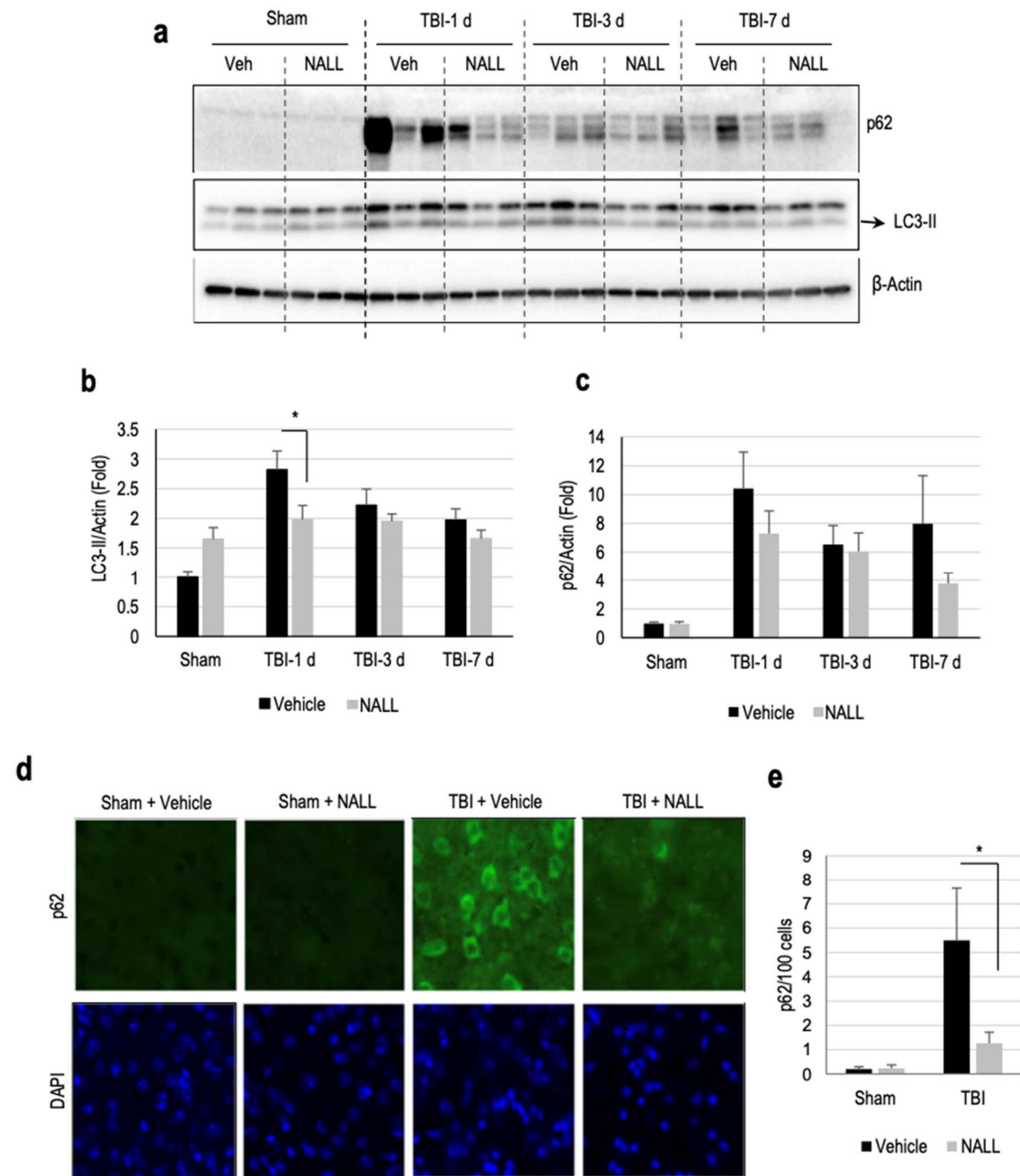


Figure 4-3. NALL restores autophagy flux after TBI. (a) Western blot for autophagosomal marker LC3 and autophagic cargo adaptor proteins p62/SQSTM1 in cortical tissue lysates from sham and TBI mice fed with NALL or vehicle and (b,c) corresponding densitometric analysis. Data are presented as mean \pm SEM. $n = 5$ (only 3/group included for representative images for western blot analysis), $*p < 0.05$ (Two-way ANOVA with Bonferroni post-tests). (d) IF staining for p62/SQSTM1 on frozen mouse cortical brain sections at 1 day after TBI. (e) Quantification of image data from d. Data are presented as mean \pm SEM. $n = 5$ /group, $*p < 0.05$ (Two-way ANOVA with Sidak post-tests).

4.2.4. NALL reduces expression of inflammatory cytokines in TBI mouse brain.

We examined whether NALL treatment can reduce neuroinflammation in the brain following TBI. We determined mRNA expression level of pro-inflammatory markers iNOS (*Nos2*), Nlrp3 (*Nlrp3*), IL-1 β (*Il1b*), TNF (*Tnf*), IFN-B1 (*Ifnb1*) and Nox2 (*Cybb*) in the perilesional area in TBI mouse cortices by qRT-PCR (**Figure. 4-4a-f**). We observed elevated levels of all inflammatory markers in TBI mouse cortices, irrespective of treatment, starting from day 1 and peaking at day 3 after injury,. However, we detected significant decreases in the mRNA levels of *Il1b*, *Ifnb1* and *Cybb* in the cortices of NALL-fed TBI mice as compared to the vehicle-fed TBI mice (**Figure 4-4c, e, and f**). No change in *Tnf* level in TBI mice fed with NALL as compared to the vehicle-fed injured mice was observed (**Figure 4-4d**). Similar to pro-inflammatory markers, we observed higher expression of anti-inflammatory markers *Socs3* (*Socs3*), YM-1 (*Chil3*), IL4ra (*Il4r*) and Arg-1 (*Arg1*) in the cortical tissue of all TBI mice as compared to sham animals (**Figure. 4-5a-d**). Among these markers, NALL treatment significantly increased *Socs3* expression and lowered levels of *Arg1* in the injured mouse cortex as compared to vehicle-fed TBI mice (**Figure. 4-5a and d**). Taken together, these results demonstrate that NALL reduces expression of several inflammatory markers, thus indicating an overall decrease in neuroinflammation following TBI in mice.

4.2.5. NALL treatment improves motor and cognitive function in mice after TBI.

We assessed whether NALL treatment can attenuate impairments in motor and memory function in injured mice following TBI. We compared functional recovery between vehicle and NALL-treated TBI and sham mice using a battery of behavioral tests as

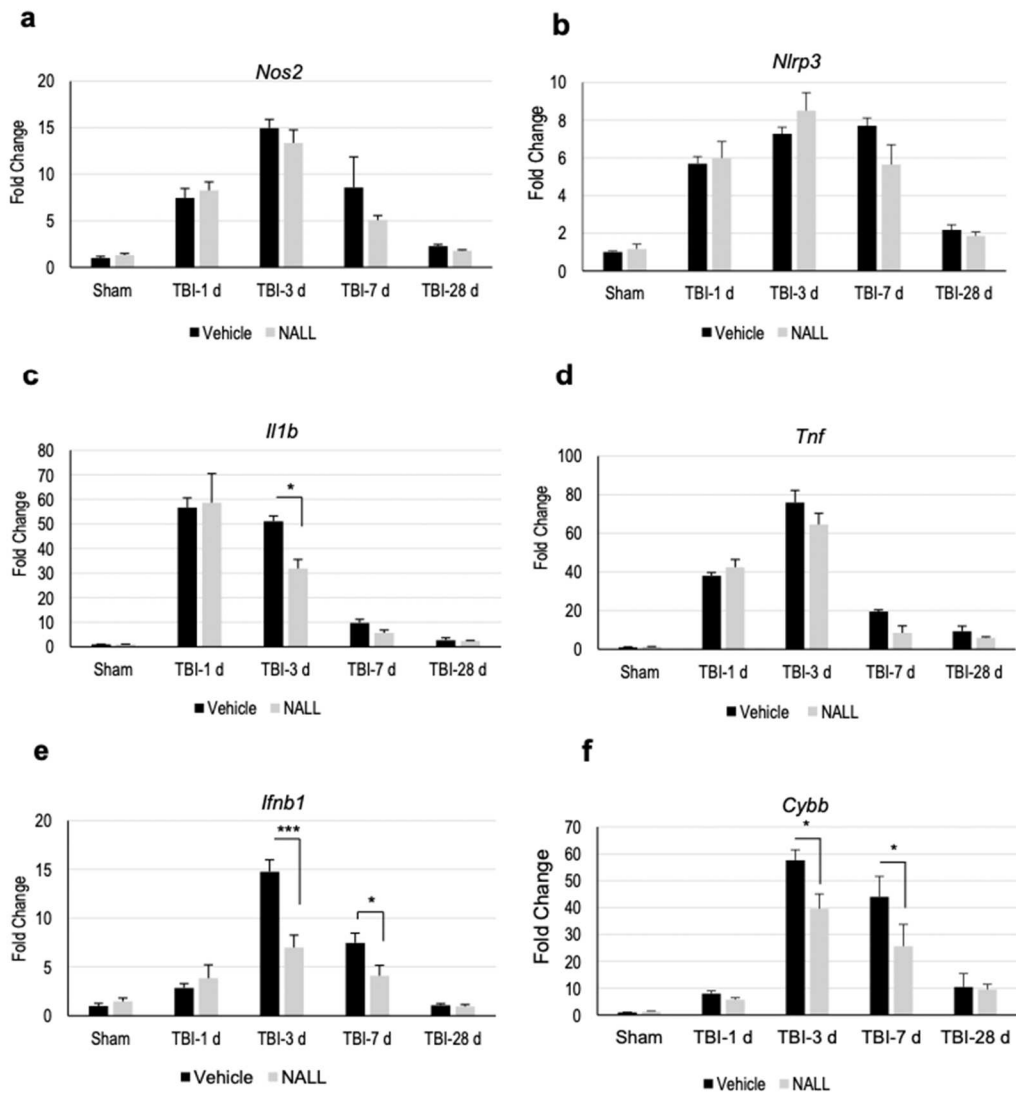


Figure 4-4. NALL reduces pro-inflammatory markers in the injured mouse cortices. Relative mRNA levels of (a) iNOS (*Nos2*), (b) NLRP3 (*Nlrp3*), (c) IL-1 β (*Il1b*), (d) TNF (*Tnf*), (e) IFN- β (*Ifnb1*) and (f) NOX2 (*Cybb*) in the cortices of sham and TBI mice fed with NALL or vehicle. Data are presented as mean \pm SEM. n = 5/group, ***p < 0.001, *p < 0.05 (Two-way ANOVA with Bonferroni post-tests).

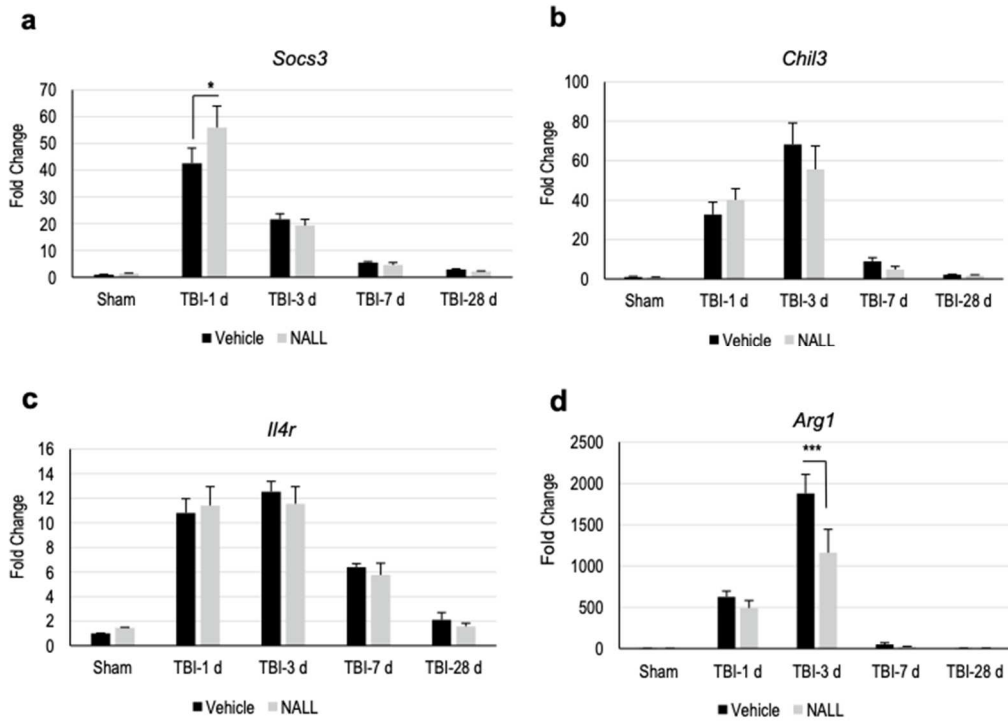


Figure 4-5. NALL alters the levels of anti-inflammatory markers in the injured mouse cortices. Relative mRNA levels of (a) SOCS3 (*Socs3*), (b) YM-1 (*Chil3*), (c) IL-4R (*Il4r*) and (d) Arginase (*Arg1*) in the cortices of sham and TBI mice fed with NALL or vehicle. Data are presented as mean \pm SEM. $n = 5/\text{group}$, *** $p < 0.001$, * $p < 0.05$ (Two-way ANOVA with Bonferroni post-tests).

depicted in **Figure 4-6**. We assessed motor coordination using Beam Walk test on days 1, 3, 7, 14, 21 and 28 post-injury. We observed gradual improvement in motor function in NALL-treated TBI mice as compared to vehicle-fed TBI mice, trending on day 7 and reaching significance on days 21 ($p=0.0096$) and 28 after injury ($p=0.012$) (**Figure. 4-6a**). This demonstrates that NALL treatment can accelerate motor function recovery in TBI mice.

To assess effects of NALL on cognitive function after TBI, we used the Novel Object Recognition (NOR) test to assess non-spatial learning and memory. All TBI mice spent significantly less time with the novel object as compared to the corresponding sham groups, confirming the expected injury effect. However, NALL-fed TBI mice spent significantly ($p=0.0395$; two-way ANOVA) longer time with the novel object as compared to the vehicle-fed TBI mice (**Figure. 4-6b**), suggesting improvement in memory retention following NALL treatment.

Finally, to determine whether NALL treatment could result in overall tissue sparing after TBI, we used stereology to compare lesion volume between NALL and vehicle-treated TBI mice. Our data demonstrated a significant decrease in lesion volume in NALL-fed TBI mice as compared to vehicle-fed TBI controls (**Figure. 4-6c and d**). Taken together, these results demonstrate attenuation of motor and cognitive deficits and decreased lesion volume in TBI mice fed with NALL as compared to the vehicle-treated TBI mice.

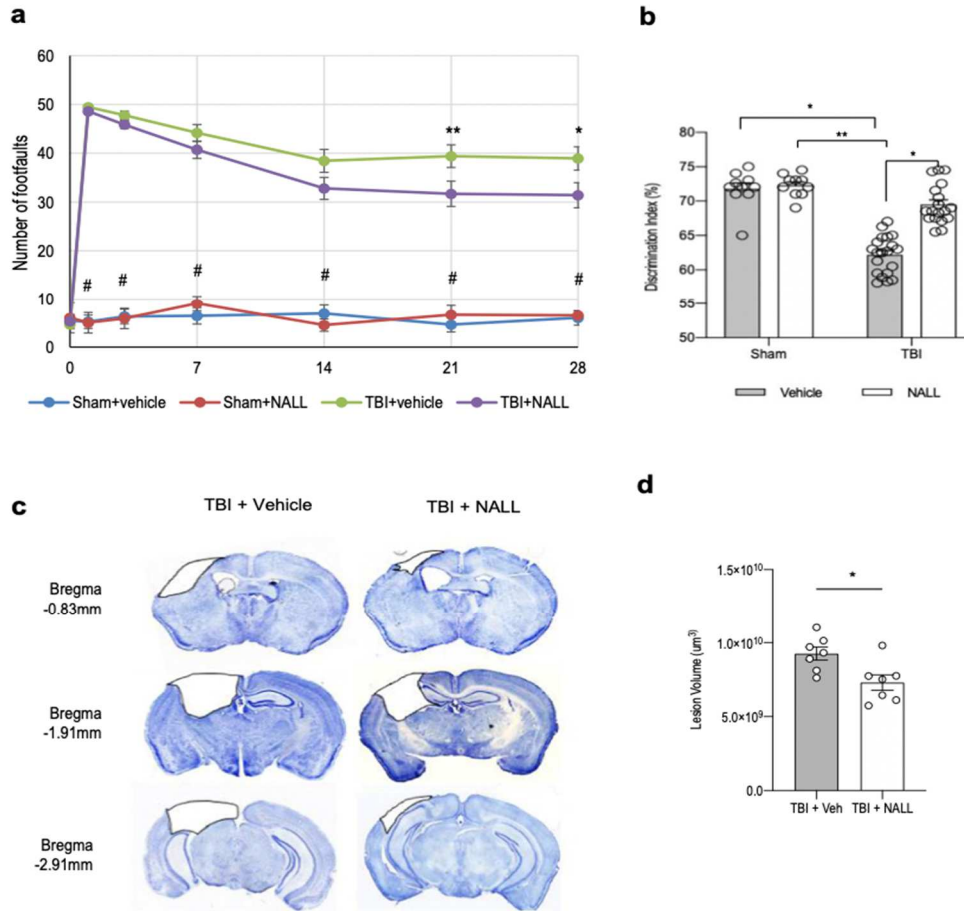


Figure 4-6. NALL attenuates motor and cognitive deficits and cortical tissue loss in mice after injury. (a) Sensory motor function was assessed in sham and TBI mice treated with vehicle or NALL using the Beam Walk test. Significant improvement in motor function was detected in the NALL-fed TBI group as compared to the vehicle-treated TBI mice on days 21 (** $p < 0.01$) and 28 (* $p < 0.05$). Data are presented as mean \pm SEM, $n = 10$ Sham + vehicle, 8 Sham + NALL, 18 TBI + vehicle and 16 TBI + NALL. (b) Novel object recognition (NOR) test was performed on days 24 and 25 after TBI to assess non-spatial memory retention in vehicle or NALL-treated sham or TBI mice. Vehicle-fed TBI mice spent significantly less time with the novel object as compared to NALL-treated TBI mice (* $p < 0.05$, Two-way ANOVA). Time spent with the novel object by the vehicle-treated TBI mice was also significantly less as compared to the vehicle (* $p < 0.05$) or NALL (** $p < 0.01$)-fed sham mice. No significant difference was observed between NALL- treated TBI and either of the sham groups. Data are presented as mean \pm SEM, (c) Representative images of lesion volume at 28 days post-injury in vehicle- and NALL-treated mouse cortices. Images were acquired on Leica DM4000 B TL (BF) microscope and generated using Stereo Investigator software, 2020.2.3 version (MBF Biosciences). Representative black lesion volume outlines seen in the images were traced on Microsoft Powerpoint (Version 16.42). (d) Stereological (Cavalieri method) quantification of lesion volume in vehicle- or NALL-fed CCI-injured mouse cortices. Data are presented as mean \pm SEM. $n = 7$ /group, * $p < 0.05$ (Two-tailed Student's t-test).

4.3. Summary

Repurposing of drugs that are already in clinical use for the treatment of certain medical conditions can be an effective and rapid way to develop useful therapeutic strategies for the treatment of highly devastating and intractable conditions like TBI. The racemic mixture of NAL has been used orally for more than 60 years in France to treat acute vertigo and dizziness (Ferber-Viart et al., 2009). It is also shown to be effective for the treatment of lysosomal storage disorders like NPC and GM2 Gangliosidosis (Tay-Sachs and Sandhoff disease) and the prophylactic treatment of migraine. It is considered a safe drug, as it does not show any major side effects at its therapeutic dose (Bremova et al., 2019). Recently, its L-enantiomer form (NALL) has been identified as the active form of NAL for disease-modification and neuroprotection (Kaya et al., 2020). In the current study, using this active L-isoform we demonstrated that NALL is neuroprotective in an experimental TBI mouse model. This suggests therapeutic potential of NALL and provides a scientific basis for exploring NALL use to treat TBI.

Early inhibition of cell death is very important in managing the devastating neurological outcome following TBI as markers of cell death peak at the acute time points following TBI, specifically in neurons (Sarkar et al., 2013). We observed marked attenuation of cell death both in cortices and in hippocampi during the acute phase at day 1 after TBI in mice that were treated orally with NALL. Our data suggest that this might be mediated through the activation or restoration of autophagy flux by NALL. Autophagy has a neuroprotective function (Nixon et al., 2013) by maintaining cellular homeostasis and removing pathogenic protein aggregates and damaged organelles that have particularly deleterious

effects in post-mitotic cells like neurons (Klionsky et al., 2014; Klionsky et al., 2007; Mizushima et al., 2011).

Impairment in autophagic function has been well documented in many neurodegenerative diseases, including Alzheimer's disease and Parkinson's disease, as well as lysosomal storage disorders like NPC and GM2 (Nixon et al., 2013; Lee et al., 2007). We also previously demonstrated that autophagy is inhibited in the mouse cortex after TBI due to impaired lysosomal function, leading to the accumulation of autophagosomes and toxic ubiquitinated proteins that contribute to neuronal death in the injured cortex (Sarkar et al., 2014; Sarkar et al., 2019). Our and others' data have also demonstrated that increasing autophagy flux after TBI has neuroprotective effects. Thus, early restoration of autophagy flux at day 1 after TBI by NALL treatment clearly demonstrates its beneficial effects in improving neuronal autophagy in the injured mouse cortices, which may contribute to its therapeutic benefits in restricting progressive neuronal death after TBI. We expect that similar mechanisms may contribute to disease-modifying benefits of NALL in other disorders where autophagy defects are observed.

NALL treatment also reduced neuroinflammation in the injured cortices of TBI mice. Acute and prolonged neuroinflammation contributes to the brain damage after TBI. Pro-inflammatory cytokines secreted by activated microglia/macrophages following TBI promote neurotoxicity either by acting directly on neurons or by activating other glial cells, including astrocytes, that secrete neurotoxic modulators (Loane et al., 2014; Kumar et al., 2012). Marked decline in pro-inflammatory cytokines like IL-1 β in the injured cortices of TBI mice fed with NALL clearly suggests attenuation of pro-inflammatory

activation by NALL treatment. Recently, detrimental effects of IFN- β -mediated neuroinflammation was demonstrated to cause chronic neurodegeneration in experimental TBI (Barrett et al., 2019). Thus, the significant decrease in *Ifnb1* gene expression in the injured cortices of TBI mice following NALL treatment further demonstrates the beneficial effects of NALL treatment in TBI.

Additionally, the inflammatory response is also associated with an increase in oxidative stress. Previous studies have demonstrated that NOX2 activation can lead to increased ROS production (Qin et al., 2004; Kumar et al., 2014; Qin et al., 2013).

Thus, the observed decrease in *Nox2* expression following NALL administration may be particularly significant as its genetic deletion or pharmacological inhibition is neuroprotective after TBI (Kumar et al., 2016). While NALL administration results in changes in anti-inflammatory genes *Arg1* and *Socs3* expression levels following brain injury, these levels gradually normalize to the levels observed in vehicle-treated TBI mice. Thus, NALL administration does not result in any long-term imbalance in anti-inflammatory responses that play an important role in tissue repair after TBI. Together, our data suggest that the early attenuation of neuroinflammation is responsible for additional neuroprotective function of NALL after brain trauma.

Early attenuation of neurodegeneration and neuroinflammation in injured mice treated with NALL was associated with improved functional recovery and smaller lesion volume for up to 28 days after injury. The improvements in both motor and cognitive function clearly support a therapeutic potential of NALL in TBI. Improvements in motor function

following NALL treatment in cerebral ataxia (Schneipp et al., 2016) and in neurodegenerative lysosomal storage diseases like NPC (de Vruchte et al., 2019; Bremova et al., 2015) and GM2 Gangliosidosis diseases have been reported previously. It has also been demonstrated that N-acetyl-leucine restores, prevents, and delays disease progression in multiple neurological circuits of the brain, the clinical manifestation of which can be visualized and captured in terms of improvements or stabilization in very different processes such as ambulation, fine motor skills, speech, and also cognition (Kaya et al., 2020; Bremova et al., 2015). The observed attenuation of memory deficit and improvement in cognition in TBI mice treated with NALL in this study supports the beneficial role of NALL treatment on cognitive function. Since TBI is a major risk factor for dementia, NALL-mediated improvement in memory function in injured mice indicates that it might be beneficial in attenuating injury-caused dementia, although further long-term studies will be necessary. It will also be necessary to perform similar studies on female mice to determine if NALL treatment after TBI can yield similar results.

Our study clearly demonstrates therapeutic potential of NALL in attenuating neurological deficits, restricting neuronal loss and neuroinflammation after TBI and provides a scientific basis for the use of NALL as a TBI treatment.

4.4. Methods

4.4.1. Controlled cortical impact (CCI)

CCI was performed as described in Chapter 2.4.2.

4.4.2. NALL treatment

N-Acetyl-L-Leucine L-enantiomer (441511, Sigma) was dissolved in ethanol to prepare a 50 mg/ml solution, which was then diluted to 10 mg/ml in water. Since the food intake decreases in mice early after TBI and cell death and neuroinflammation peak at days 1 and 3, respectively, following brain injury in mice, NALL was given to the mice via oral gavage for four days after CCI-induced TBI so that the effective therapeutic concentration of NALL can be maintained in mice early after injury. Around 0.25 ml of NALL solution (10 mg/ml) was orally administered to mice at a 100 mg/kg/day dose (2.5 mg NALL/25 g mouse) via oral gavage, starting at one hour after CCI-induced TBI and continuing once daily for four days. NALL has been shown to be safe even upon long-term administration (up to several months) and to improve outcomes in animal models in neurodegenerative diseases when administered IV at 10-15 mg/kg (Gunther et al., 2015). Because of the lower bioavailability of NALL when given orally (10-15%), 100 mg/kg of NALL was administered in mice per day orally to maintain its effective concentration. Oral administration was chosen because this route of administration is more clinically relevant and has been shown to be safe and effective in human patients and laboratory animals. Mice were also fed with NALL at 0.5 g/kg of chow for up to 28 days after injury (**Figure 4-1a**). This amount was determined based on the average food intake of mice, which is between 17 and 23% (\approx 20% average) of their own body weight per day (Priestman et al., 2008) that equates to 0.5g NAL/kg chow powder.

4.4.3. Western Blot Analysis

Western blots were performed as described in Chapter 3.4.

Primary antibodies for this study were: LC3 (1:1000; Novus, NB100-2220), p62/SQSTM1 (1:1000; BD Bioscience, 610832), β -actin/ACTB (1:10,000; A1978) and fodrin/spectrin (1:5000; Enzo Life Science International, BML-FG6090).

4.4.4. TUNEL assay

Twenty μ m frozen cortical brain sections were obtained from vehicle- or NALL-fed sham or TBI mouse brains (n=6/group and 4 sections/mouse) at day 1 post-TBI, followed by fixation with 4% paraformaldehyde (PFA, pH 7.4) and protection in 30% sucrose, as previously described. TUNEL-positive cells were detected in brain sections from NALL-fed sham and TBI mice at 1 day post-TBI using ApopTag In Situ Apoptosis Detection Kit (Millipore, S7165) as per the manufacturer's protocol. Images of TUNEL positive cells in the cortical region proximal to the injury site were acquired using a fluorescent Nikon Ti-E inverted microscope at 20X (CFI Plan APO VC 20X NA 0.75 WD 1 mm) and quantified using Nikon Elements software (V4.12.01, Nikon).

We quantified the number of TUNEL+ cells relative to the total number of cells counted. The average number of total cells counted/mouse was approximately 4000 cells/mouse. After the number of TUNEL+ cells were normalized to the total cell number, they were then expressed as TUNEL+ cells/100 cells.

4.4.5. Immunohistochemistry

Twenty μm frozen sections were obtained from vehicle- or NALL-fed sham and TBI mouse brains at 1 day post-TBI ($n=5/\text{group}$) following fixation with 4% paraformaldehyde (PFA, pH 7.4) and protection in 30% sucrose, as previously described (27). Sections were blocked with 5% goat serum (Millipore, S30-100) in 1X phosphate-buffered saline (PBS; Quality Biological, INC., 119-069-101) containing 0.025% Triton X-100 (Sigma, T8787). Sections were incubated overnight with primary antibodies at 4°C and then with secondary antibodies in the blocking solution for 2 h at room temperature. Nuclei were stained with DAPI. 20X images of the immune-stained sections were acquired using a Nikon Eclipse Ti-E/Ni-E microscope and analyzed and quantified by Elements software.

Primary antibodies used include: SQSTM1 (1:200; Progen, GP62-C), LC3 (1:250, Novus Biologics), NeuN (1:500; Millipore, MAB377), Cleaved caspase-3 (1: 200; Cell Signaling Technology, 9661). Secondary antibodies used include: Alexa Fluor 488 goat anti-rabbit (A11034), Alexa Fluor 633 goat anti-guinea pig (A11075), and Alexa Fluor 546 goat anti-mouse (A11030).

We quantified the number of p62+ cells relative to the number of total cells counted. The average number of total cells counted/mouse was approximately 4000 cells/mouse. Once the number of p62+ cells were normalized to the total cell number, they were then expressed as p62+/100 cells. For cleaved caspase-3 and NeuN double staining, the quantification was expressed as number of cleaved caspase 3+ neurons/100 cells.

4.4.6. Real-Time PCR

Around 5 mm tissue of ipsilateral cortex around the site of injury from TBI mice (1 day, 3 days and 7 days post-TBI) or the corresponding tissue of same volume around the same cortical region from sham mice was dissected and processed as described²³. Total RNA isolated using miRNeasy Mini Kit (Qiagen, Cat No. 217004) was converted into cDNA using High-Capacity RNA to cDNA kit (Applied Biosystem, Cat. No. 4387406) as per manufacturer's instruction. cDNA TaqMan® Universal Master Mix II (Applied Biosystems, Cat. No. 4440040) was used to perform quantitative real-time PCR amplification as described previously²³ using 20X TaqMan® Gene Expression Assay (Applied Biosystems) for the following mouse genes: *Gapdh* (Mm99999915_g1), *Nlrp3* (Mm00840904_m1), *Cybb* (Mm01287743_m1), *Nos2* (Mm00440502_m1), *Tnf* (Mm00443258_m1), *Ifnb1* (Mm00439552_s1), *Il1b* (Mm00434228_m1), *Arg1* (Mm00475988_m1), *Socs3* (Mm00545913_s1), *Chil3* (Mm00657889_mH) and *Il4r* (Mm01275139_m1) (Applied Biosystems). Reactions were amplified and quantified by using a 7900HT Fast Real-Time PCR System and corresponding software (Applied Biosystems). Relative gene expression normalized to *Gapdh* was calculated based on the comparative Ct method described earlier. For this study n=5/group for all time points.

4.4.7. Behavioral methods

A battery of behavioral tests were performed at time points depicted in **Figure 4-1a**. All functional assessment and behavioral tests were performed and scored blinded.

4.4.7.1. Beam Walk Test

Fine motor coordination was assessed in sham and vehicle- or NALL-fed TBI mice using the Beam Walk test performed on days 0 (before injury), 1, 3, 7, 14, 21 and 28 after TBI as described in Chapter 3.4.4.1.

4.4.7.2. Novel Object Recognition (NOR) test

Hippocampal spatial memory was measured on days 24 and 25 after TBI using the NOR test as per the method described in Chapter 3.4.4.2. Relative time spent with the novel object over total time spent with novel and familiar object is expressed as discrimination index.

4.4.8. Lesion Volume

Cortical lesion volume was assessed in vehicle- and NALL-treated injured mouse brains at day 28 after TBI. Sixty μm sections located approximately 240 μm apart across the entire lesion volume were stained with cresyl violet (FD Neurotechnologies Inc) and images were acquired on a Leica DM4000 B TL (BF) microscope. Quantification was based on the Cavalieri method using Stereo Investigator software (MBF Biosciences) and the lesion volume was quantified by outlining the missing tissue on the injured hemisphere using the Cavalieri estimator with a grid spacing of 0.1 mm.

4.4.9. Statistical Analysis

All data are presented as mean \pm standard error of the mean (SEM). One-way ANOVA or two-way ANOVA was performed followed by appropriate post-hoc test as specified in the figure legends. For data with only two groups two-tailed student t-test with equal

variance was used. Statistical analyses were performed using GraphPad Prism program, version 3.02 for Windows (GraphPad Software, San Diego, CA, USA). A p value ≤ 0.05 was considered statistically significant. Two-way ANOVA with repeated measures was performed for beam walk analysis. Behavioral and stereological analyses were performed by an individual who was blinded to injury or treatment groups. Number of animals used in this study was determined by power analysis (power of 0.8; alpha value 0.05).

CHAPTER 5: Discussions

The pathophysiology of TBI is complex and heterogeneous, and the multifactorial nature of the involved secondary injury processes makes it challenging to develop effective therapeutic interventions. Neuroinflammation is a well-established key secondary injury mechanism following TBI and can have both detrimental and beneficial effects depending on the phase after injury. In the acute phase of TBI, neuroinflammation can be beneficial as it aids in the clearance of cellular debris and promotes brain repair and tissue regeneration. However, when neuroinflammation is excessive or persists into the chronic phase of TBI, it exacerbates secondary cell death, particularly neuronal cell death, interferes with endogenous repair mechanisms, and is associated with worse neurological outcomes and increased predisposition to neurodegenerative diseases and early-onset dementia. Improvements in our knowledge of the molecular mechanisms that govern neuroinflammation can help guide the development of therapeutics after TBI.

Inhibition of autophagy is also observed in the injured brain after TBI. Our previous data demonstrated that inhibition of autophagy after TBI affects several cell-types, and occurs in different cells at different time points after injury. In the activated immune cells autophagy is inhibited in the acute phase following TBI, but prior to this study the role of autophagy in regulating inflammatory responses after TBI was limited. Thus, the purpose of this study was to characterize the inflammatory status of microglia and infiltrating monocytes/macrophages with inhibited autophagy and to determine the role that autophagy dysregulation plays in neuroinflammation.

5.1 Role of Autophagy in Neuroinflammation

Our lab has previously shown that activated CD68-expressing immune cells accumulate autophagosomes and p62 after TBI (Sarkar et al., 2014), suggesting inhibition of autophagy flux within these cells. The current work demonstrated that inhibition of autophagy flux occurs in both resident microglia and infiltrating monocytes/macrophages as early as 24 hours after TBI and that infiltrating macrophages are impacted to a greater degree than the resident microglia. Moreover, we demonstrated that immune cells with inhibited autophagy flux after CCI expressed increased levels of pro-inflammatory markers, including IL-1 β and TNF α as compared to corresponding immune cells with normal levels of autophagy. These impairments in autophagy and corresponding inflammatory phenotypes persisted through day 28- post CCI, suggesting that autophagy flux impairment following TBI has long-term neuroinflammatory consequences. Moreover, we showed through *in vitro* experiments (Chapter 2) and our *in vivo* studies on *Becn1* cKO mice (Chapter 3) that the autophagy-neuroinflammation link is not a mere correlation, but rather inhibition of autophagy can potentiate pro-inflammatory responses. These findings are consistent with other published work that describing the function of autophagy in regulating inflammatory responses in macrophages and other immune cells. Defects in autophagy have been associated with increased inflammation. For example, cancer researchers have shown that defective autophagy in peripheral myeloid cells enhanced tumor-promoting inflammation and compromised antigen presentation. Conversely, stimulation of autophagy suppressed tumor-promoting inflammation and enhanced anti-cancer immunity (Szabo and Csak, 2012; Zhong et al., 2016). Our data are consistent with the observed anti-inflammatory role of autophagy.

5.2 Role of Autophagy in Innate Immunity after TBI

Our work demonstrates that autophagy dysregulation exacerbates innate immune responses after TBI, particularly the NLRP3 inflammasome pathway and the cGAS/STING signaling pathway. These pathways are activated in the brain when specific DAMPs released from damaged or dying cells post-injury stimulate PPRs present on immune brain cells. As such, these DAMPs act as endogenous danger signals to regulate the subsequent inflammatory and immune response. A crucial role of the autophagic machinery is clearance and degradation of these DAMPS to prevent prolonged activation of innate immune responses (Zhang et al., 2013).

Previous work has supported the role of autophagy in regulating inflammasome activation. Under homeostatic conditions, autophagy negatively regulates inflammasome activation, and decrease in autophagy function leads to activation of these hyperactivation of the pathway and increased production of its downstream such as IL-1 β and IL-18 (Deretic et al., 2013; Levine et al., 2011). Regulation of inflammasome activation by autophagy occurs in multiple ways, through either removal of endogenous inflammasome activators or removal of inflammasomes components directly through selective autophagy. Selective autophagy is a more targeted and receptor-specific form of autophagy that entails cooperation between specific target recognition and assembly of the autophagic apparatus. In recent years, the tripartite motif (TRIM) family (particularly TRIM20) has been shown to act as an autophagy receptor for delivery of the NLRP3 inflammasome components for autophagic degradation. Our data (**Figure 3-7**) shows increase of TRIM20 protein levels in response to TBI, which suggest a role for this precision autophagy in regulating inflammasome pathway activation following injury. In

context of TBI, we hypothesize that inhibition of autophagy in microglia and infiltrating immune cells leads to both decreased removal of inflammasome-activating DAMPs as well decreased removal of inflammasome components through p62 or other TRIM proteins.

5.3. Role of Autophagy in TBI: Expansion of existing paradigm

Overall, this work strengthens the need to study autophagy dysregulation in TBI and its role in all cell types. In the CNS field, autophagy has been studied in greater detail in neurons, where it plays a crucial role as a checkpoint for protein and organelle quality control. Dysregulated autophagy plays a critical role in the development and progression of neurodegenerative diseases such as AD, PD, HD, and ALS. The depletion of key autophagy-related genes (such as *Atg5*, *Atg7*) in neurons results in neurodegeneration in mice. On the other hand, upregulation of autophagy in neurons can be a protective mechanism that slows the advance of neurodegenerative disorders (Martinez-Vicente and Cuervo, 2007).

In TBI, autophagy flux inhibition in neurons results in excessive ER stress and neuronal loss. Our current data demonstrate that autophagy flux inhibition in microglia/monocytes in the acute phase of TBI exacerbates inflammation. Thus, inhibition of autophagy after TBI directly contributes to both neurodegeneration and neuroinflammation. Furthermore, excessive inflammation can indirectly result in increased neuronal cell death. In our studies, microglia and monocyte/macrophage-specific inhibition of autophagy in mice, mediated through knockout of the autophagy gene *Becn1*, resulted in worse functional outcomes. This was associated with excessive neuroinflammation as well as increased

hippocampal neuronal loss and overall neurodegeneration. This finding is consistent with the previously reported spatial and temporal correlation of microglial activation with levels of neuronal loss in the brain (Farfel-Becker et al., 2011b).

Although we need to more thoroughly understand the complex and heterogeneous autophagic response triggered by the TBI, these data suggests that enhancement of autophagy can play a multivalent protective role to help restore homeostasis within the injured brain. As we have demonstrated in Chapter 4 (Hegdekar et al., 2021), therapies that upregulate autophagy in the early phase post-injury can result in both decreased neuronal cell death and decreased neuroinflammation, and ultimately translate to better functional outcomes. Thus, autophagy-enhancing drugs could positively affect multiple cell types, promoting neuron and oligodendrocyte survival, oligodendrocyte differentiation, and decreasing neuroinflammation in the brain (Lipinski & Wu, 2015).

5.4. Autophagy, TBI & Aging

Epidemiological data implicate history of TBI as a major predisposing factor to development of neurodegenerative diseases and dementia later in life. However, the mechanisms how TBI may contribute to development of neurodegeneration years or even decades later remain poorly understood. Our data indicate that although inhibition of autophagy in the microglia and monocytes/macrophages occurs in the acute phase following TBI, it persists into the chronic phase, suggesting possible long-term consequences. Therefore, our work has potential implications in the field of aging and chronic outcomes following TBI.

One of the major changes that occur during aging is the dysregulation of the immune response, leading to a chronic systemic inflammatory state. Among the dysregulated proinflammatory mediators, cytokines and chemokines are major culprits in the development of chronic inflammation and the immunosenescence process. For instance, interleukin (IL)-6, tumor necrosis factor (TNF)- α , and their receptors, are upregulated in aged tissues and cells. Elevated levels of chemokines and C-reactive protein (CRP) have been found to be involved in age-related pathogenesis (Gordon et al., 2011). Moreover, several key intra- or inter-cellular signaling pathways are closely associated with age-related chronic inflammatory changes during aging (Kwon et al., 2001).

In the aging literature, there are currently two major hypotheses related to age-related inflammation: inflammaging (Franceschi et al., 2000; Franceschi et al., 2007). and molecular inflammation (Chung et al., 2006; Chung et al., 2000; Chung 2001). These two are complementary to each other to a large extent but differ in their focus on age-related inflammatory phenomena. Inflammaging refers to a low-grade pro-inflammatory phenotype which accompanies aging in mammals. The aging process is also associated with a decline in autophagic capacity which impairs cellular housekeeping, leading to protein aggregation. Long-term defects in autophagy in brain immune cells also results in aberrant clearance of damaged mitochondria, leading to elevated inflammation and accumulation of ROS and protein aggregates that can cause ER stress (Bujak et al., 2015; Komatsu et al., 2006). Recent studies have clearly indicated that the ROS production induced by damaged mitochondria can stimulate inflammasomes. Nod-like receptor 3 (NLRP3) can be activated by many danger signals, e.g. ROS, cathepsin B released from destabilized lysosomes and aggregated proteins, all of which evoke cellular stress and are

involved in the aging process. NLRP3 activation is also enhanced in many age-related diseases, e.g., atherosclerosis, obesity and type 2 diabetes. NLRP3 activates inflammatory caspases, mostly caspase-1, which cleave the inactive precursors of IL-1 β and IL-18 and stimulate their secretion. Consequently, these cytokines provoke inflammatory responses and accelerate the aging process by inhibiting autophagy. This suggests that inhibition of autophagic capacity with aging generates the inflammaging condition via the activation of inflammasomes, in particular NLRP3.

Overall, effective function of autophagic uptake and lysosomal degradation of dysfunctional mitochondria and aggregated proteins is a crucial element in maintaining tissue homeostasis. There are indications that autophagic capacity is compromised in certain diseases e.g., in Alzheimer's disease (Nixon et al., 2011). On the other hand, there is growing evidence implying that inflammasomes are activated in many pathological conditions (Martinez-Vicente et al., 2007; Levine & Kroemer, 2008) and thus a deficiency in autophagic housekeeping could trigger an inflammatory component and aggravate their pathogenesis. As TBI inhibits autophagy function in microglia after TBI, this could potentially accelerate aging-related inflammaging and contribute to predisposition to neurodegeneration and dementia after TBI.

5.5. Future Directions

1. Molecular mechanisms by which autophagy mediates neuroinflammation: Our work provides interesting insights into the neuroinflammatory landscape after TBI due to autophagy dysregulation in microglia and monocytes/macrophages. However, we did not study molecular mechanisms or elucidate the components of the autophagy machinery that might be potentiating innate immune signaling pathways after TBI. Future work

should focus on the role that non-selective autophagy plays in DAMP removal and that precision autophagy plays in mediating inflammasome activation after TBI.

2. Sex-based differences in autophagy regulation after TBI: One future avenue that should be explored in further detail is whether there are sex-based differences in autophagy regulation/dysregulation after TBI. Sex has emerged as a contributing factor that influences the development and progression of multiple psychiatric and neurodegenerative conditions. For example, data suggests that while both men and women are affected by neurodegenerative diseases (such as AD and PD), women are at greater risk for both developing the disease and have more severe pathology (Yoshitake et al., 1995; Fratiglioni et al., 1997; Andersen et al., 1999; Letenneur et al., 1999; Di Carlo et al., 2002; Miech et al., 2002). One possible cause of the differences between males and females is the effects of sex, both chromosomal makeup and hormones, on autophagy during the individual's lifetime. This would be an exciting area to explore in TBI, especially because sex is a factor that plays a role in TBI outcomes. We performed this work primarily on male mice, and experiments should be carried on female mice to obtain a sex-based comparison of autophagy regulation on inflammation.

3. Effects of autophagy inhibition on long-term TBI outcomes: Our data indicate that dysregulated autophagy plays a vital role in the pathogenesis of neuroinflammation in the acute phases following injury. Our studies were performed until the day 28 time point following TBI, and future work should examine the long-term effects beyond this time point. As autophagic function decrease with age (Barbose et al., 2019), we hypothesize that long-term autophagy dysregulation, will enable us to further understand differences between our *Becn1* cKO/Sham mice and Control/mice. In addition, long-term studies will

provide key insights into the long-term impact of autophagy dysregulation on TBI outcomes and neuroinflammation in aging.

4. The impact of autophagy inhibition on other cell types in the brain and periphery For this study, we determined that autophagy dysregulation in microglia and monocytes/macrophage exacerbated (to some extent) neurodegeneration after TBI. Given the heterogeneity of cells in the brain, future work should examine the impact of autophagy dysregulation on other cell types such as astrocytes and oligodendrocytes.

5.6. Final Thoughts on this Project

TBI is a devastating condition with high personal and socioeconomic burden. While the current treatments can help mask symptoms and improve patient quality of life, they are unable to prevent or reverse the underlying damage to the brain. Understanding the mechanism of a disease is essential to finding a cure. Even today, the complete pathophysiology of TBI is not fully understood, but it is well established that chronic neuroinflammation contributes to TBI disease progression and poor neurological outcomes. The present work has characterized the functional role of autophagy in microglia and infiltrating monocytes/macrophages in regulating neuroinflammation levels after TBI. We demonstrated that inhibition of autophagy exacerbates neuroinflammation and particularly the innate immune responses after TBI. This work has expanded the field's knowledge of a mechanism that could potentiate neuroinflammation after TBI, lays the groundwork for investigating pathways by which autophagy mediates innate immune responses after TBI and opens up potential novel therapeutic avenues to treat TBI.

REFERENCES

- Abdullah, A., Zhang, M., Frugier, T. (2018). STING-mediated type-I interferons contribute to the neuroinflammatory process and detrimental effects following traumatic brain injury. *J Neuroinflammation*; 15, 323.
doi:10.1186/s12974-018-1354-7.
- Ahmed, S., Maratha, A., Butt, A.Q., Shevlin, E., Miggin, S.M. (2013). TRIF-mediated TLR3 and TLR4 signaling is negatively regulated by ADAM15. *J Immunol*;190(5):2217-28.
doi: 10.4049/jimmunol.1201630.
- Algattas, H., Huang, J.H. (2013). Traumatic Brain Injury pathophysiology and treatments: early, intermediate, and late phases post-injury. *Int J Mol Sci*;15(1):309-41.
doi: 10.3390/ijms15010309.
- Alirezaei, M., Kemball, C.C., Flynn, C.T., Wood, M.R., Whitton J.L., Kiosses W.B. (2010). Short-term fasting induces profound neuronal autophagy. *Autophagy*;6(6):702-710. doi:10.4161/auto.6.6.12376.
- Andriessen, T.M., Jacobs, B., Vos, P.E. (2010). Clinical characteristics and pathophysiological mechanisms of focal and diffuse traumatic brain injury. *J Cell Mol Med*;14(10):2381-92.
doi: 10.1111/j.1582-4934.2010.01164.
- Arroyo, D.S., Gaviglio, E.A., Peralta B., Ramos, J.M., Bussi, C., Rodriguez-Galan, M.C., Iribarren, P. (2014). Autophagy in inflammation, infection, neurodegeneration and cancer. *Int. Immunopharmacol.* 18, 55–65.
doi: 10.1016/j.intimp.2013.11.001.
- Au, T.M., Sauer-Zavala, S., King, M.W., Petrocchi, N., Barlow, D.H., Litz, B.T. (2017). Compassion-Based Therapy for Trauma-Related Shame and Posttraumatic Stress: Initial Evaluation Using a Multiple Baseline Design. *Behav Ther*; 48(2):207-221.
doi: 10.1016/j.beth.2016.11.012.
- Aungst, S.L., Kabadi S.V., Thompson, S.M., Stoica, B.A., Faden, A.I. (2014). Repeated mild traumatic brain injury causes chronic neuroinflammation, changes in hippocampal synaptic plasticity, and associated cognitive deficits. *J Cereb Blood Flow Metab*; 34(7):1223-32.
doi: 10.1038/jcbfm.2014.75
- Bao, H.J., Zhang, L., Han, W.C., Dai, D.K. (2015). Apelin-13 attenuates traumatic brain injury-induced damage by suppressing autophagy. *Neurochem. Res*; 40, 89–97.
doi: 10.1007/s11064-014-1469-x.

Barrett J.P., Knoblach, S.M., Bhattacharya, S., Gordish-Dressman, H., Stoica, B.A., Loane D.J. (2021). Traumatic Brain Injury Induces cGAS Activation and Type I Interferon Signaling in Aged Mice. *Front Immunol*; 12:710608.
doi: 10.3389/fimmu.2021.710608.

Barrett, J.P., Henry R.J., Shirey K.A., Doran S.J., Makarevich O.D., Ritzel R.M., Meadows V.A., Vogel S.N., Faden A.I, Stoica B.A., Loane D.J. (2020). Interferon-beta plays a detrimental role in experimental traumatic brain injury by enhancing neuroinflammation that drives chronic neurodegeneration. *J. Neurosci.* 40, 2357–2370.
doi: 10.1523/JNEUROSCI.2516-19.2020.

Baxendale, S., Heaney, D., Rugg-Gunn, F. & Friedland, D. (2019). Neuropsychological outcomes following traumatic brain injury. *Pract. Neurol.*
Doi:10.1136/practneurol-2018-002113.

Bendlin, B.B., Ries, M.L., Lazar, M., Alexander, A.L., Dempsey, R.J., Rowley, H.A., Sherman J.E., Johnson S.C. (2008). Longitudinal changes in patients with traumatic brain injury assessed with diffusion-tensor and volumetric imaging. *Neuroimage*; 42(2):503-14.
doi: 10.1016/j.neuroimage.2008.04.254.

Bieri, G., Lucin, K.M., O'Brien, C.E. (2018). Proteolytic cleavage of Beclin 1 exacerbates neurodegeneration. *Mol Neurodegeneration* 13, 68.
Doi:10.1186/s13024-018-0302-4.

Bremova-Ertl, T., Platt, F., Strupp, M. (2020). Sandhoff disease: Improvement of gait by acetyl-DL-leucine: A case report. *Neuropediatrics*; 51(6):450-452.
doi:10.1055/s-0040-1715486.

Bremova, T., Malinová, V., Amraoui, Y., Mengel, E., Reinke, J., Kolníková, M., Strupp, M. (2015). Acetyl-dl-leucine in Niemann-Pick type C: A case series. *Neurology*85, 1368–1375.
doi:10.1212/WNL.0000000000002041.

Bruns, J. Jr., Hausar, W.A. (2003). The epidemiology of traumatic brain injury: a review. *Epilepsia*, 44(s10):2-10.
doi: 10.1046/j.1528-1157.44.s10.3.x.

Chan, V., Mollayeva, T., Ottenbacher, K.J., Colantonio, A. (2017). Clinical profile and comorbidity of traumatic brain injury among younger and older men and women: a brief research notes. *BMC Res Notes*, 10(1):371.
doi:10.1186/s13104-017-2682-x.

Churchill, G.C., Strupp, M., Galione, A. and Platt, F.M. (2020). Unexpected differences in the pharmacokinetics of N-acetyl-DL-leucine enantiomers after oral dosing and their clinical relevance. *PLoS ONE*; 15, e0229585.
doi: 10.1371/journal.pone.0229585.

Clark, R.S., Schiding, J.K., Kaczorowski, S.L., Marion, D.W., Kochanek, P.M. (1994). Neutrophil accumulation after traumatic brain injury in rats: comparison of weight drop and controlled cortical impact models. *J Neurotrauma*; 11(5):499-506.
doi: 10.1089/neu.1994.11.499.

Cole, J., Ritchie, S., Bastin, M. et al. Brain age predicts mortality (2018). *Mol Psychiatry*; 23, 1385–1392.
doi: 10.1038/mp.2017.62

Cortes, D., Pera, M.F. (2021) The genetic basis of inter-individual variation in recovery from traumatic brain injury. *npj Regen Med* 6, 5.
doi:10.1038/s41536-020-00114-y.

Cortina-Borja, M. (2018). Annual severity increment score as a tool for stratifying patients with Niemann-Pick disease type C and for recruitment to clinical trials. *Orphanet. J. Rare Dis*;13, 143.
doi:10.1186/s13023-018-0880-9.

Corso, P., Finkelstein, E., Miller, T., Fiebelkorn, I., Zaloshnja, E. (2015). Incidence and lifetime costs of injuries in the United States. *Inj. Prev*; 21, 434–440.
doi: 10.1136/ip.2005.010983.

Coughlin, J.M., Wang, Y., Munro, C.A. (2015). Neuroinflammation and brain atrophy in former NFL players: An in vivo multimodal imaging pilot study. *Neurobiol Dis*; 74:58-65.
doi: 10.1016/j.nbd.2014.10.019.

Crişan, T.O., Plantinga, T.S., van de Veerdonk, F.L., Farcaş, M.F., Stoffels, M., Kullberg, B.J., van der Meer, J.W., Joosten, L. A., & Netea, M. G. (2011). Inflammasome-independent modulation of cytokine response by autophagy in human cells. *PLoS One*; 7;6(4):e18666.
doi: 10.1371/journal.pone.0018666.

Daglas, M., Draxler, D.F., Ho, H., McCutcheon, F., Galle, A., Au, A.E., Larsson, P., Gregory, J., Alderuccio, F., Sashindranath, M., Medcalf, R.L. (2019). Activated CD8+ T Cells Cause Long-Term Neurological Impairment after Traumatic Brain Injury in Mice. *Cell Rep*; 29(5):1178-1191.e6.
doi: 10.1016/j.celrep.2019.09.046.

Dams-O'Connor K., Spielman L., Singh A., Gordon, W.A., Lingsman, H.F., Maas, A.I., Manley, G.T., Mukherjee, P., Okonkwo, D.O., Puccio AM, Schnyer DM, Valadka AB, Yue JK, Yuh EL; TRACK-TBI Investigators (2013).The impact of previous traumatic brain injury on health and functioning: a TRACK-TBI study. *J Neurotrauma*; 15;30(24):2014-20.
doi: 10.1089/neu.2013.3049.

De Luca, L., Olivari, Z., Bolognese, L., Lucci, D., Gonzini, L., Di Chiara, A., Casella G., Chiarella, F., Boccanelli, A., Di Pasquale, G., Bovenzi, F.M., Savonitto, S. (2014). A decade of changes in clinical characteristics and management of elderly patients with non-ST elevation myocardial infarction admitted in Italian cardiac care units. *Open Heart*;13;1(1):e000148.

doi: 10.1136/openhrt-2014-000148.

Deretic, V., Saitoh, T., and Akira, S. 2013. Autophagy in infection, inflammation and immunity. *Nat. Rev. Immunol*; 13:722–737.

doi:10.1038/nri3532.

Ding, Z., Liu S., Deng, X., Fan, Y., Wang, X., Mehta, J.L. Hemodynamic shear stress modulates endothelial cell autophagy: Role of LOX-1. *Int J Cardiol.* 2015 Apr 1;184:86-95.

doi: 10.1016/j.ijcard.2015.01.065.

Dupont, N., Jiang, S., Pilli M., Ornatowski W., Bhattacharya D., and Deretic V. (2011). Autophagy-based unconventional secretory pathway for extracellular delivery of IL-1 β . *EMBO J*; 30(23):4701-4711.

doi:10.1038/emboj.2011.398

Duran, A, Linares, J.F., Galvez, A.S., Wikenheiser, K., Flores, J.M., Diaz-Meco, M.T., Moscat, J. (2008). The signaling adaptor p62 is an important NF-kappaB mediator in tumorigenesis. *Cancer Cell*; 13(4):343-54.

doi: 10.1016/j.ccr.2008.02.001

Egea-Guerrero, J.J., Murillo-Cabezas, F., Gordillo-Escobar, E., Rodríguez-Rodríguez, A, Enamorado-Enamorado, J., Revuelto-Rey, J., Pacheco-Sánchez, M., León-Justel A, Domínguez-Roldán J.M., Vilches-Arenas A. (2013). S100B protein may detect brain death development after severe traumatic brain injury. *J Neurotrauma*; 15;30(20):1762-9.

doi: 10.1089/neu.2012.2606.

Erlich, S., Alexandrovich A., Shohami E., Pinkas-Kramarski R. (2007). Rapamycin is a neuroprotective treatment for traumatic brain injury. *Neurobiol Dis.*; 26(1):86-93.

doi: 10.1016/j.nbd.2006.12.003.

Faden, A.I., Loane D.J. (2015) Chronic neurodegeneration after traumatic brain injury: Alzheimer disease, chronic traumatic encephalopathy, or persistent neuroinflammation? *Neurotherapeutics*; 12(1):143-50.

doi: 10.1007/s13311-014-0319-5.

Faden, A.I., Wu, J., Stoica, BA, Loane, DJ. (2016). Progressive inflammation-mediated neurodegeneration after traumatic brain or spinal cord injury. *J Pharmacol.*; 173(4):681-691.

doi:10.1111/bph.13179.

Faul, M., Coronado V. (2015). Epidemiology of traumatic brain injury. *Handb Clin Neurol*;127:3-13.
doi: 10.1016/B978-0-444-52892-6.00001-5.

Ferber-Viart, C., Dubreuil, C. & Vidal, P. P. (2009). Effects of acetyl-DL-leucine in vestibular patients: A clinical study following neurotomy and labyrinthectomy. *Audiol. Neurotol.*; 14, 17–25.
doi:10.1159/000148206.

Fields, T., Patterson, M., Bremova, T., Belcher, G., Billington, I. (2021). A master protocol to investigate a novel therapy acetyl-L-leucine for three ultra-rare neurodegenerative diseases: Niemann-Pick disease type C, The GM2 Gangliosidosis, and Ataxia-Telangiectasia. *Trial*; 22(1), 84.
doi: 10.1186/s13063-020-05009-3(2021).

Fleminger, S (2008). Long-term psychiatric disorders after traumatic brain injury. *Eur. J. Anaesthesiol. Suppl.* **42**, 123–130.
doi:10.1017/S0265021507003250

Frati, A., Cerretani D., Fiaschi A.I., Frati P., Gatto V., La Russa R., Pesce A., Pinchi E., Santurro A., Frascetti F., Fineschi V. (2017). Diffuse Axonal Injury and Oxidative Stress: A Comprehensive Review. *Int J Mol Sci*; 2;18(12):2600.
doi: 10.3390/ijms18122600.

French FMF Consortium (1997). A candidate gene for familial Mediterranean fever. *Nat. Genet.* 17:25–31.
doi:10.1038/ng0997-25.

Gao, Y., Zhuang, Z., Gao, S., Li, X., Zhang, Z., Ye, Z., Li, L., Tang, C., Zhou, M., Han, X., Li, J (2017). Tetrahydrocurcumin reduces oxidative stress-induced apoptosis via the mitochondrial apoptotic pathway by modulating autophagy in rats after traumatic brain injury. *Am J Transl Res*; 15;9(3):887-899.

Gao, D., Wu, J., Wu, Y.T., Du, F., Aroh, C., Yan, N., Sun, L., and Chen, Z.J. 2013. Cyclic GMP-AMP synthase is an innate immune sensor of HIV and other retroviruses. *Science*; 341:903–906.
doi:10.1126/science.1240933.

Ginhoux, F., Greter, M., Leboeuf, M., Nandi, S., See, P., Gokhan, S., Mehler, M.F., Conway, Stanley E.R., Samokhvalov, Merad, M. (2010). Fate mapping analysis reveals that adult microglia derive from primitive macrophages. *Science*; 330(6005):841-5.
doi: 10.1126/science.1194637.

Gomes, L.C., Dikic, I. (2014). Autophagy in antimicrobial immunity. *Mol. Cell.* 54:224–233.
doi: 10.1016/j.molcel.2014.03.009.

Gordon, S., Martinez, F.O. (2010). Alternative activation of macrophages: mechanism and functions. *Immunity* 32, 593–604.
doi: 10.1016/j.immuni.2010.05.007

Green, R.E.A., Colella, B., Maller, J.J., Bayley, M., Glazer, J., Mikulis, D.J. (2014). Scale and pattern of atrophy in the chronic stages of moderate-severe TBI. *Front. Hum. Neurosci.* 8:67.
doi: 10.3389/fnhum.2014.00067

Gruenbaum, S.E., Zlotnik, A., Gruenbaum, B.F., Hersey, D., Bilotta, F. (2016). Pharmacologic Neuroprotection for Functional Outcomes After Traumatic Brain Injury: A Systematic Review of the Clinical Literature. *CNS Drugs*; 30(9):791-806.
doi:10.1007/s40263-016-0355-2.

Günther, L., Beck, R., Xiong, G., Potschka, H., Jahn, K., Bartenstein, P., Brandt, T., Dutia M., Dieterich, M., Strupp, M., la Fougère, C., Zwergal, A. (2015). N-acetyl-L-leucine accelerates vestibular compensation after unilateral labyrinthectomy by action in the cerebellum and thalamus. *PLoS One*; 10(3):e0120891.
doi: 10.1371/journal.pone.0120891.

Gupte, R., Brooks, W., Vukas, R., Pierce, J., Harris, J. (2019). Sex Differences in Traumatic Brain Injury: What We Know and What We Should Know. *J Neurotrauma*;c36(22):3063-3091.
doi: 10.1089/neu.2018.6171.

Gyoneva, S., Hosur, R., Gosselin, D., Zhang, B., Ouyang, Z., Coteleur, A. C., Peterson, M., Allaire, N., Challa, R., Cullen, P., Roberts, C., Miao, K., Reynolds, T. L., Glass, C. K., Burkly, L., & Ransohoff, R. M. (2019). *Cx3cr1*-deficient microglia exhibit a premature aging transcriptome. *Life science alliance*, 2(6), e201900453.
Doi:10.26508/lsa.201900453

Gyoneva, S., Kim, D., Katsumoto, A., Kokiko-Cochran, O.N., Lamb, B.T., Ransohoff, R.M. (2015). *Ccr2* deletion dissociates cavity size and tau pathology after mild traumatic brain injury. *J Neuroinflammation*;12:228.
doi: 10.1186/s12974-015-0443-0.

Gyoneva, S., Ransohoff, R.M. (2015). Inflammatory reaction after traumatic brain injury: therapeutic potential of targeting cell-cell communication by chemokines. *Trends Pharmacol Sci*;36(7):471-80.
doi: 10.1016/j.tips.2015.04.003.

Hanscom, M., Loane D.J., Aubretch, T. (2021). Acute colitis during chronic experimental traumatic brain injury in mice induces dysautonomia and persistent extraintestinal, systemic, and CNS inflammation with exacerbated neurological deficits. *J Neuroinflammation*;18(1):24.
doi:10.1186/s12974-020-02067-x.

Harris, J., Hartman, M., Roche, C., Zeng, S.G., O'Shea, A., Sharp F.A., Lambe E.M., Creagh E.M., Golenbock D.T., Tschopp J., Kornfeld H., Fitzgerald K.A., Lavelle E.C. (2011). Autophagy controls IL-1beta secretion by targeting pro-IL-1beta for degradation. *J Biol Chem*; 286(11):9587-97.
doi: 10.1074/jbc.M110.202911.

Heckmann, B.L., Boada-Romero, E., Cunha, L.D., Magne, J., Green, D.R. (2017). LC3-Associated Phagocytosis and Inflammation. *J Mol Biol*;429(23):3561-3576.
doi: 10.1016/j.jmb.2017.08.012.

Heneka, M.T., Carson, M.J., El Khoury, J., Landreth, G.E, Brosseron, F., Feinstein, D.L. (2015) Neuroinflammation in Alzheimer's disease. *Lancet Neurol*; 14:388–405

Hegdekar, N., Lipinski, M. M., & Sarkar, C. (2021). N-Acetyl-L-leucine improves functional recovery and attenuates cortical cell death and neuroinflammation after traumatic brain injury in mice. *Scientific reports*; 11(1), 9249.
doi:10.1038/s41598-021-88693-8

Hickman, S., Kingery, N., Ohsumi, T. (2013). The microglial sensome revealed by direct RNA sequencing. *Nat Neurosci*; 16, 1896–1905.
doi:10.1038/nn.3554

Houtman, J., Freitag, K., Gimber, N., Schmoranzer, J., Heppner, F.L., Jendrach, M. (2019). Beclin1-driven autophagy modulates the inflammatory response of microglia via NLRP3. *EMBO J*; 38(4):e99430.
doi: 10.15252/embj.201899430.

Hutson, C.B., Nichol, J.W., Aubin, H., Bae, H., Yamanlar, S., Al-Haque, S., Koshy, S.T., Khademhosseini, A. (2011). Synthesis and characterization of tunable poly(ethylene glycol): gelatin methacrylate composite hydrogels. *Tissue Eng Part A*; 17(13-14):1713-23.
doi: 10.1089/ten.TEA.2010.0666.

Iankova, A. (2006). The Glasgow Coma Scale: clinical application in emergency departments. *Emerg Nurse*; 14(8):30-5.
doi: 10.7748/en2006.12.14.8.30.c4221..

International Consortium for Systemic Lupus Erythematosus Genetics (SLEGEN), Harley, J. B., Alarcón-Riquelme, M. E., Criswell, L. A., Jacob, C. O., Kimberly, R. P., Moser, K. L., Tsao, B. P., Vyse, T. J., Langefeld, C. D., Nath, S. K., Guthridge, J. M., Cobb, B. L., Mirel, D. B., Marion, M. C., Williams, A. H., Divers, J., Wang, W., Frank, S. G., Namjou, B., Kelly, J. A. (2008). Genome-wide association scan in women with systemic lupus erythematosus identifies susceptibility variants in ITGAM, PXX, KIAA1542 and other loci. *Nat Genet.*; 40(2):204-10.
doi: 10.1038/ng.81.

Izzy, S., Liu, Q., Fang, Z. (2019). Time-Dependent Changes in Microglia Transcriptional Networks Following Traumatic Brain Injury. *Front Cell Neurosci.*; 13:307.
doi:10.3389/fncel.2019.00307.

Jassam, Y.N., Izzy, S., Whalen, M., McGavern, D.B., El Khoury J. (2017). Neuroimmunology of Traumatic Brain Injury: Time for a Paradigm Shift. *Neuron*; 95(6):1246-1265.
doi: 10.1016/j.neuron.2017.07.010.

Jiang, Y., Huang, W., Wang, J., Xu Z., He, J., Lin, X., Zhou, Z., Zhang J. (2014). Metformin plays a dual role in MIN6 pancreatic β cell function through AMPK-dependent autophagy. *Int J Biol Sci.*;10(3):268-77.
doi: 10.7150/ijbs.7929.

Johansen, T., T. Lamark. (2011). Selective autophagy mediated by autophagic adapter proteins. *Autophagy*; 7:279–296.
Doi:10.4161/ auto.7.3.14487.

Johnson, V.E., Stewart, J.E., Begbie, F.D., Trojanowski, J.Q., Smith, D.H., Stewart, W. (2013). Inflammation and white matter degeneration persist for years after a single traumatic brain injury. *Brain*; 136(Pt 1):28-42.
doi: 10.1093/brain/aws322.

Johnson, V. E., Meaney, D. F., Cullen, D. K. & Smith, D. H. (2015). Animal models of traumatic brain injury. *Handb. Clin. Neurol.*; 127, 115–128.
doi:10.1016/B978-0-444-52892-6.00008-8.

Jounai, N., F. Takeshita, K. Kobiyama, A. Sawano, A. Miyawaki, K.Q. Xin, K.J. Ishii, T. Kawai, S. Akira, K. (2007). The Atg5 Atg12 conjugate associates with innate antiviral immune responses. *Proc. Natl. Acad. Sci. USA*; 104:14050–14055.
doi.:10.1073/ pnas.0704014104

Karsli-Uzunbas, G., Guo, J.Y., Price, S., Teng, X., Laddha, S.V., Khor, S., Kalaany, N.Y., Jacks, T., Chan, C.S., Rabinowitz, J.D., White, E. (2014). Autophagy is required for glucose homeostasis and lung tumor maintenance. *Cancer Discov.*; 4(8):914-27.
doi: 10.1158/2159-8290.CD-14-0363.

Kawai, T., Akira, S. (2010). The role of pattern-recognition receptors in innate immunity: update on Toll-like receptors. *Nat Immunol*;11(5):373-84.
doi: 10.1038/ni.1863.

Kaya, E. (2020). Acetyl-leucine slows disease progression in lysosomal storage disorders. *Brain Commun.*; 3(1).
doi.org/10.1093/braincomms/fcaa148(2020).

Kaya, E., Smith, D.A., Smith, C., Boland, B., Strupp, M., Platt, F.M. (2020). Beneficial Effects of Acetyl-DL-Leucine (ADLL) in a Mouse Model of Sandhoff Disease. *Journal of clinical medicine*, 9(4), 1050.
doi.org/10.1093/braincomms/fcaa148.

Khaksari, M., Hajializadeh, Z., Shahrokhi, N., and Esmaeili-Mahani, S. (2015). Changes in the gene expression of estrogen receptors involved in the protective effect of estrogen in rat's traumatic brain injury. *Brain Research*; 1618, 1–8.
doi: 10.1016/j.brainres.2015.05.017.

Klionsky, D. J. (2007) Autophagy: From phenomenology to molecular understanding in less than a decade. *Nat. Rev. Mol. Cell Biol.* 8, 931–937.
doi: 10.1038/nrm2245.

Kirisako, T., Ichimura, Y., Okada, H. (2000). The reversible modification regulates the membrane-binding state of Apg8/Aut7 essential for autophagy and the cytoplasm to vacuole targeting pathway. *J Cell Biol*;151(2):263-276.
doi:10.1083/jcb.151.2.263.

Kawai, T., Akira, S. (2011) Toll-like receptors and their crosstalk with other innate receptors in infection and immunity. *Immunity*134:637–50
doi: 10.1016/j.immuni.2011.05.006

Kraft, C., Peter, M., Hofmann, K. (2010). Selective autophagy: ubiquitin-mediated recognition and beyond. *Nature Cell Biology*.;12(9):836-41.
doi: 10.1038/ncb0910-836.

Kumar, A., Alvarez-Croda, D.M., Stoica, B.A., Faden, A.I, and Loane, D.J. (2015) Microglial/Macrophage Polarization Dynamics following Traumatic Brain Injury. *Journal of Neurotrauma*; 1;33(19):1732-1750.
doi: 10.1089/neu.2015.4268.

Kumar, A., Barrett, J.P., Alvarez-Crod,a D.M., Stoica, B.A., Faden, A.I., and Loane, D.J. (2016). NOX2 drives M1-like microglial/macrophage activation and neurodegeneration following experimental traumatic brain injury. *Brain Behavior and Immunology*; 58:291-309.
doi: 10.1016/j.bbi.2016.07.158.

Lakso, M., Sauer, B., Mosinger, B. Jr, Lee, E.J., Manning R.W., Yu S.H., Mulder K.L., and Westphal H. (1992). Targeted oncogene activation by site-specific recombination in transgenic mice. *Proceedings of the National Academy of Sciences of the United States of America*; 15;89(14):6232-6.
doi: 10.1073/pnas.89.14.6232.

Langlois, J.A., Rutland-Brown W., Wald M.M. (2006). The epidemiology and impact of traumatic brain injury: a brief overview. *Journal of Head and Trauma Rehabilitation*;21(5):375-8.

doi: 10.1097/00001199-200609000-00001.

Lawson, L.J., Perry V.H., Dri P., Gordon S. (1990). Heterogeneity in the distribution and morphology of microglia in the normal adult mouse brain. *Neuroscience*; 39(1):151-70.

doi: 10.1016/0306-4522(90)90229-w

Lee, Y.K., Lee J.A. (2016). Role of the mammalian ATG8/LC3 family in autophagy: differential and compensatory roles in the spatiotemporal regulation of autophagy. *BMB Rep.*;49(8):424-430.

doi:10.5483/bmbrep.2016.49.8.081

Lee, J.H., Yu, W.H., Kumar, A., Lee, S., Mohan, P.S., Peterhoff, C.M., Wolfe, D.M., Martinez-Vicente, M., Massey, A.C., Sovak, G., Uchiyama, Y., Westaway, D., Cuervo A.M., Nixon, R.A. (2010). Lysosomal proteolysis and autophagy require presenilin 1 and are disrupted by Alzheimer-related PS1 mutations. *Cell*; 141, 1146–1158.

doi: 10.1016/j.cell.2010.05.008.

Leitgeb, R.A., Werkmeister R.M., Blatter C., Schmetterer L. (2014). Doppler optical coherence tomography. *Prog Retin Eye Res*;41(100):26-43.

doi:10.1016/j.preteyeres.2014.03.004.

Levine, B., Kroemer G. (2008). Autophagy in the pathogenesis of disease. *Cell*;132(1):27-42.

doi: 10.1016/j.cell.2007.12.018.

Levine, B., Mizushima N., Virgin H.W. (2011). Autophagy in immunity and inflammation. *Nature*; 469(7330):323-35.

doi: 10.1038/nature09782.

Levine, B., and Klionsky, D.J. (2004). Development by self-digestion: molecular mechanisms and biological functions of autophagy. *Developmental cell* 6, 463-477.

Liesz, A., Dalpke, A., Mracsko E., Antoine D.J., Roth S., Zhou W., Yang H., Na S.Y., Akhisaroglu M., Fleming T., Eigenbrod T., Nawroth P.P., Tracey K.J., Veltkamp R. (2019). DAMP signaling is a key pathway inducing immune modulation after brain injury. *J Neurosci*;35(2):583-98.

doi: 10.1523/JNEUROSCI.2439-14.2015.

Lippai, M., and Low, P. (2014). The role of the selective adaptor p62 and ubiquitin-like proteins in autophagy. *BioMed research international*, 832704.

Liu, S., Li, Y., Choi, H., Sarkar, C., Koh, E.Y., Wu, J., Lipinski M.M. (2018). Lysosomal damage after spinal cord injury causes accumulation of RIPK1 and RIPK3 proteins and potentiation of necroptosis. *Cell Death Dis*;9(5):476.

doi: 10.1038/s41419-018-0469-1.

Liu, S., Li, Y., Choi, H.M.C., Sarkar, C., Koh, E.Y., Wu, J., and Lipinski, M.M. (2018). Lysosomal damage after spinal cord injury causes accumulation of RIPK1 and RIPK3 proteins and potentiation of necroptosis. *Cell death & disease*; 9, 476.

Liu, S., Sarkar, C., Dinizo, M., Faden, A.I., Koh, E.Y., Lipinski, M.M., and Wu, J. (2015). Disrupted autophagy after spinal cord injury is associated with ER stress and neuronal cell death. *Cell death & disease*; 6, e1582.

Loane, D.J., Byrnes, K.R. (2010). Role of microglia in neurotrauma. *Neurotherapeutics*;7(4):366-77.
doi: 10.1016/j.nurt.2010.07.002.

Loane, D.J., Faden, AI. Neuroprotection for traumatic brain injury: translational challenges and emerging therapeutic strategies. *Trends Pharmacol Sci*;31(12):596-604.
doi: 10.1016/j.tips.2010.09.005.

Loane, D.J., and Kumar, A. (2016). Microglia in the TBI brain: The good, the bad, and the dysregulated. *Exp. Neuro*; 275, 316–327.
doi: 10.1016/j.expneurol.2015.08.018

Lodder, J., Denaës T., Chobert M.N., Wan J., El-Benna J., Pawlowsky J.M., Lotersztajn S., Teixeira-Clerc F. Macrophage autophagy protects against liver fibrosis in mice. *Autophagy*;11(8):1280-92.
doi: 10.1080/15548627.2015.1058473.

Loos, B., du Toit, A., and Hofmeyr, J.H. (2014). Defining and measuring autophagosome flux—concept and reality. *Autophagy*; 10, 2087-2096.

Lupfer, C., Thomas, P.G., Anand, P.K., Vogel, P., Milasta, S., Martinez J., Huang G., Green M., Kundu M., Chi. H., Xavier R.J., Green, D.R., Lamkanfi, M., Dinarello C.A., Doherty P.C., Kanneganti T.D. (2013). Receptor interacting protein kinase 2-mediated mitophagy regulates inflammasome activation during virus infection. *Nat Immunol*;14(5):480-8.
doi: 10.1038/ni.2563.

Lye, T.C., Shores, E.A. (2000). Traumatic brain injury as a risk factor for Alzheimer's disease: a review. *Neuropsychol Rev*;10(2):115-29.
doi: 10.1023/a:1009068804787.

Ma, Y., L. Galluzzi, L. Zitvogel, and G. Kroemer. (2013). Autophagy and cellular immune responses. *Immunity*; 39:211–227.
doi:10.1016/j.immuni.2013.07.017.

Maejima, I., A. Takahashi, H. Omori, T. Kimura, Y. Takabatake, T. Saitoh, A. Yamamoto, M. Hamasaki, T. Noda, Y. Isaka, and Yoshimori, T. 2013. Autophagy sequesters damaged

lysosomes to control lysosomal biogenesis and kidney injury. *EMBO J.* 32:2336–2347.
Doi:10.1038/emboj.2013.171.

Majeski, A.E., and Dice, J.F. (2004). Mechanisms of chaperone-mediated autophagy. *The International Journal of Biochemistry & Cell Biology*; 36, 2435-2444.

Makinde, H.M., Cuda, C.M., Just, T.B., Perlman, H.R., and Schwulst, S.J. (2017). Nonclassical Monocytes Mediate Secondary Injury, Neurocognitive Outcome, and Neutrophil Infiltration after Traumatic Brain Injury. *J Immunol*;199(10):3583-3591.
doi: 10.4049/jimmunol.1700896.

Mansour, A., and Lajiness-O'Neill, R. (2015). Call for an integrative and multi-disciplinary approach to traumatic brain injury (TBI). *Psychology*; 06, 323–374.
doi: 10.4236/psych.2015.64033.

Martin, D.D., Ladha, S., Ehrnhoefer, D.E., & Hayden, M.R. (2015). Autophagy in Huntington disease and Huntingtin in Autophagy. *Trends in Neurosciences*; 38, 26-35.

Maruyama, T., and Noda, N.N. (2017). Autophagy-regulating protease Atg4: structure, function, regulation and inhibition. *The Journal of antibiotics*; 71, 72–78 (2018).
doi:10.1038/ja.2017.104

Masel, B.E., and DeWitt, D.S. (2010). Traumatic brain injury: a disease process, not an event. *J Neurotrauma*; 27(8):1529-40.
doi: 10.1089/neu.2010.1358.

Masters, S.L., A. Simon, I. Aksentijevich, and Kastner D.L. (2009). Horror autotoxicus: the molecular pathophysiology of autoinflammatory disease. *Annu. Rev. Immunol*; 27:621–668.
doi:10.1146/annurev.immunol.25.022106.141627

Mathew, R., Khor, S., Hackett, S.R., Rabinowitz, J.D., Perlman, D.H., and E. White (2014). Functional role of autophagy-mediated proteome remodeling in cell survival signaling and innate immunity. *Mol. Cell.* 55:916–930.
doi:10.1016/j.molcel.2014.07.019

McKinlay, A., Grace R.C., Dalrymple-Alford J.C., Anderson T., Fink J., and Roger D. (2008). A profile of neuropsychiatric problems and their relationship to quality of life for Parkinson's disease patients without dementia. *Parkinsonism Relat Disord*;14(1):37-42.
doi: 10.1016/j.parkreldis.2007.05.009.

Mira, R.G., Lira, M, and Cerpa, W. (2021). Traumatic Brain Injury: Mechanisms of Glial Response. *Front Physiol*; 12:740939.
doi: 10.3389/fphys.2021.740939.

Mizushima, N., and Komatsu, M. (2011). Autophagy: Renovation of cells and tissues. *Cell*; 147, 728–741.
doi:10.1016/j.cell.2011.10.026

Morganti, J.M., Jopson, T.D., Liu, S., Riparip, L.K., Guandique, C.K., Gupta, N., Ferguson A.R., and Rosi, S. CCR2 antagonism alters brain macrophage polarization and ameliorates cognitive dysfunction induced by traumatic brain injury. *J Neurosci*. 2015 Jan 14;35(2):748-60.

doi: 10.1523/JNEUROSCI.2405-14.2015

Mortimer, J.A., L. Ronald, F.J., Thomas H., and Schuman L.M. (1985). Head injury as a risk factor for Alzheimer's disease, *Neurology*; 35 (2) 264.

doi: 10.1212/WNL.35.2.264.

Muhammad, S., Barakat W., Stoyanov S., Murikinati S., Yang H., Tracey K.J., Bendszus M., Rossetti G., Nawroth P.P., Bierhaus A., and Schwaninger M. (2008). The HMGB1 receptor RAGE mediates ischemic brain damage. *J Neurosci*; 28(46):12023-12031.

doi: 10.1523/JNEUROSCI.2435-08.

Murthy, A., Li Y., Peng I., Reichelt M., Katakam A.K., Noubade R., Roose-Girma M., DeVoss J., Diehl L., Graham R.R., and van Lookeren Campagne M. (2014). A Crohn's disease variant in Atg16l1 enhances its degradation by caspase 3. *Nature*; 506(7489):456-62.

doi: 10.1038/nature13044.

Nakahira, K., Haspel, J.A., Rathinam, V.A., Lee, S.J., Dolinay, T., Lam, H.C., Englert, J.A. Rabinovitch, M. and Cernadas, H.P. (2011). Autophagy proteins regulate innate immune responses by inhibiting the release of mitochondrial DNA mediated by the NALP3 inflammasome. *Nat. Immunol*; 12:222–230.

doi:10.1038/ni.1980

Nakamura, Y. (2002). Regulating factors for microglial activation. *Biol Pharm Bull*; 25(8):945-53.

doi: 10.1248/bpb.25.945.

Neuzil, E., Ravaine, S., Cousse, H. L. (2002). N-acetyl-DL-leucine, medicament symptomatique des etats vertigineux. *Bull. Soc. Pharm. Bordeaux*;141, 15–38.

doi: 10.3389/fphys.2021.740939.

Nixon, R. A. (2007). Autophagy, amyloidogenesis and Alzheimer disease. *J. Cell Sci*; 120, 4081–4091.

doi: 10.1242/jcs.019265.

Nixon, R. A. (2013). The role of autophagy in neurodegenerative disease. *Nat. Med*; 19, 983–997.

doi:10.1038/nm.3232.

Noda, N.N., Kumeta H., Nakatogawa H., Satoo K., Adachi W., and Ishii J. (2008). Structural basis of target recognition by Atg8/LC3 during selective autophagy. *Genes Cells*; 13, 1211–1218.

doi:10.1111/j.1365-2443.2008.01238.x.

Nott, M.T., Gates, T.M., and Baguley, I.J. (2015). Age-related trends in late mortality following traumatic brain injury: A multicentre inception cohort study. *Australas. J. Ageing*; 34, E1–E6.
<https://doi.org/10.1111/ajag.12151>.

Orban, P.C., Chui D., and Marth, J.D. (1992). Tissue- and site-specific DNA recombination in transgenic mice. *Proc Natl Acad Sci U S A*;89(15):6861-5.
doi: 10.1073/pnas.89.15.6861.

Paola, F., Scopetti, M., Santurro, A., Gatto, V., and Fineschi, V. (2017). Stem Cell Research and Clinical Translation: A Roadmap about Good Clinical Practice and Patient Care *Stem Cells International*, 8.
Doi: 10.1155/2017/5080259.

Parzych, K.R., and Klionsky, D.J. (2014). An overview of autophagy: morphology, mechanism, and regulation. *Antioxid Redox Signal*;20(3):460-73.
doi: 10.1089/ars.2013.5371.

Peterson, A.B., and Thomas, K.E. (2018). Incidence of Nonfatal Traumatic Brain Injury-Related Hospitalizations - United States. *MMWR Morb Mortal Wkly Rep*; 70(48):1664-1668.
doi: 10.15585/mmwr.mm7048a3.

Petherick, K.J., Conway, O.J., Mpamhanga, C., Osborne, S.A., Kamal, A., Saxty, B., and Ganley, I.G. (2015). Pharmacological inhibition of ULK1 kinase blocks mammalian target of rapamycin (mTOR)-dependent autophagy. *The Journal of biological chemistry*; 290, 11376-11383.
doi: 10.1074/jbc.C114.627778.

Pickford, F., Masliah E., Britschgi M., Lucin K., Narasimhan R., Jaeger P.A., Small S., Spencer B., Rockenstein E., Levine B., and Wyss-Coray T. (2008). The autophagy-related protein beclin 1 shows reduced expression in early Alzheimer disease and regulates amyloid beta accumulation in mice. *J Clin Invest*; 118(6):2190-9.
doi: 10.1172/JCI33585.

Plassman, B.L., Havlik, R.J., Steffens, D.C., Helms, M.J., Newman, T.N., Drosdick, D., Phillips, C., Gau, B.A., Welsh-Bohmer, K.A., Burke, J.R., Guralnik, J.M., Breitner, J.C. (2000). Documented head injury in early adulthood and risk of Alzheimer's disease and other dementias. *Neurology*; 55(8):1158-66.
doi: 10.1212/wnl.55.8.1158.

Platt, F., Strupp, M. (2016). An anecdotal report by an Oxford basic neuroscientist: effects of acetyl-DL-leucine on cognitive function and mobility in the elderly. *J. Neurol*; 263, 1239–1240.
doi:10.1007/s00415-016-8048-9(2016).

Plesnila, N. (2016). The immune system in traumatic brain injury. *Curr Opin Pharmacol*; 26:110-7.

doi: 10.1016/j.coph.2015.10.008.

Qin, L., Liu, Y., Wang, T., Wei, S. J., Block, M. L., Wilson, B., Liu, B., & Hong, J. S. (2004). NADPH oxidase mediates lipopolysaccharide-induced neurotoxicity and proinflammatory gene expression in activated microglia. *Jou bio chem*, 279(2), 1415–1421. <https://doi.org/10.1074/jbc.M307657200>

doi:10.1074/jbc.M307657200.

Qin, L., Liu, Y., Hong, J.S., Crews, F.T. (2013). NADPH oxidase and aging drive microglial activation, oxidative stress, and dopaminergic neurodegeneration following systemic LPS administration. *Glia*; 61, 855–868.

doi:10.1002/glia.22479.

Qu, X., Yu, J., Bhagat, G. (2003). Promotion of tumorigenesis by heterozygous disruption of the beclin 1 autophagy gene. *J Clin Invest*;112(12):1809-1820.

doi:10.1172/JCI20039

Ramlackhansingh, A.F., Brooks, DJ, Greenwood, R.J., Bose, S.K., Turkheimer, F.E., Kinnunen, K.M., Gentleman, S., Heckemann, R.A., Gunanayagam, K., Gelosa, G., Sharp, D.J. (2016). Inflammation after trauma: microglial activation and traumatic brain injury. *Ann Neurol*; 70(3):374-83.

doi: 10.1002/ana.22455.

Ren, J.L., Pan, J.S., Lu, Y.P., Sun, P., Han, J. (2009). Inflammatory signaling and cellular senescence. *Cell Signal*; 21(3):378-383.

doi:10.1016/j.cellsig.2008.10.011.

Richards, N., Schaner, P., Diaz, A., Stuckey, J., Shelden, E., Wadhwa, A. (2001). Interaction between pyrin and the apoptotic speck protein (ASC) modulates ASC-induced apoptosis. *J Biol Chem*. (2001) 276:39320–9.

doi: 10.1074/jbc.M104730200

Risdall, J.E., & Menon, D. K. (2011). Traumatic Brain Injury. *Philosophical Transactions of the Royal Society*, 366, 241-250.

doi:10.1098/rstb.2010.0230.

Roth, T.L., Nayak, D., Atanasijevic, T., Koretsky, A.P., Latour, L.L., McGavern, D.B. (2014). Transcranial amelioration of inflammation and cell death after brain injury. *Nature*;505(7482):223-8.

doi: 10.1038/nature12808.

- Russo, M.V., Latour, L.L., McGavern, D.B. (2008). Distinct myeloid cell subsets promote meningeal remodeling and vascular repair after mild traumatic brain injury article. *Nat. Immunol.*; 19, 442–452.
doi: 10.1038/s41590-018-0086-2.
- Sahu, R., Kaushik, S., Clement, C.C., Cannizzo, E.S., Scharf, B., Follenzi, A., Potalicchio, I., Nieves, E., Cuervo, A.M., and Santambrogio, L. (2011). Microautophagy of cytosolic proteins by late endosomes. *Developmental cell*; 20, 131-139.
doi: 10.1016/j.devcel.2010.12.003.
- Saitoh, T., Akira, S. Regulation of innate immune responses by autophagy-related proteins. *J Cell Biol*;189(6):925-35.
doi: 10.1083/jcb.201002021.
- Salter, M.W., Beggs, S. (2014). Sublime microglia: expanding roles for the guardians of the CNS. *Cell*; 158(1):15-24.
doi: 10.1016/j.cell.2014.06.008.
- Sandsmark, D.K., Bashir, A., Wellington, C.L., Diaz-Arrastia, R. (2019). Cerebral Microvascular Injury: A Potentially Treatable Endophenotype of Traumatic Brain Injury-Induced Neurodegeneration. *Neuron*;103(3):367-379.
doi: 10.1016/j.neuron.2019.06.002.
- Santeford, A., Wiley, L.A., Park, S., Bamba, S., Nakamura R., Gdoura A., Ferguson T.A., Rao P.K., Guan J.L., Saitoh T., Akira S., Xavier R., Virgin H.W. (2016). Impaired autophagy in macrophages promotes inflammatory eye disease. *Autophagy*;12(10):1876-1885.
doi: 10.1080/15548627.2016.1207857.
- Sarkar C., Jones J.W., Hegdekar N., Thayer J.A., Kumar A., Faden A.I., Kane M.A., Lipinski M.M. (2019). PLA2G4A/cPLA2-mediated lysosomal membrane damage leads to inhibition of autophagy and neurodegeneration after brain trauma. *Autophagy*; 16(3):466-485.
doi: 10.1080/15548627.2019.1628538.
- Sarkar, S., Zhao, Z., Aungst, S., Sabirzhanov, B., Faden, A.I., and Lipinski, M.M. (2014). Impaired autophagy flux is associated with neuronal cell death after TBI. *Autophagy*; 10, 2208-2222.
doi: 10.4161/15548627.2014.981787.
- Schoch, K.M., Madathil, S.K., Saatman, KE. Genetic manipulation of cell death and neuroplasticity pathways in traumatic brain injury. *Neurotherapeutics*. 2012;9(2):323-337. doi:10.1007/s13311-012-0107-z.
- Selassie, A.W., Zaloshnja E., Langlois, J.A., Miller, T., Jones P., Steiner C. (2008). Incidence of long-term disability following traumatic brain injury hospitalization, United States, 2003. *J Head Trauma Rehabil.*;23(2):123-31.

doi: 10.1097/01.HTR.0000314531.30401.39.

Semple, B.D., Bye N., Rancan, M., Ziebell, J.M., Morganti-Kossmann MC. (2010). Role of CCL2 (MCP-1) in Traumatic Brain Injury (TBI): Evidence from Severe TBI Patients and CCL2^{-/-} Mice. *Journal of Cerebral Blood Flow & Metabolism*;3 0(4):769-782. doi:10.1038/jcbfm.2009.262.

Shi Y., Kirwan P., Livesey F.J. (2012). Directed differentiation of human pluripotent stem cells to cerebral cortex neurons and neural networks. *Nat Protoc*;7(10):1836-46. doi: 10.1038/nprot.2012.116.

Shpilka, T., and Elazar, Z. (2011). Shedding light on mammalian microautophagy. *Developmental Cell*; 20, 1-2. doi: 10.1016/j.devcel.2010.12.010.

Spencer, B., Potkar, R, Trejo, M., Rockenstein, E., Patrick, C., Gindi, R., Adame, A., Wyss-Coray, T., Masliah, E. (2009). Beclin 1 gene transfer activates autophagy and ameliorates the neurodegenerative pathology in alpha-synuclein models of Parkinson's and Lewy body diseases. *J Neurosci*;29(43):13578-88. doi: 10.1523/JNEUROSCI.4390-09.2009.

Spencer, J. L., Theadom, A. (2019). Global, regional, and national burden of traumatic brain injury and spinal cord injury, 1990–2016: A systematic analysis for the Global Burden of Disease Study 2016. *Lancet Neurol*; 18, 56–87. doi:10.1016/S1474-4422(18)30415-0.

Staib-Lasarezik, I., Nagel, N., Sebastiani, A., Griemert, E.V., Thal, S. C. Analgesic treatment limits surrogate parameters for early stress and pain response after experimental subarachnoid hemorrhage. *BMC Neurosci*; 20, 49. doi:10.1186/s12868-019-0531-7(2019).

Strupp, M. Effects of acetyl-dl-leucine in patients with cerebellar ataxia: A case series. *J. Neurol*; 260, 2556–2561. doi:10.1007/s00415-013-7016-x(2013).

Strupp, M., Bayer, O., Feil, K., Straube, A. (2019) Prophylactic treatment of migraine with and without aura with acetyl-DL-leucine: A case series. *J. Neurol*; 266, 525–529. doi:10.1007/s00415-018-9155-6.

Tan, C.C., Yu, J.T., Tan, M.S., Jiang, T., Zhu, X.C., Tan, L. (2014). Autophagy in aging and neurodegenerative diseases: implications for pathogenesis and therapy. *Neurobiol Aging*; 35(5):941-57. doi: 10.1016/j.neurobiolaging.2013.11.019.

Tanzi R. E. (2012). The genetics of Alzheimer disease. *Cold Spring Harbor perspectives in medicine*, 2(10). doi:10.1101/cshperspect.a006296

- Te Vruchte, D., Galione, A., Strupp, M. & Mann, M. Effects of N-acetyl-leucine and its enantiomers in Niemann-Pick disease type C cells. doi:10.1101/826222v1 (2019).
- Teasdale, G., and Jennett, B. (1974). Assessment of coma and impaired consciousness. A practical scale. *Lancet*; 2(7872):81-4. doi: 10.1016/s0140-6736(74)91639-0.
- Thurman, D.J., Alverson, C., Dunn K.A., Guerrero J., Sniezek J.E. (1999). Traumatic brain injury in the United States: A public health perspective. *J Head Trauma Rehabil*; 14(6):602-15. doi: 10.1097/00001199-199912000-00009.
- Tighilet, B., Leonard, J., Bernard-Demanze, L., Lacour, M. (2015). Comparative analysis of pharmacological treatments with N-acetyl-DL-leucine (Tanganil) and its two isomers (N-acetyl-L-leucine and N-acetyl-D-leucine) on vestibular compensation: Behavioral investigation in the cat. *Eur. J. Pharmacol.*, 769, 342–349. doi:10.1016/j.ejphar.2015.11.041.
- Tiret, L., Hausherr E., Thicoipe, M., Garros B., Maurette P., Castel J.P., Hatton F. (1990). The epidemiology of head trauma in Aquitaine (France), 1986: a community-based study of hospital admissions and deaths. *Int J Epidemiol*;19(1):133-40. doi: 10.1093/ije/19.1.133.
- Tsuboyama, K., Koyama-Honda, I., Sakamaki Y., Koike M., Morishita H., Mizushima N. (2016). The ATG conjugation systems are important for degradation of the inner autophagosomal membrane. *Science*;354(6315):1036-1041. doi: 10.1126/science.aaf6136.
- Twenge, J.M., Campbell, W.K. (2018). Associations between screen time and lower psychological well-being among children and adolescents: Evidence from a population-based study. *Prev Med Rep* 2018; 12:271-283. doi:10.1016/j.pmedr.2018.10.003
- Vagnerova, K., Koerner, I.P., and Hurn, P.D. Gender and the injured brain. *Anesth. Analg.* 107, 201–214. doi:10.1213/ane.0b013e31817326a5(2008).
- Vibert, N., Vidal, P. P. (2001). In vitro effects of acetyl-DL-leucine (tanganil) on central vestibular neurons and vestibulo-ocular networks of the guinea-pig. *Eur. J. Neurosci*; 13, 735–748.
- Vitner, E. B., Farfel-Becker, T., Eilam, R., Biton, I., & Futerman, A. H. (2012). Contribution of brain inflammation to neuronal cell death in neuronopathic forms of Gaucher's disease. *Brain : a journal of neurology*, 135(Pt 6), 1724–1735. Doi:10.1093/brain/aws095

- Virgin, H.W., and Levine, B. (2009). Autophagy genes in immunity. *Nat Immunol*; 10(5):461-70.
doi: 10.1038/ni.1726.
- Wang, T., Zhang, L., Zhang, M., Bao, H., Liu, W., and Wang, Y. (2013). [Gly14]-Humanin reduces histopathology and improves functional outcome after traumatic brain injury in mice. *Neuroscience*; 231, 70–81.
doi:10.1016/j.neuroscience.2012.11.019
- Wen, H., Gris, D., Lei, Y., Jha, S., Zhang, L., Huang, M.T., Brickey, W.J., and Ting, J.P. (2011). Fatty acid-induced NLRP3-ASC inflammasome activation interferes with insulin signaling. *Nat Immunol*; 12(5):408-15.
doi: 10.1038/ni.2022.
- Wilson L., Stewart W., Dams-O'Connor K., Diaz-Arrastia R., Horton L., Menon D.K., and Polinder S. (2017). The chronic and evolving neurological consequences of traumatic brain injury. *Lancet Neurol*;16(10):813-825.
doi: 10.1016/S1474-4422(17)30279-X.
- Wilson, P.M., Petticrew, M., and Calnan, M.W. (2010). Disseminating research findings: what should researchers do? A systematic scoping review of conceptual frameworks. *Implementation Sci*; 5, 91.
doi: 10.1186/1748-5908-5-91.
- Wild, P., Farhan, H., McEwan, D.G., Wagner, S., Rogov, V.V., Brady, N.R., Richter, B., Korac, J., Waidmann, O., Choudhary, C., Dötsch, V., Bumann, D., and Dikic, I. (2011). Phosphorylation of the autophagy receptor optineurin restricts Salmonella growth. *Science*; 333(6039):228-33.
doi: 10.1126/science.1205405.
- Wong, P.M., Puente, C., Ganley, I.G., and Jiang, X. (2013). The ULK1 complex: sensing nutrient signals for autophagy activation. *Autophagy* 9, 124-137.
- Woodcock, T, and Morganti-Kossmann, M.C. (2013). The role of markers of inflammation in traumatic brain injury. *Front Neurol*; 4, 4:18.
doi: 10.3389/fneur.2013.00018.
- Yang, Z., and Klionsky, D.J. (2009). An overview of the molecular mechanism of autophagy. *Current topics in microbiology and immunology*; 335, 1-32.
doi:10.1007/978-3-642-00302-8_1
- Yang, Z., and Klionsky, D.J. (2010). Mammalian autophagy: core molecular machinery and signaling regulation. *Current opinion in cell biology*; 22, 124-131.
doi: 10.1016/j.ceb.2009.11.014.

Yao J., Zheng K., and Zhang X. (2015). Rosiglitazone exerts neuroprotective effects via the suppression of neuronal autophagy and apoptosis in the cortex following traumatic brain injury. *Mol. Med. Rep.* 12, 6591–6597.

Doi:10.3892/mmr.2015.4292

Yorimitsu, T., and Klionsky, D.J. (2005). Autophagy: molecular machinery for self-eating. *Cell death and differentiation* 12 Suppl 2, 1542-1552.

Yoshii, S.R., Kuma, A., Akashi, T., Hara, T., Yamamoto, A., Kurikawa, Y., Itakura, E., Tsukamoto, S., Shitara, H., Eishi, Y., Mizushima, N. (2016). Systemic Analysis of Atg5-Null Mice Rescued from Neonatal Lethality by Transgenic ATG5 Expression in Neurons. *Dev Cell*; 39(1):116-130.

doi: 10.1016/j.devcel.2016.09.001. Epub 2016 Sep 29.

Yoshii, S.R., and Mizushima, N. Monitoring and Measuring Autophagy. *Int J Mol Sci.* 2017 Aug 28;18(9):1865.

doi: 10.3390/ijms18091865.

Yue, Z., Jin, S., Yang, C., Levine, A.J., and Heintz, N. (2003). Beclin 1, an autophagy gene essential for early embryonic development, is a haploinsufficient tumor suppressor. *Proc Natl Acad Sci U S A*;100(25):15077-82.

doi: 10.1073/pnas.2436255100.

Yue, Z., Jin, S., Yang, C., Levine, A.J., and Heintz, N. (2003). Beclin 1, an autophagy gene essential for early embryonic development, is a haploinsufficient tumor suppressor. *Proceedings of the National Academy of Sciences of the United States of America* 100, 15077-15082.

Zaloshnja, E., Miller, T, Langlois, J.A., and Selassie, A.W. Prevalence of long-term disability from traumatic brain injury in the civilian population of the United States, 2005. *J Head Trauma Rehabil.* 2008 Nov-Dec;23(6):394-400.

doi: 10.1097/01.HTR.0000341435.52004.ac.

Zhang, D., Wang, W., Sun, X., Xu, D., Wang, C., Zhang, Q., Wang, H., Luo, W., Chen, Y, Chen, H., Liu, Z. (2017). AMPK regulates autophagy by phosphorylating BECN1 at threonine 388. *Autophagy*;12(9):1447-59.

doi: 10.1080/15548627.2016.1185576.

Zhang L., Ding K., Wang, H., Wu Y., Xu J. (2016). Traumatic brain injury-induced neuronal apoptosis is reduced through modulation of PI3K and autophagy pathways in mouse by FTY720. 36(1):131-42.

doi: 10.1007/s10571-015-0227-1.

Zhang L., Wang, H., Fan, Y., Gao Y., Li X., Hu Z., et al. . (2017). Fucoxanthin provides neuroprotection in models of traumatic brain injury via the Nrf2-ARE and Nrf2-autophagy pathways. *Sci. Rep*; 7:46763.

doi:10.1038/srep46763

Zhang, Y., He, X., Yu, F. (2013). Characteristic and functional analysis of toll-like receptors (TLRs) in the lophotrocozoan, *Crassostrea gigas*, reveals ancient origin of TLR-mediated innate immunity. *PLoS One*;8(10):e76464.
doi:10.1371/journal.pone.0076464

Zhang, Y.B., Li, S.X., Chen, X.P., Yang, L., Zhang, Y.G., Liu, R. (2008). Autophagy is activated and might protect neurons from degeneration after traumatic brain injury. *Neurosci. Bull.*24, 143–149.
Doi: 10.1007/s12264-008-1108-0.

Zhang, Q., Kang, R., Zeh, H. J., 3rd, Lotze, M. T., & Tang, D. (2013). DAMPs and autophagy: cellular adaptation to injury and unscheduled cell death. *Autophagy*, 9(4), 451–458. <https://doi.org/10.4161/auto.23691>

Zhao, M., Liang, F., Xu, H., Yan, W., Zhang, J. (2016). Methylene blue exerts a neuroprotective effect against traumatic brain injury by promoting autophagy and inhibiting microglial activation. *Mol. Med. Rep.* 13, 13–20.
Doi:10.3892/mmr.2015.4551.

Zhao, Z., Loane, D. J., Murray, M.G. 2nd., Stoica, B. A. & Faden, A. I. Comparing the predictive value of multiple cognitive, affective, and motor tasks after rodent traumatic brain injury. *J. Neurotrauma* 29, 2475–2489.
Doi:10.1089/neu.2012.2511 (2012).

Zheng, H., Fletcher, D., Kozak, W., Jiang, M., Hofmann, K., Conn, C. C., et al. (1995). Resistance to fever induction and impaired acute-phase response in interleukin-1 β deficient mice. *Immunity* 3, 9–19.
doi:10.1016/1074-7613(95)90154-X

Zhong, Z., Umemura, A., Sanchez-Lopez, E., Liang, S., Shalapour, S., Wong, J., He, F., Boassa, D., Perkins, G., Ali, S.R., McGeough, M.D., Ellisman, M.H., Seki, E., Gustafsson, A.B., Hoffman, H.M., Diaz-Meco, M.T., Moscat, J., Karin, M. (2016). NF- κ B Restricts Inflammasome Activation via Elimination of Damaged Mitochondria. *Cell*; 164(5):896-910.
doi: 10.1016/j.cell.2015.12.057.

Zhou, K., Shi, L., Wang, Y, Chen, S., and Zhang, J. (2016). Recent Advances of the NLRP3 Inflammasome in Central Nervous System Disorders. *J Immunol Res*; 2016:9238290. doi:10.1155/2016/9238290

Zhou, R., Yazdi, A. S., Menu, P., and Tschopp, J. (2011). A role for mitochondria in NLRP3 inflammasome activation. *Nature* 469, 221–225.
doi:10.1038/nature09663